DEPARTMENT OF THE INTERIOR

U.S. GEOLOGICAL SURVEY

Reconnaissance geologic map of the southern Sierra Nevada, Kern, Tulare, and Inyo counties, California

by

Donald C. Ross[1]

Open-File Report 90-337

[1]Menlo Park, California

1990

CONTENTS

ILLUSTRATIONS

Plate

Figures

Tables

INTRODUCTION

The map accompanying this report (Plate 1) completes reconnaissance coverage at a scale of 1:125,000 of the southern Sierra Nevada south of lat 36° north, supplementing the geologic map in U.S.G.S. Professional Paper 1381 (Ross, 1989c) that covers the southernmost part of the Sierra Nevada south of lat 35°30' north. Detailed geologic descriptions do not accompany this map as much of these data have already been released in a series of topical open-file reports on the entire southern Sierra Nevada. These reports include data acquired since Ross (1989c) was first submitted for publication in 1981! A list of the abbreviated titles of these open-file reports follows:

1. Hornblende-rich, high-grade metamorphic terranes and implications for crustal depth and batholith roots (Ross, 1983a)

2. Petrographic (thin section) notes on selected samples from hornblende-rich metamorphic terranes (Ross, 1983b)

3. Metamorphic framework rocks (Ross, 1987a)

4. Mafic plutonic rocks (Ross, 1987b)

5. Generalized geologic map -- scale, 1:250,000 (Ross, 1987c)

6. Granitic rock modal data (Ross, 1987d)

7. Specific gravity, granitic rocks (Ross, 1988a)

8. Chemical traits and trends, granitic rocks (Ross, 1988b)

9. Magnetic susceptibility, granitic rocks (Ross, 1989a)

10. Lineaments (Ross, 1989b)

Modal data collected in 1987 and 1988 after the publication of Ross (1987d -- Open-File no. 6 in the above list) are presented here as an appendix, with the same format as modal Open-File 6 (modal table, modal triangular plot, and sample location map for each unit). To aid comparison with the earlier modal data, the modal triangular plots of the appendix show the outline of the modal field of the earlier data by a dashed line; the sample location maps show the earlier modal samples by black dots.

PREVIOUS WORK

Many previous geologic studies in this area were undertaken for special purposes or cover only limited areas, and general-purpose geologic mapping of the basement rocks was normally not a prime objective. For example, many previous studies made no attempt to delineate and describe the intermediate to felsic granitic rocks. Several of the studies, particularly those covering large areas, were made to appraise the mineral resources. These, by necessity, had severe time constraints, which limited mapping and description of basement rock units. Nevertheless, these, and other special-purpose studies, have provided petrographic, structural, modal, chemical, and radiometric age data for parts of the map area. The areal extent of these studies is shown in Figure 1.

The present study has attempted to integrate these previous studies into a regional picture by additional geologic mapping and sampling. Conflicting data have been arbitrarily "resolved" by me -- often leaving "unresolved" conclusions that suggest that much more geologic work is needed in this region. The area of "granitic rocks, undivided in the north-central part of the map

area" is an obvious place to start!

Areal studies

(1) Bartow and Doukas, (1978) -- contacts and faults between basement rocks and Cenozoic deposits along the eastern margin of the San Joaquin Valley.

(2) Bergquist and Nitkiewicz, (1982) -- limited contacts and minor modal and radiometric age data in Domelands.

(3) Best and Weiss, (1964) -- petrographic and mineralogical data on metamorphic rocks near Isabella Lake; chemical analyses of several biotites, cordierites, and garnets.

(4) Bruce, (1981) -- some contacts and petrographic data on metasedimentary rocks of the eastern part of the Indian Wells mining district.

(5) Diggles et al., (1987) -- some contacts on the east face of the Sierra Nevada; some modal and chemical data of granitic rocks.

(6) Elan, (1985) -- contacts and petrographic data on metamorphic rocks on the north side of Isabella Lake.

(7) Fox, (1981) -- petrographic data and abundant modal and chemical data on granitic rocks near Cyrus Flat.

(8) Harner et al., (1983) -- scattered contacts and thin sections (no hand specimens) from granitic and metamorphic rocks of the Scodie Mountains.

(9) Jenkins, (1961) -- petrographic and structural data on metasedimentary rocks north of Kernville on the west side of the Kern Canyon fault.

(10) Kennedy et al., (1983) -- petrographic data on basement rocks from field notes and thin sections (no hand specimens). Limited area east of Havilah.

(11) MacKevett, (1960) -- petrographic data on granitic and metamorphic rocks near Kern River southwest of Isabella Lake; numerous thin sections and hand specimens, modal plots of granitic rocks, and semi-quantitative spectrographic data.

(12) Miller and Webb, (1940) -- limited petrographic data on granitic and metamorphic rocks, and general outline of many metamorphic bodies in a large area (2700 km^2) northeast of Isabella Lake -- a pioneering reconnaissance study.

(13) Prout, (1940) -- contacts, faults, and petrographic data near the Big Blue mine southwest of Kernville. (Big Blue shear zone is probably a branch of the Kern Canyon fault zone.)

(14) Saleeby and Sharp, (1980) -- outline of major mafic and ultramafic bodies in northwest corner of the map area, and some petrographic and radiometric data.

(15) Taylor et al., (1986) -- some petrographic data on basement rocks.

(16) Treasher, (1948) -- delineation of Kern Canyon fault zone near Isabella dam, based on extensive drilling and trenching.

Other studies (not on index map)

Saleeby and Busby-Spera, (1986) -- petrographic and structural data on basement rocks at selected spots along the Kern River from near Fairview to south of Lake Isabella; also some radiometric age data.

Smith, (1965) -- outlines of major metamorphic bodies in previously unmapped areas of the Bakersfield AMS sheet of the geologic map of California.

Lawson, (1906) -- historic reports that locate and describe various segments
Webb, (1936) of the Kern Canyon fault zone.
Webb, (1946)

Webb, (1955) -- describes several segments of the Kern Canyon "lineament" from Wheeler Ridge north to Golden Trout Creek and concludes that "the concept of a single structure important in today's geology should be abandoned." He also concludes that "the possibility of a direct present relationship between separate faults known in this regional lineament must be admitted.

DESCRIPTION OF MAP UNITS

Surficial Deposits

Deposits and alluvial sedimentary rocks, undivided (Quaternary and Tertiary -- surficial deposits lapping up on the basement at the east and west sides of the Sierra Nevada, and larger valleys within the range itself, mostly floored with unconsolidated alluvial material.

Qb Basalt (Quaternary) -- extensive exposures near Little Lake of basaltic flows, pyroclastic deposits, and cinder cones, and minor rhyolite deposits in the south end of the Coso volcanic field (outline generalized from Duffield and Bacon, 1981).

Tb Basalt (Tertiary) -- remnants of flows and cinder cones scattered about the north-central part of map area and minor exposures north of Little Lake.

Plutonic Rocks

Kce Fine-grained granitic rocks of Cedar Creek (Cretaceous) -- dikes and small masses of widely varying mineral content, ranging from granite to quartz diorite. At least in part intrusive into the Poso Flat and Walt Klein Ranch units. Some quartz diorite resembles dark inclusions common in many Sierra Nevada plutonic units.

gru Granitic rocks, undivided (Cretaceous and Jurassic) -- areas in the northeast part of the map area underlain chiefly by granitic rocks, as shown on earlier maps. These rocks have not been examined in the present study.

Lamprophyric dikes of the Independence dike swarm of Moore and Hopson (1961) (Late Jurassic) -- dark, porphyritic, diabasic dikes composed chiefly of andesine and green hornblende; lesser brown biotite -- correspond most closely to spessartite lamprophyres. Many dikes are altered to masses of chlorite, epidote, sericite, and calcite. The dikes are abundant and intrude the granodiorite of Sacatar along the eastern Sierra Nevada front (location of selected dikes shown by attitude symbols on Plate 1); they are less common in the quartz diorite of Walker Pass and have been noted locally cutting the gabbro of Bodfish at the Wofford Heights marina. Many of these lamprophyric dikes are located and petrographically described in Ross (1987b). Dikes cutting the granite of Little Lake (J11) and granitic rocks, undivided (gru) in the northeast part of the map area, are noted only as "steeply dipping dikes" by Duffield and Bacon (1981). Air photo inspection suggests that the dikes are mafic, but I have not examined them in the field. They probably are part of the Independence dike swarm (Moore and Hopson, 1961), but could also be Cenozoic volcanic dikes. U/Pb determinations on zircon from silicic dikes associated with lamprophyre dikes give concordant ages of 148 Ma from localities in the Argus Range (about 45 km southeast of the Eastern Sierra Nevada dike localities) (Chen and Moore, 1979).

Granite

(radiometric ages shown)

Knc Granite of Noname Canyon (Late Cretaceous) -- leucocratic alaskite with minor amounts of muscovite and garnet. K-Ar muscovite age, 80.1±5.3 Ma (Diggles, 1984). Rb/Sr whole rock isochron on 4 samples is 80.5±1.7 Ma (R.W. Kistler, written commun., 1986).

Kcc Granite of Cannell Creek (Late Cretaceous) -- coarse-grained, strongly sheared rock. U-Pb zircon age of 80 ± 2 Ma (Saleeby and Busby-Spera, 1986. Rb/Sr whole rock ages for 5 samples average 107.5±5 Ma (R.W. Kistler, written commun., 1986). K-Ar biotite ages of 50.5 Ma (Evernden and Kistler, 1970) and 55 Ma (Jenkins, 1961 -- location uncertain).

Kkr Granite of Kern River (Late Cretaceous) -- dark-colored hornblende and biotite-bearing rock with distinctive centimeter-sized dark clots. U-Pb zircon age of 80±3 Ma (Saleeby and Busby-Spera, 1986, p. 92). K-Ar biotite ages of 86.8, 87.2, and 88.8 Ma (Evernden and Kistler, 1970). Rb/Sr whole rock isochron age on 4 samples is 81.1±11.1 Ma (R.W. Kistler, written commun., 1986).

Kgo Granite of Onyx (Late Cretaceous) -- fine-grained, sugary textured rocks with about 4 percent biotite. K-Ar biotite age of 80.7 Ma (Evernden and Kistler, 1970).

Kff Granite of Five Fingers (Late Cretaceous) -- weathers into impressive, light-colored spires. Noted for abundant small mafic inclusions and scattered hornblende, otherwise similar to the granodiorite of Castle Rock. Estimated 90-Ma age from Rb/Sr whole rock data (R.W. Kistler, written commun., 1986).

Ksp Alaskite* of Sherman Pass (Cretaceous) -- coarse-grained with minor biotite and some hornblende. Rb/Sr whole rock age of 91 Ma from samples just to north of the map area in the Hockett Peak quadrangle (R.W. Kistler, written commun., 1987). May be correlative with the alaskite of Coyote Pass and/or the alaskite of Hells Hole in the Golden Trout Wilderness Area to the north of the map area (du Bray and Dellinger, 1981).

Kbp Granite of Baker Point (Late Cretaceous) -- fine-grained, biotite-bearing rocks. A large dike cutting the granite of Kern River. Questionable K-Ar age on biotite of 92 Ma (Jenkins, 1961).

Kpp Granite of Portuguese Pass (Early Cretaceous) -- coarse-grained, biotite-bearing rock with some hornblende. May be correlative with texturally similar Hatchet Peak unit. Rb/Sr determinations on whole rock samples give an age of 105.6±9.2 Ma (R.W. Kistler, written commun., 1986).

J11 Granite of Little Lake (Jurassic) -- exposed as a window in Cenozoic volcanic rocks just east of the east front of the Sierra Nevada. Not examined by me. Physical descrip-

---

*In the IUGS classification the term "alaskite" is restricted to rocks with a plagioclase fraction of An_{0-5}. This is unusually restrictive and virtually eliminates the term from the Cordilleran batholithic belt. I prefer the time-worn usage of "alaskite": felsic, granitic rock with less than 5 percent mafic constituents, and normally subequal amounts of plagioclase, K-feldspar, and quartz.

tion and chemical analysis of one sample collected for age determination (Kistler and Peterman, 1978) suggest a relation to the granite of Paiute Monument (Ross, 1969) in the Inyo Mountains to the north. Rb/Sr isochron from five samples collected outside the map area gives a 175±5-Ma age (R.W. Kistler, written commun., 1986).

Granite

(no radiometric ages)

Kac Granite of Arrastre Creek (Cretaceous) -- coarse-grained, felsic rocks.

Kblm Granite of Black Mountain (Cretaceous) -- a small, nearly round plug of biotite granite intruded into the granite of Kern River and the tonalite of Wofford Heights.

Kbra Granite of Bob Rabbit Canyon (Cretaceous) -- felsic, coarse-grained, biotite-bearing rocks with minor hornblende. Intrudes granodiorite of Rabbit Island and probably granodiorite of Castle Rock.

Kbo Granite of Bodfish Canyon (Cretaceous) -- typically coarse-grained, but some variation, contains a few percent of biotite and only local hornblende.

Kb Granite of Brown (Cretaceous) -- small plug on east front of the Sierra Nevada. Distinctly different from nearby felsic dikes and plugs. Has some textural resemblance to the quartz diorite of Walker Pass.

Kgg Quartz Syenite of Grapevine Grade (Cretaceous) -- small plug about 6 km east of White River that is quartz-poor (13 percent).

Klm Granite of Long Meadow (Cretaceous) -- an ovoid pluton of fine- to medium-grained, felsic rocks containing a few percent biotite. Intrudes the granodiorite of Castle Rock.

Kmf Miscellaneous felsic bodies in granodiorite of Sacatar (Cretaceous) -- vari-textured dikes and small stocks on east face of the Sierra Nevada. Granite of Brown and the stock correlated with Granite of Onyx about 6 km to the northwest of the granite of Brown may be related to the small stocks and dikes. Some of these dikes may be part of the Jurassic Independence dike swarm of Moore and Hopson (1961).

Khs Granite of Old Hot Springs Road (Cretaceous) -- small medium-grained heart-shaped alaskitic stock. Contains traces of garnet.

Krr Alaskite of Robbers Roost (Cretaceous) -- coarse-grained, orange-weathering craggy rocks with small amounts of biotite, opaque minerals, and garnet.

Kss Granite of Saddle Springs Road (Cretaceous) -- fine-grained, vari-shades of gray, and characterized by small mafic clots and inclusions to several millimeters in diameter.

Ksc Granite of Sand Canyon (Cretaceous) -- low-dipping, fine-grained mass along eastern Sierra Nevada front; may be a dike-like offshoot of granodiorite of Castle Rock.

Kpw Pegmatite of Wofford Heights (Cretaceous) -- massive dike of simple pegmatite about 2 km west of Wofford Heights on south side of State Highway 155. Crops out as a lens-shaped body 600 m long and as wide as 150 m. This large dike is representative of many smaller pegmatites in the immediate area.

Granodiorite

(radiometric ages shown)

Kas Granodiorite of Alta Sierra (Late Cretaceous) -- fine-grained, but sprinkled with coarser biotite. Dikes of this unit intrude the granodiorite of Wagy Flat, but textural

gradation between these two masses suggests the Alta Sierra unit is a slightly younger, finer-grained pulse of the Wagy Flat. K-Ar biotite age of 89.0±2.1 Ma (Evernden and Kistler, 1970).

Kcr Granodiorite of Castle Rock (Late Cretaceous) -- generally porphyritic rocks with pink to salmon K-feldspar phenocrysts to 5 cm. Modal average close to granite field. Probably correlative with granite of White Mountain to north (du Bray and Dellinger, 1981). K-Ar biotite ages of 80.2, 80.7 Ma (Evernden and Kistler, 1970), 67.1±2, 78.7±2, 74.8±2 Ma (Kistler and Peterman, 1978), and 81.1±2 Ma (R.M. Tosdal in Bergquist and Nitkiewicz, 1982). K-Ar ages may reflect resetting by the younger Granite of Onyx. One Pb/U age of 90±2 Ma (Sams, 1986) from the Whiterock facies of the Granodiorite of Castle Rock (south of the map area) suggests the entire body may have been intruded about 90 Ma. In the southernmost Sierra Nevada this unit was formerly called Granodiorite of Claraville (Ross, 1989c).

Kcw Whiterock facies of the granodiorite of Castle Rock (Late Cretaceous) -- rocks separated from the granodiorite of Castle Rock chiefly because of very low magnetic susceptibility (average of 30 x 10^{-5} Siu) contrasted to "normal" Castle Rock with susceptibility values greater than 1000 x 10^{-5} Siu. (Ross, 1989a). These rocks, near the south border of the map area, are a presumed extension of rocks farther south that were originally defined as the Whiterock facies and that also have similarly low magnetic susceptibility. U-Pb age on zircon is 90±2 Ma, based on one sample south of lat 35°30' N (Sams, 1986) in the area originally defined as Whiterock.

Kbru Granodiorite of Brush Creek (Late Cretaceous) -- varied, but generally dark-colored, in part, contaminated rock containing abundant biotite and hornblende. Dark, ovoid inclusions common, as are centimeter-sized mafic clots reminiscent of the granite of Kern River. May correlate with granodiorite of Loggy Meadow to the north (du Bray and Dellinger, 1981). K-Ar age on biotite of 90 ± 2 Ma (Evernden and Kistler, 1970).

Kal Granodiorite of Alder Creek (Late Cretaceous) -- facies of tonalite of Dunlap Meadow that contains more K-feldspar and less mafic minerals. Has higher measured $^{87}Sr/^{86}Sr$ (average of 6 samples = 0.7085) than Dunlap Meadow (average of 7 samples = 0.7069); both are higher than nearby Poso Flat unit (average of 4 samples = 0.7057), but no contact has been seen. Rb/Sr age assumed to be same as that of Dunlap Meadow (91.4±11.3 Ma). K-Ar ages on biotite of 93.9 and 94.6 Ma (Evernden and Kistler, 1970).

Kpi Granodiorite of Pine Flat (Late Cretaceous) -- medium-grained, felsic rocks with biotite and some hornblende. Dikes of granodiorite intrude tonalite of Dunlap Meadow at several localities -- no age-relations seen; however, Rb/Sr whole rock data indicate that this body has an age of 91.4±11.3 Ma and cannot be distinguished from the tonalite of Dunlap Meadow on the basis of age (R.W. Kistler, written commun., 1986).

Kri Granodiorite of Rabbit Island (Early Cretaceous) -- medium-grained, dark rock containing more biotite than hornblende. Mafic inclusions generally common. U-Pb age on zircon of 99±2 Ma (Saleeby and Busby-Spera, 1986).

Kpf Granodiorite of Poso Flat (Early Cretaceous) -- texturally much like tonalite of Bear Valley Springs with abundant biotite, hornblende, and K-feldspar. May well be the same age as the tonalite of Bear Valley Springs, dated by U-Pb on zircon as about 100 Ma (Sams, 1986).

Kpm Granodiorite of Peppermint Meadow (Early Cretaceous) -- medium-grained, abundant biotite and some hornblende. Sprinkled with scattered coarser mafic minerals. Extends some distance north of the map area and may be correlative with the granodiorite of Pecks Canyon (du Bray and Dellinger, 1981). Rb/Sr whole rock data give an age of 106.7±21.1 Ma (R.W. Kistler, written commun., 1986).

Js Granodiorite of Sacatar (Jurassic) -- dark rock of varied grain size, in part porphyritic -- may well be a composite body. Abundant biotite and hornblende, surprisingly abundant K-feldspar (about 15 percent) in so dark a rock. Quartz quite variable, but generally relatively low (about 15 percent average). Examined in detail only along eastern Sierra Nevada front, where it is intruded by mafic lamprophyric dikes that belong to the 148-Ma Independence dike swarm (Chen and Moore, 1979). K-Ar ages on hornblende of 146.3±4.4, 145.3±4.4, and 144.5±4.3 Ma have been determined from samples of the Sacatar unit about 4 km north of the map area (R.M. Tosdal in Bergquist and Nitkiewicz, 1982). R.W. Kistler (written commun., 1986) has determined an isochron of 177.4±4.9 Ma from whole rock data for Rb/Sr for a large number of samples from the northeast part of the map area and from just north of the map area between Kennedy Meadows (near the north margin of the map area) and Blackrock Mountain (about 20 kilometers NNW of Kennedy Meadows).

Granodiorite

(no radiometric ages)

Kba Granodiorite of Basket Pass (Cretaceous) -- sparsely sampled medium-to coarse-grained distinctive craggy, orange-colored felsic rock that may be related to Kpc.

Kdc Granodiorite of Deer Creek (Cretaceous) -- medium-grained, gray rock with abundant biotite and varied amounts of hornblende. Characterized by abundant inclusion-schlieren swarms that are migmatic and gneissic in part. Rather common opaque minerals and average magnetic susceptibility of about 1400 x 10^{-5} siu. Seems to cut off foliation in the nearby tonalite of Carver-Bowen Ranch and may be younger.

Kds Granodiorite of Democrat Springs (Cretaceous) -- medium-grained, relatively felsic

body that intrudes the tonalite of Bear Valley Springs (body of unknown size -- not fully mapped -- along State Highway 178).

Kef Granodiorite of Evans Flat (Cretaceous) -- peppered with abundant biotite crystals and weakly porphyritic with distinctive blue-gray anhedral quartz crystals to 1 cm in diameter--map pattern suggests Evans Flat intrudes the granodiorites of Alder Creek and Wagy Flat, but no age relations have been seen.

Kgc Granodiorite of Goat Ranch Canyon (Cretaceous) -- isolated body south of Isabella Lake originally correlated with Rabbit Island rocks. Called "dark Rabbit Island" in the field, and has a color index of about 27 contrasted to about 18 for main Rabbit Island body. The Goat Ranch Canyon body is particularly rich in hornblende. A Goat Ranch Canyon sample has $^{87}Sr/^{86}Sr = 0.7065$ contrasted to values above 0.7071 for several samples from the main Rabbit Island outcrops. Also, the Goat Ranch Canyon body has a low magnetic susceptibility with a range of 40 to 160 x 10^{-5} siu with only one aberrant sample of 2200 x 10^{-5} siu that is in the range of Rabbit Island samples.

Khp Granodiorite of Hatchet Peak (Cretaceous) -- coarse-grained, with abundant biotite and some hornblende.

Khr Granodiorite of Hershey Ranch (Cretaceous) -- medium-grained, gray rock, physically similar to the granodiorite of Deer Creek, but has somewhat more hornblende and a lower magnetic susceptibility (average of about 550 x 10^{-5} siu). Formerly called the "East body" of the Deer Creek unit (Ross, 1987d).

Kkp Granodiorite of Kelso Peak (Cretaceous) -- sparsely sampled body originally included with Rabbit Island mass. Modally has less K-feldspar, biotite, and quartz, and more plagioclase than average of Rabbit Island samples. Magnetic susceptibility is very low

(less than 50 x 10^{-5} siu) contrasted to more than 1000 x 10^{-5} siu for Rabbit Island. May instead be part of the granodiorite of Whiterock (Ross, 1989c).

Klp Granodiorite of Lime Point (Cretaceous) -- small bodies of fine-grained gray rock cropping out north and south of Isabella Lake east of conspicuous marble-rich belt of metasedimentary rocks.

Kpc Granodiorite of Poso Creek (Cretaceous) -- possibly a felsic variant of the granodiorite of Poso Flat.

Kwf Granodiorite of Wagy Flat (Cretaceous) -- medium-grained, with abundant, relatively coarse, subhedral to euhedral biotite and hornblende crystals. Texturally similar to Mount Adelaide pluton, but contains about 10 percent of K-feldspar.

Tonalite

(radiometric ages shown)

Kwh Tonalite of Wofford Heights (Late Cretaceous?) -- dark rocks with abundant biotite and hornblende. Texturally and modally resemble the tonalite of Bear Valley Springs. K-Ar ages on biotite of 87.7 and on hornblende from the same sample of 89.9 Ma (Evernden and Kistler, 1970) are similar to the ages of a near-concordant pair from the tonalite of Bear Valley Springs about 25 km south of Caliente. The latter samples are presumed to have been reset, but their near concordance poses a problem.

Kdm Tonalite of Dunlap Meadow (Late Cretaceous) -- another medium-grained, fairly dark rock much like the Bear Valley Springs mass (perhaps the Dunlap has somewhat better formed mafic minerals and does not have noticeable gneissic patches and stringers). Rb/Sr whole rock data indicate an age of 91.4±11.3 Ma, indistinguishable from the age of the granodiorite of Pine Flat (R.W. Kistler, written commun., 1986).

Kma Tonalite of Mount Adelaide (Early Cretaceous) -- distinctive, medium-grained rock with abundant coarse biotite crystals, in part euhedral, and lesser subhedral to euhedral coarse hornblende crystals. Very small amounts of K-feldspar, but abundant quartz. Probably intrudes tonalite of Bear Valley Springs. U-Pb age on zircon of 100±2 Ma (Sams, 1986).

Kbv Tonalite of Bear Valley Springs (Early Cretaceous) -- dark-gray, medium-grained rocks with abundant anhedral and patchy biotite and hornblende, and characteristically foliated and with abundant mafic inclusions and streaks and patches of gneiss. Grades westward into the mafic gneiss complex of the San Emigdio and Tehachapi Mountains. Six U-Pb zircon ages of 98±2, 100±2, 100±2, 100±2, 100±2, and 100±2 Ma (Sams, 1986). K-Ar age on biotite of 85.9±3 Ma and on hornblende from the same sample of 88.1±3 Ma (J.L. Morton, written commun., 1979). The near concordance of this latter pair of ages in the midst of concordant and much older U-Pb ages is an enigma and requires very special conditions (such as very rapid cooling) to reset both biotite and hornblende at roughly the same time.

Kfs Tonalite of Fountain Springs (Early Cretaceous) -- medium-grained, moderate gray tonalite averaging 11 percent biotite and 5 percent hornblende. U-Pb age on zircon of 102 Ma (Saleeby and Sharp, 1980).

Kwk Tonalite of Walt Klein Ranch (Early Cretaceous) -- medium-grained and texturally similar to the Mount Adelaide mass with abundant coarse, well-formed biotite and hornblende crystals. Random bar pattern east of Eclipse Hill shows area of contaminated (?) rocks (approximate extent outlined by dash-dot line). K-Ar ages on biotite of 105 Ma and hornblende from same sample of 111 Ma (Evernden and Kistler, 1970). K-Ar age determination on biotite and hornblende of another sample yielded respectively 100.4 and 105 Ma (Evernden and Kistler, 1970). Another K-Ar

determination on biotite gave an age of 100.6 Ma (Evernden and Kistler, 1970). More recent evaluation of the data of Evernden and Kistler (1970) indicates a K-Ar age on hornblende of 111±2.5 Ma (R.W. Kistler, written commun., 1986).

Tonalite

(no radiometric ages)

Kcb Tonalite of the Carver-Bowen Ranch (Early Cretaceous) -- medium-grained, very dark rock with more than 10 percent each of biotite and hornblende.

Kzr Tonalite of the Zumwalt Ranch (Cretaceous) -- dark-colored, medium-grained body in the northwest corner of the map area that is much like the tonalite of Bear Valley Springs in texture and modal content.

Quartz diorite

(radiometric ages shown)

Kcf Quartz diorite of Cyrus Flat (Early Cretaceous) -- medium-grained, dark colored rock with abundant, but variable amounts of biotite and hornblende. Also a few percent of clinopyroxene and/or orthopyroxene. On west side, Fox (1981) mapped a gabbro body made up of mostly plagioclase and hornblende, with lesser amounts of biotite, clinopyroxene, orthopyroxene, and opaque minerals. U-Pb age on zircon of 100±3 Ma (Saleeby and Busby-Spera, 1986).

Trfj Quartz diorite of Freeman Junction (Triassic) -- small, dark-gray body of varied grain size and texture. Some samples resemble the quartz diorite of Walker Pass. Rb/Sr whole rock determinations, on only 2 samples, give an age of about 222 Ma (R.W. Kistler, written commun., 1986).

Trwp Quartz diorite of Walker Pass (Triassic) -- medium-grained, moderately dark-gray rock that has distinctly coarser mafic minerals that are anhedral and patchy, giving rock a distinctive "fuzzy" texture. Few mafic inclusions, which is unusual for so dark a rock. Strongly foliated northeast margin (shown by wiggly line pattern on Plate 1) may mark suture of possible regional extent between Mesozoic metasedimentary rocks to the west and bedded-barite-bearing Paleozoic metasedimentary rocks to the east. Intruded by mafic lamprophyric dikes that are possibly related to the Independence dike swarm of 148 Ma (Chen and Moore, 1979). Rb/Sr on whole rock of 86 Ma with a relatively low Sri of 0.7049 (Kistler and Peterman, 1973). K-Ar ages on biotite and hornblende from the same sample are respectively 74 and 86 Ma (Evernden and Kistler, 1970). Preliminary Rb/Sr determinations on several other samples from this body indicate these ages are anomalously low, as recent determinations of Rb/Sr on whole rocks give ages of 240.4±14 Ma (R.W. Kistler, written commun., 1986).

Quartz diorite

(no radiometric ages)

Krc Quartz diorite of Rhymes Campground (Cretaceous) -- small dark-gray, fine- to medium-grained, orthopyroxene-bearing bodies that may be related to the gabbronorite of Quedow Mountain (fine-grained facies?).

(?) Quartz diorite of Long Valley (Triassic?) -- sparsely sampled; texture

Trlv and mineral content compatible with some Sacatar samples, texture is unlike distinctive Walker Pass. Measured $^{87}Sr/^{86}Sr$ = 0.70558, much lower than Sacatar to the east (0.708-0.709) and higher than Walker Pass (0.7046). Some physical resemblance to quartz diorite of Freeman Junction that has a measured $^{87}Sr/^{86}Sr$ of 0.7051.

Mafic and ultramafic rocks

(radiometric ages shown)

Kqm Gabbronorite of Quedow Mountain (Early Cretaceous) -- a number of probably related remnants in the largely granitic terrane of the northwest part of the map area. Medium- to coarse-grained, darkly colored rocks composed of various mixtures of labradorite, orthopyroxene, clinopyroxene, and opaque minerals; also minor olivine. Small amount of quartz is present in most samples. Many bodies are dominated by retrograded rocks composed dominantly of plagioclase and hornblende (amphibolite) with only minor remnants of the original gabbronorite and norite. U-Pb age on zircon of 115 Ma (Saleeby and Sharp, 1980).

Pzgm Gabbro-basalt serpentinite melange of Saleeby and Sharp (1980) (Late Paleozoic?) -- disrupted and internally mixed oceanic lithosphere exposed in far northwest corner of map area. U-Pb determinations on zircon from a plagiogranite block give widely discordant ages from 165 to 191 Ma (Saleeby and Sharp, 1980). They interpret these discordant data as suggesting a "safe age assignment" of 270 to 305 Ma (representing the age of the ocean-floor assemblage of which these blocks were originally a part).

Mafic and ultramafic rock
(no radiometric ages)

Jbo Olivine gabbro of Bodfish (Jurassic?) -- olivine gabbro, gabbro, anorthositic gabbro, and lesser dunite and wehrlite, in part serpentinized. In some gabbro outcrops, olivine occurs as distinctive, small, rounded, reddish to black spots enclosed by thin reaction mantles of pale amphibolite intergrown with green spinel (kelyphitic rims) which are particularly conspicuous on weathered faces or in thin section. These spotted gabbros commonly weather to eye-catching spheroidal piles ("cannonballs"). Gabbros are cut locally by mafic dikes that may be related to the Independence dike swarm of Moore and Hopson (1961), which suggests that these gabbros are Jurassic.

KJlo Gabbro of Live Oak (Cretaceous or Jurassic) -- dark, hornblende gabbro (and amphibolite?) with patches of remnant olivine norite with diffuse contacts with surrounding tonalite. Possible correlative with Breckenridge remnants (about 10 km to the southeast).

Mzmsc Miscellaneous gabbroic rocks (Mesozoic) -- hornblende-gabbro and amphibolite in small bodies at Freeman Canyon, Horse Canyon, and Sand Canyon. Some may be related to the Summit Gabbro of Miller and Webb (1940)?

Trs Summit gabbro of Miller and Webb (1940) (Triassic) -- commonly occurs as vari-sized patches of hornblende-gabbro remnants in the granodiorite of Sacatar, the largest of which are southwest of Big Pine Meadow and in the Spanish Needle Creek area. Possibly intruded by quartz diorite of Walker Pass. Original definition of unit also included olivine gabbro of Bodfish (KJbo), quartz diorite of Cyrus Flat (Kcf), and tonalite of Wofford Heights (Kwh).

Metamorphic rocks

(some age data)

Kf Fairview metasedimentary and metavolcanic belt (Cretaceous?) --consists of numerous
Kfv roof pendants, extends 55 km south-southeast from near the northern border of the map area, and is diagonally bisected by the White Wolf-Breckenridge-Kern Canyon fault. Most pendants are dominantly composed of deposits of dark, fine-grained-to-granular, thick-bedded to massive quartzite. Angular to subrounded clasts, largely unsorted, suggest rapid deposition (from turbidity currents?) for these beds. Tuffaceous layers and other metavolcanic types are also present. The associated and possibly related (in age?) French Gulch metavolcanic pendant (Kfv) extends for about 25 km on the east side of the Kern Canyon fault, mostly south of Isabella Lake. The metavolcanic pendant contains various felsic and intermediate volcanic rock and tuff types, including

felsic layers with strong fluxion structure that probably represent ash flow tuff layers. In addition, there are interlayers of coarse, granular, unsorted quartzite found only in the Fairview belt, which suggests that the dominantly metavolcanic pendant is part of the Fairview belt. The offset counterparts of the Fairview belt east of the Kern Canyon fault (south of Isabella Lake and west of the French Gulch pendant) also contain both granular, unsorted quartzite and metavolcanic layers, suggesting further an age tie between the Fairview and French Gulch pendants. No fossil evidence of the age of the Fairview belt has been found. Metavolcanic rocks from the possibly related French Gulch pendant have been radiometrically dated, however. Ash flow tuff from just south of the map area has been dated by U-Pb on zircon at 98± Ma (Saleeby and Busby-Spera, 1986). Rb/Sr whole rock data from the same locality indicate an age of 97±0.5 Ma (R.W. Kistler, written commun., 1986). A rhyolite sill in Erskine Canyon has been dated by the U-Pb method on zircon at 102±5 Ma (Saleeby and Busby-Spera, 1986). These radiometric data indicate that the French Gulch pendant and, by association, the Fairview belt are mid-Cretaceous and much younger than the metamorphic rocks to the east and west, which are considered to be part of the Kings sequence of Late Triassic to Early Jurassic age (based on sparse fossil evidence).

JTrlc Long Canyon Metasedimentary belt (Jurassic and/or Triassic) --irregualr, west-north--northwest-trending pendant and several correlative masses to the north, including one series of beds offset along, and west of, the Kern Canyon fault. Mostly well-layered sequence of siliceous to pelitic schist (in part, coarse, containing andalusite and sillimanite), pure to impure quartzite, marble, and calchornfels. Main pendant contains one locality of bivalves that indicate a late Triassic or early Jurassic age (Saleeby and others, 1978).

Pzrb Rockhouse Basin Metasedimentary belt (Paleozoic?) -- several isolated pendants of thin-bedded mica schist, pure and impure quartzite, and calcareous beds. Possibly Paleozoic age, based on bedded barite in largest pendant (Taylor and others, 1986), and

intrusion of belt by Triassic granitic rocks. Geraci and others (1987) suggest that the Indian Wells Canyon pendant, the southeasternmost pendant of the Rockhouse Basin metasedimentary belt, is lithologically similar to Ordovician to Devonian eugeoclinal strata in Nevada and in the nearby El Paso Mountains. Also, conglomeratic strata in the pendant are strikingly similar to Mississippian "Antler" in the El Paso Mountains.

Metamorphic rocks

(no age data)

Mzbm Big Meadow Metasedimentary belt (Mesozoic?) -- a group of several north-west-trending pendants distinguished by gray to green calc-horn-fels layers that have purplish spots that commonly weather out ("fish eye holes"); otherwise, they are much like Rockhouse Basin belt. From the north boundary of the map area, the Big Meadow belt extends south-southeast for 50 km. This metasedimentary belt continues north of the map area, and there contains bedded barite, suggesting that the Big Meadow Belt may be, at least in part, Paleozoic. The easternmost pendants of the poorly studied Big Meadow Belt may as well be on-strike continuations of the Rockhouse Basin belt.

Mzp? Pampa Schist (Mesozoic?) -- dominantly dark pelitic schist and quartzo-feldspathic hornfels. The White River and Fountain Springs pendants are possibly correlative with the Pampa Schist to the south.

Mzt Tehachapi Metasedimentary belt (Mesozoic?) -- one irregular, but generally north-trending pendant and several related masses to the south, northeast, and northwest. Includes some bodies offset on the west side of the Kern Canyon fault. Also, tentatively included with this belt are several, as yet poorly studied, pendants (Mzt?) west of the Kern Canyon fault. The group includes a metavolcanic pendant with ash flow tuff (King George Ridge metavolcanic pendant -- shown as "Mztv"). The Tehachapi belt contains the usual siliceous, pelitic, and calcareous thin beds (some

rather massive marble). Extension of rocks formerly referred to as "Metasedimentary rocks of the Keene area" in the southernmost Sierra Nevada (Ross, 1989c).

DISCUSSION

The following comments on a wide variety of topics summarize geologic and chemical data not only from the area of Plate 1, but also from the entire southern Sierra Nevada. Basically, these discussions include topics, large and small, that either were not included in the previously listed open-file reports, or that represent ideas largely developed after their release.

Geologic relations

Relation of the Fairview pendant to the rest of the metamorphic section. The quartzitic turbidite (?) sequence of the Fairview pendant is unlike the metamorphic rocks both to the east and west (Ross, 1987a), the bulk of which are assigned to the Kings sequence of early Mesozoic age (Saleeby and others, 1987).

The unique Fairview pendant and its correlative quartzitic rocks form a giant lens among the metamorphic rocks to the east and west, particularly if some 10-15 kilometers of right-lateral displacement (Ross, 1986) are restored on the Kern Canyon fault (fig. 2). Although there is no direct evidence of the age of the Fairview rocks, the presence of volcanic layers and a possible volcanic component in some quartzite layers, as well as the proximity to the unique French Gulf pendant of metavolcanic rocks that contains some Fairview-like quartzite layers, suggests the Fairview-French Gulch "lens" is all of the same general age. Several radiometric dates on zircon about 100 Ma have been determined on metavolcanic rocks of the French Gulch pendant, and on hypabyssal intrusives, including vent breccias, in the Fairview rocks (Saleeby and Busby-Spera, 1986). Even though the hypabyssal rocks intrude the Fairview rocks, they may be relatively close to them in age.

If these are valid suggestions, the Fairview pendant is significantly younger than the Kings sequence and is closely related in age to the French Gulch volcanic rocks. However, my cursory field observations did not distinguish any significant stratigraphic breaks; Elan (1985) noted interbedding of metavolcanic and metasedimentary rocks in a detailed study of the contact between the French Gulch pendant and the Long Canyon pendant (a Kings sequence type) in an area north of Isabella Lake.

Rocks of the Fairview-French Gulch belt are generally of a lower metamorphic grade than the metamorphic rocks to the east and west, and also generally have less structural complexity. On rather sparse data I postulated a large open fold near the north end of the Fairview pendant, based largely on the strike of a series of marble lenses, and to a lesser extent on complementary attitudes in the associated quartzite (Ross, 1987a). This is in contrast to the complexly folded rocks to the east and west, for example in the main pendant of the Long Canyon metasedimentary belt (L.E. Weiss, unpublished data, cited in Saleeby and Busby-Spera, 1986). Busby-Spera (1983) has characterized the French Gulch rocks as dominantly greenschist-grade. Argillaceous layers in the Fairview pendant at the north end of the map area contain andalusite, but no sillimanite is seen. In contrast, sillimanite is common in the metamorphic rocks to the east and west. Some amphibolite-grade rocks are found in both the French Gulch and Fairview pendants, but, in general, the metamorphic grade is lower than in the adjoining metamorphic rocks to the east and west. In summary, the Fairview-French Gulch belt may be significantly younger than the other metamorphic rocks in the southern Sierra Nevada, which might account for the Fairview-French Gulch belt being less structurally complex than surrounding metamorphic rocks.

Are the Hatchet Peak and Portuguese Pass bodies original parts of the same granitic unit? The Hatchet Peak and Portuguese Pass are the only two bodies of relatively coarse-grained granitic bodies in the Southern Sierra Nevada. The bull's-eye map pattern and sparse radiometric data (Ross, 1987c) suggest that the Dunlap Meadow-Pine Flat masses (Plate 1) intruded and split apart these two texturally similar rocks. As such, they represent remnants of what was originally

one NNW-trending granitic unit.

The Hatchet Peak body has an average modal composition of granodiorite, whereas the Portuguese Pass body, by modal average, is a granite (fig. 3). Nevertheless, the two units have a considerable overlap of modal fields (fig. 3), and the vast majority of samples fall in the area of overlap. Interestingly, the four most "potassic" of the Portuguese Pass samples (those not in the overlap area) are in the south part of the mass, furthest from the Hatchet Peak rocks. The two most "calcic" samples from the Hatchet Peak mass are from the northern boundary of the map area, and one of the Reservation Road samples is similarly "calcic" (Table 1, sample 671OB). This fact suggests a regional "gradient" in the composition of the two bodies, certainly within the range of many granitic bodies in the region.

Reservation Road samples. A reconnaissance traverse along the Reservation Road just north of the map area (fig. 4) was helpful in delineating some granitic units along the north boundary of the map area where access is limited. Coarse-grained granitic rocks (6709, 6710), physically and modally comparable (Table 1) to samples from the granodiorite of Hatchet Peak (Ross, 1987d), suggest that the Hatchet Peak unit extends at least this far north and that it is continuous with outcrops to the south in the map area. The Reservation Road samples (6709, 6710) also have fine granular (probably quenched) quartz, also typical of some Hatchet Peak samples. However, the Reservation Road samples have less mafic minerals, particularly hornblende, than the Hatchet Peak samples. Further west, both a felsic and a mafic body were sampled (samples 6712, 6713, 6715, 6716, 6717), which do not appear to connect with granitic bodies to the south, being "blocked" by metasedimentary rocks of the Deer Creek pendant. Still further west, beyond the westernmost belt of the Deer Creek pendant, several samples (6719, 6721, 6722, and 6723) suggest compatibility with the tonalite of Zumwalt Ranch (see Appendix). Only one (6723) of the four samples is an undoubted Zumwalt Ranch correlative; the other three samples, though modally compatible with the Zumwalt Ranch unit (see Table 1), may be Deer Creek or Carver-Bowen correlatives (as suggested by field notes). With the presently sparse data, however, all four samples are tentatively correlated with the Zumwalt Ranch unit.

Tejon Canyon pendant. Ross (1987a) stated that the Tejon Canyon pendant is tentatively lumped with the mixed rocks and considered related to the mafic gneiss complex. New data suggest that this pendant is more closely allied to the Tehachapi metasedimentary belt. The dominance of thinly layered quartzite, marble, and argillaceous layers (some with sillimanite) is atypical of metasedimentary layers in the mafic gneiss complex, even if compared to the paragneisses of Comanche Point.

Field notes describe these rocks as: "lack of real gneiss" and "entirely different from gneiss terrane to west." Abundant migmatitic injections of sills and dikes of tonalite of Bear Valley Springs produce gneissic-looking rocks, but the overall lithologies and outcrop appearance are not compatible with the gneissic terrane to the west.

White River pendant. Proceeding west from Eclipse Hill to Grizzly Gulch (Plate 1), the typical lithology in the White River pendant, the large, irregularly shaped, metamorphic mass about 6 kilometers south of Fountain Springs, is gray "punky," thin- to medium-bedded, argillaceous, metasedimentary rock with abundant spots of micaceous material that suggests the former presence of andalusite. These rocks, probably typical of much of the pendant, are reminiscent of layers in the Pampa Schist (about 45 kilometers south of the pendant).

Elsewhere, particularly around the north end of the pendant, samples of tremolite schist, amphibolite, and amphibolite schist have been collected that are associated with White River metasedimentary types, but the relation is unclear. All may be related to the gabbroic rocks of the Quedow Mountain type, but they display extensive retrograde metamorphism. There seems to be no connection between these retrograded mafic rocks (?) and the metasedimentary rocks. However, the nearby presence of relatively large Quedow Mountain-like gabbronorite bodies (Bald Mountain and the Flynn Ranch mass) suggests that these regraded mafic rocks are remnants of the Quedow Mountain type that intrude into the White metasedimentary pile. Abundant localized gabbroic float on the east slope of Eclipse Hill is evidence for the small gabbroic mass mapped in the White River pendant on Plate 1.

Chemical relations

Chemical trends across the southern Sierra Nevada batholith. Chemical trends across the southern Sierra Nevada batholith were determined by projecting oxide values from located chemically analyzed granitic rocks onto two southwest- northeast-trending lines for areas north of and south of lat 35°30' N (fig. 5). A composite was compiled from these two lines for each oxide to show chemical trends at approximately right angles to the general trend of elongation of most plutons for the entire southern part of the batholith. The west part of the southern line is perhaps distorted by the anomalous east-west trend of the southernmost part of the Sierra block (San Emidgio and western Tehachapi Mountains) and particularly by the structurally disrupted granitic rocks south of the Garlock and Pastoria faults. Also, the eastern part of the northern line contains data from Triassic and Jurassic bodies that are chemically anomalous to the great bulk of the younger Cretaceous rocks. For this reason the composite section is modified for most oxides. The modified composite cross-section omits the Triassic and Jurassic samples, as well as those samples found south of the Pastoria and Garlock faults. Omitting these samples emphasizes the trend of relatively undisturbed Cretaceous granitic rocks across the southern part of the Sierra Nevada batholith. Chemical trends for the Triassic and Jurassic rocks cannot be determined because of the limited lateral extent of these older rocks.

The chemical trends noted in the following discussion may be unduly influenced by a relatively few samples at each end of the composite section, particularly when locating the "visually-estimated trend-line." Essentially, a few mafic samples on the west end and a few felsic samples on the east end "dictate" a trend across the great mass of central samples that would otherwise show no discernible trend for some oxides. (Note, for example, the modified composite plot for CaO in figure 13D.) Only the modified composite plot for K_2O (fig. 15D) and the oxidation ratio (fig. 6D) show unequivocal trends in the great bulk of central samples; these trends can be projected to the eastern and western samples.

The chemical parameters that are plotted are: oxidation ratio (ferrous-ferric iron ratio), SiO_2, Al_2O_3, Fe_2O_3, FeO, total iron (Fe_2O_3 + FeO), MgO, CaO, Na_2O, K_2O, and TiO_2. Some oxides such as Al_2O_3, Na_2O, and TiO_2 showed no visually apparent trend across the batholith; only a composite plot is shown to emphasize this lack of a trend. Perhaps the best trend is shown by the eastward increase of K_2O across the batholith. However, the oxidation ratio also shows a good eastward increase in the Cretaceous rocks. Further north, in the central Sierra Nevada, Bateman and Dodge (1970) and Bateman (1988) note a significant eastward increase in amounts of K_2O.

Oxidation ratios--Plotting the oxidation ratio [mol (2 Fe_2O_3 x 100 / 2 F_2O_3 + FeO)] for each of the chemically analyzed granitic rocks in the southern Sierra, shows a variation in the ferrous-ferric ratio. Both north and south cross-sections (fig. 6 A, B) show a discernibly progressive increase in the oxidation ratio eastward across the batholith, with a somewhat greater increase in the area north of lat 35°30' N. (fig. 6A). The data show considerable scatter with ratios ranging from 10 to 80. A visually estimated trend-line on the composite section ranges from about 15 on the west to about 50 on the east (fig. 6C). Particularly noticeable on the composite section are 10 samples (identified in fig. 6C) that have extremely high oxidation ratios (Table 2). These samples are spread throughout the width of the batholith. The anomalously high samples south of lat 35°30'N are all granites with low FeO; the amount of FeO is lower than Fe_2O_3 (unusual for southern Sierra Nevada granitic rocks). The rocks north of lat 35°30'N are similarly lower in FeO than Fe_2O_3, but have a much larger compositional range. Although all the samples selected for chemical analysis were "relatively" unweathered, there is noticeable alteration in some samples (particularly of biotite in the granites), which might contribute to these marked anomalies. Three of the anomalously high oxidation ratios are from the samples of Tejon Lookout, where the granite is, at the very least, somewhat altered through much of its outcrop area. The other high samples are single samples from the granites of Brush Mountain (3221), Bodfish (5071), Tehachapi Airport (4100A), and from the granodiorites of Alder Creek (6245), Castle Rock (6539), Deer Creek (6117), and Poso Flat (6292).

The Triassic and Jurassic granitic samples plot in distinct and separate fields on the composite cross-section for both Fe_2O_3 (ferric iron) and FeO (ferrous iron) (figs. 9A and 10A). However, on the plots for oxidation ratio (fig. 6A), these samples are mostly compatible with the progressively eastward increase of oxidation ratio across the batholith. Also, on the oxidation ratio plot south of lat 35°30'N, (fig. 6B) there is no clear difference between granitic samples north and south of the Pastoria and Garlock faults. There is considerable scatter at the west end of the cross-section, but most samples, both north and south of the faults, are relatively close to the visually-estimated trend-line. However, when points south of the Garlock and Pastoria Faults are omitted, along with omisssion of the Triassic and Jurassic samples, the plot (fig. 6D) has a slightly steeper increase to the east.

Dodge (1972) recorded a similar increase in the oxidation ratio from west to east across the central Sierra Nevada batholith. He suggests this variation may reflect a lower water content in the more western magmas. The variation in water content may have been due, in part, to deeper levels of magma generation for the more western magmas. Dodge (1972) further suggests that it is equally likely that variation in water content reflects westward changes in source materials for the magmas. Either westward increase in relatively mafic volcanic and anhydrous volcanogenic sedimentary material, or westward increase in relatively anhydrous mantle-derived material seems a likely cause of water variation.

SiO_2--The composite plot of all the silica values from the granitic samples of the southern Sierra Nevada shows a broad belt of points with no discernible change across the batholith (fig. 7C). However, there is a somewhat systematic west-east increase in SiO_2 (fig. 7D) if Triassic and Jurassic samples on the east side and the samples south of the Pastoria and Garlock faults are omitted from the plot (as indicated on figs. 7A and 7B). Even though the end points of this trend-line are constrained by very few samples, and this is a visually estimated line, there is a definite suggestion of an eastward increase in SiO_2 in Cretaceous rocks across the batholith. This trend would be predicted from the geologic map, as the dominantly tonalitic rocks on the west

give way to more silicic granodiorite and granite on the east.

Table 2. Anomalously high oxidation rates

Sample	Fe_2O_3	FeO	Oxidation ratio
Granite			
Tejon Lookout (3401)	1.4	0.5	72
Tejon Lookout (3466)	1.2	0.5	70
Tejon Lookout (3752A)	1.1	0.3	78
Brush Mountain (3221)	0.9	0.2	80
Bodfish (5071)	0.6	0.3	67
Tehachapi Airport (4100a)	0.6	0.4	63
Granodiorite			
Alder Creek (6245)	3.1	1.2	69
Castle Rock (6539)	1.2	0.5	70
Deer Creek (6117)	1.2	1.0	53
Poso Flat (6292)	2.8	1.5	63

Note that all but one (Deer Creek - 6117) of the samples with anomalously high oxidation ratios are also anomalous on the plot of oxidation ratio against magnetic susceptibility (fig. 6E). This latter plot further emphasizes that the 10 samples with very high oxidation ratios are probably more altered than they appear to be.

Al_2O_3--The Al_2O_3 values, ranging from 12.7 to 20.8 percent, show no noticeable trend across the batholith (fig. 8). The Triassic and Jurassic granitic rocks at the east end of the composite section have generally higher values than geographically related Cretaceous samples, whereas on the

west side of the batholith there is overlap of Al_2O_3 values for samples on opposite sides of the Garlock and Pastoria faults. With its wide spread of values, Al_2O_3 is a poor indicator of pattern or variation across the batholith.

Fe_2O_3--Fe_2O_3 values produce on the composite plot a somewhat subtle increase eastward across the batholith (fig. 9A). Part of the "subtlety" of the trend concerns the easternmost granitic rocks. The ferric iron values for these rocks basicly group into two clusters (fig. 9B). The lower cluster includes the samples from the granite of Five Fingers and one sample of the granodiorite of Castle Rock that is far removed from other analyzed samples of Castle Rock. This lone sample, however, is representative of a large body of rock that may or may not be correlative with the great bulk of the Castle Rock. These samples represent the easternmost Cretaceous units of the batholith. The higher cluster, the samples richer in ferric iron, is from the Triassic and Jurassic units, which dominate the northwest corner of the map area. A visual trend-line can be drawn though either the lower or upper cluster. The trend-line including the lower cluster passes through, or relatively near, the greatest number of samples. As such, it probably represents the trend of ferric iron in the Cretaceous part of the batholith. The higher level of ferric iron in the eleven Triassic and Jurassic samples suggests a "steeper" ferric iron trend for these older batholithic rocks, but the slope of the trend-line cannot be determined because no older rocks are present to the west. The Fe_2O_3 values in granitic rocks on the west side of the batholith (fig. 9C) do not permit a ready separation of samples located north and south of the Pastoria and Garlock faults, as is evident from other oxides. Some of the rocks to the south of these faults are definitely below the visually estimated trend line; but most samples, both north and south of these faults, fall near the trend-line.

FeO--Omitting the eleven Triassic and Jurassic samples, there seems to be a subtle FeO decrease in rocks toward the east (fig. 10A). Though diffuse, this trend is also evident within the northern cross-section (fig. 10B). The marked separation of rocks by the Pastoria and Garlock faults, which is so evident for some oxides, does not seem to be significant for FeO on the south section

(fig. 10C). Excluding the samples south of the Pastoria and Garlock faults, an eastwardly decreasing trend can be visualized on figure 10C; but the sample distribution here is even more diffuse than it is on the northern section. A trend-line from the Tehachapi Mountain samples on the west, to the Five Fingers samples on the east, shows an even sharper eastward decrease in FeO. However, the trend-line on figure 10A encompasses even more points. The above waffling suggests that FeO is not a very sensitive indicator of compositional change across the batholith. Bateman and Dodge (1970) reported an eastwardly decrease in FeO in the central Sierra Nevada, but in their figure 3, the trend is subtle, at best.

Total iron (Fe_2O_3 + FeO)--To check for a systematic variation in total iron across the southern Sierra Nevada, the sum of Fe_2O_3 + FeO for each of the chemically analyzed samples of the granitic rocks was projected onto the cross-sections. The resulting plots (figs. 11A, and 11B) are scattered. A spread of 1 to 8 percent total iron oxides is evident throughout the width of the batholith. However, the composite plot of these data (fig. 11C), with proper imagination, has some suggestion of an eastward increase. This trend, however, may be more apparent than real. On the east side of the north section (fig. 11A) the sampling is dominated by relatively iron-rich Triassic and Jurassic granitic rocks. On the west side of the south section (fig. 11B) the relatively iron-poor granodiorites and granites south of the Garlock and Pastoria faults are structurally separated from the more iron-rich samples in the relatively in-place Sierra Nevada block. If these possibly anomalous samples from the north and south sections (figs. 11A, and 11B) are eliminated, a modified composite plot (fig. 11D) shows an eastward decrease in total iron oxides across the batholith, the opposite of the suggested eastward increase in the unmodified composite section (fig. 11C). Total iron decrease to the east is more logically based on the rock type distribution of tonalites dominant on the west and granodiorites and granites dominant further east, at least for the Cretaceous granitic bodies (the bulk of the batholith at this latitude).

MgO--The composite plot of MgO values (fig. 12C across the southern Sierra Nevada batholith follows a common pattern with anomalous values for the structurally displaced samples on the

west side of the south section (fig. 12B) south of the Pastoria and Garlock faults. Also on the east side of the batholith the values of the Triassic and Jurassic granitic rocks are distinctly separated from, and higher than the Cretaceous values (fig. 12A). If the Triassic and Jurassic MgO values as well as the ones south of the Pastoria and Garlock faults are expunged, there is a marked eastward decrease in MgO across the batholith for the Cretaceous granitic rocks. The central Sierra Nevada batholith shows a somewhat more subtle decrease in MgO to the east (Bateman and Dodge, 1970). The decrease is illustrated by a least-squares line; a visually-estimated trend-line through the data would seem hard to draw!

CaO--The pattern of sample distribution for CaO, not surprisingly, more-or-less mimics the pattern of MgO (fig. 12). The composite plot (fig. 13C) shows a diffuse belt of points with no readily obvious trend, but when the structural dislocated samples south of the Garlock and Pastoria faults (fig. 13B) and the Triassic and Jurassic samples on the east (fig. 13A) are removed, a trend of decreasing CaO to the east across the batholith is evident (fig. 13D). This also is predictable from the rock distribution, with more of the anorthitic fraction in the feldspar and rocks richer in hornblende both more abundant in the west. Bateman and Dodge (1970) also note a similar eastward decrease across the central part of the Sierra Nevada batholith, but the plot of points used to define the least squares line, to me, has no readily discernible pattern (certainly no obvious visual trend-line could be drawn through those data).

Na_2O--A composite plot of Na_2O values (fig. 14) shows that Na_2O has no discernible trend across the batholith. Soda is notoriously non-responsibe with regard to age, variation in rock type, or geographic position in most common granitic rock types. Irregardless of age (Triassic, Jurassic, or Cretaceous) or structural position (south or north of the Pastoria and Garlock faults) soda extends across the southern part of the Sierra Nevada batholith in a narrow range of values of mostly 3 to 4 volume percent (more than 100 samples fall in this range out of a total of 134 samples).

K_2O--K_2O increases eastward on both the north (fig. 15A) and south (fig. 15B cross-sections.

The eastward increases in K_2O are reflected as much by the great central bulk of the samples as by the two "end-members." This eastward increase in K_2O in the central concentration of samples is also evident in the composite plot (fig. 15C). The eastward increasing trend-line is even more evident in the modified composite plot (fig. 15D) where the samples from the Triassic and Jurassic rocks and the structurally displaced bodies south of the Pastoria and Garlock faults are deleted.

K_2O is perhaps the best oxide for reflecting change across the south part of the Sierra Nevada batholith. Bateman and Dodge (1970) also noted that K_2O convincingly decreases westward across the central part of the Sierra Nevada batholith. In my opinion K_2O is the only oxide in the central Sierra Nevada with a clearly evident "visual" trend.

TiO_2--The composite belt of TiO_2 values shows much scatter with no obvious trend (fig. 16). The common separation on the east side of Triassic and Jurassic samples from the Cretaceous samples for most oxides is not clear cut for TiO_2. Likewise, on the west there is no clear distinction between the samples north and south of the Garlock and Pastoria fault.

The general compositional change eastward across the batholith from dominantly tonalite to dominantly granodiorite and granite is not reflected by TiO_2. Granites have less TiO_2 (an average of 0.2 percent) but there are relatively few granite samples. The great bulk of the granitic samples are granodiorite, tonalite, and quartz diorite, which all average about 0.6 percent TiO_2 in the southern Sierra Nevada.

Average chemical composition of granitic rocks, southern Sierra Nevada, California. Chemical analyses of 133 granitic rocks ranging in composition from quartz diorite to granite were determined and reported in Ross (1988b). As a supplement to that report, average composition data are presented here for each rock type (granite, granodiorite, tonalite, and quartz diorite) as well as an average composition for the granitic rocks as a whole. The samples selected for

chemical analysis were chosen to represent the modal range and the areal extent of the large bodies. For smaller plutons commonly only one, hopefully representative, sample was analyzed. In most cases unweathered samples were selected. The analyzed samples are probably a fair representation of the composition of the various plutons, but no statistically significant coverage was attempted.

More samples were analyzed from the larger plutons, but there was no attempt to sample strictly proportionally to the areal extent of the various plutons. The weighted averages on Table 3, which take in to account the areal extent of each sampled pluton are not significantly different from the raw averages.

In the oxide averages for all the rock types the variation between raw and weighted averages rarely exceeded 0.2 percent. Exceptions are the weighted average of SiO_2 in the granite which is 0.5 percent lower that the raw average, and the weighted averages of SiO_2, Al_2O_3, Fe_2O_3, Na_2, and K_2O in the quartz diorite which are from 0.3 to 0.4 percent greater that the raw average, and the weighted average of FeO which is 0.8 percent lower. The overall oxide averages of all granitic rocks by both methods are almost identical.

One of the conventions in calculating these averages by rock type was to assign all analyses of each pluton to the rock type represented by the modal average of that pluton. Some modal averages were marginal, particularly between granite and granodiorite. Silica variation ("Harker") diagrams of all oxides (fig. 17) are as expected with all oxides except SiO_2, K_2O, and Na_2O decreasing from quartz diorite to granite. Na_2O has virtually no variation across the compositional range.

Not all plutons in the southern Sierra Nevada were chemically analyzed, but most of those not analyzed are small and their omission probably does not markedly affect the average granitic compositons. Of unknown, but possibly of significant extent are granitic rocks within the mafic gneiss complex and the "transition zone." These are mostly mafic tonalites and quartz

diorites and their omission may somewhat skew an average composition toward the more felsic end of the granitic spectrum.

Daly (1933) compiled data on the average composition of various igneous rock types. His average granodiorite is very close to the average southern Sierra Nevada rock. This is predictable as granodiorite is predominant in the southern Sierra Nevada. It also suggests that the southern Sierra Nevada granitic rocks are comparable to average crustal granodiorite.

Many estimates have been made of average crustal abundance of igneous rocks. Granite and granodiorite are dominant components of these averages as Daly (1933) suggested that the "areal abundance of granite and granodiorite is more than 20 times that of all other intrusives combined." Gilluly (1954), in calculating the composition of continental plates, has suggested that Kuenen's estimate of average igneous rock is perhaps the most realistic, although Gilluly noted that the inclusion of "simatic" rocks from ocean basins results in an average that is probably too low in SiO_2 to represent average continental crust. The southern Sierran rocks are 5.5 percent higher in SiO_2, 2.8 percent lower in total iron, and 1.5 percent lower in MgO than Kuenen's (1941) average. This suggests, as Gilluly (1954) noted, that Kuenen weighted mafic (oceanic?) igneous rocks too greatly in his average igneous crustal rock. Perhaps a better average igneous crustal estimate is that of Vogt ((1931) which is within 1 percent of the southern Sierran averages for all oxides (Sierran granitic rocks are somewhat higher in SiO_2 and Al_2O_3, lower in total iron, MgO, and K_2O, and virtually identical in Na_2O, CaO, and TiO_2).

These somewhat dated abundance estimates may change somewhat with the addition of more modern chemical data, but probably not significantly. The southern Sierra Nevada rocks are probably a good representative of average continental crust.

Rubidium and strontium in granitic rocks. Rubidium and strontium values and strontium isotopic ratios have been determined on about 240 samples of granitic rocks from the southern Sierra Nevada. The data reported here are abstracted from a more comprehensive report on rubidium

and strontium by Kistler and Ross (in press).

The range and average of rubidium and strontium for each sampled pluton are shown in Table 4. Rubidium is least abundant in the quartz diorite samples (generally 20-50 ppm), more abundant in the tonalites (50-75 ppm) and the granodiorites (75-100 ppm), and most abundant in the granites (150-175 ppm). Strontium has a much wider range of values as can be seen by the histograms of the distribution of values for each rock type (figs. 18 and 19) and does not show a progressive change by rock type as does rubidium. The areal distribution of rubidium and strontium, based on pluton averages, is shown on generalized geologic index maps of the southern Sierra Nevada (figs. 20 and 21). Table 4 also shows the initial strontium ratio (Sri) for each sampled pluton. A similar index map shows the pattern of the initial strontium ratio (Sri), based on pluton averages, for the southern Sierra Nevada (fig. 22). This index map shows a general northeast increase in Sri (with some exceptions, most notably by the "out of place" low values of the Triassic quartz diorite of Walker Pass). Figure 22 also shows the rather abrupt change in Sri values from below 0.706 to the west and above 0.706 east of a discontinuous belt of metasedimentary pendants that trend more-or-less southerly from lat 36°00' N, long 118°50' W to the Garlock fault. The metasedimentary belt marking the Sri "break" is more graphically shown on fig. 25.

A variation diagram plotting strontium (in ppm) against the ratio of rubidium to strontium (fig. 23) reflects the rather wide range of the rubidium-strontium ratio in the granites, the more restricted range in granodiorites, and the rather low ratios for tonalites and quartz diorites, which reflects the relatively low rubidium values for these compositions (fig. 18).

The previously described figures 20, 21, and 22 all demonstrate the eastward increase in rubidium, strontium, and the Sri across the batholith based on average values from each sampled pluton. The eastward progression of values is only interrupted by relatively low values in Triassic plutons near the east front of the Sierra Nevada and in a relatively small body south of Isaabella Lake, whose locations are shown on fig. 25.

The position of the 0.706 Sri line in the Sierra Nevada has traditionally been considered the boundary between plutons intruded into crystalline Precambrian crust east of this line (Sri > 0.706) and plutons intruding more oceanic primitive crust west of the line (Sri < 0.706). In other words, west of the 0.706 line plutons are largely mantle-derived, and east of the line plutons have some component of crustal contamination (Kistler, in press).

Recent work by Kistler (in press) suggests that the Sri 0.706 line is not the sole criterion in this crustal distinction. He notes that two distinct lithospheric types underlie the Sierra Nevada. One has Proterozoic crystalline basement (North American lithosphere) and the second (Panthalassan lithosphere) consists largely of oceanic crust that encroaches on and was subducted beneath western North America in the early Mesozoic. Plutons intruding Panthalassan lithosphere can also have an Sri greater than 0.706, having acquired that character by assimilating sedimentary material that was deposited on top of the oceanic crust. Plutons with Sri greater than 0.706 and with $\delta^{18}O$ greater than +9 per mil SMOW suggest significant sedimentary contamination and derivation through Panthalassan lithosphere. Figure 24 shows the distribution of plutons in the southern Sierra Nevada with those characteristics. Kistler also suggests that plutons with Sri less than 0.706 and Rb less than 100 ppm are characteristic of Panthalassan lithosphere. Plutons in the southern Sierra Nevada that meet these criteria are shown on fig. 25.

These criteria along with the available $\delta^{18}O$ and Rb and Sr data from the southern Sierra Nevada, indicate that all the plutonic rocks were derived from Panthalassan lithosphere except the granodiorite of Sacatar whose characteristics suggest derivation through North American crystalline basement.

Regardless of the validity of Kistler's two-fold crustal model, the fact remains that the strong Sri discordance east of the western belt of tonalites and dark granodiorites (marked by the discontinuous belt of metasedimentary pendants) is a most striking and significant marker horizon in the southern Sierra Nevada.

Ideally each pluton would show a pronounced linear trend (isochron) on an Rb-Sr evolution diagram. An example is the tonalite of Dunlap Meadow (fig. 26B) where several samples produce an isochron that projects to a rather well-constrained initial strontium ratio. In contrast, some equally mappable and coherent plutons show a wide spread of points on the Rb-Sr evolution diagram as for example does the tonalite of Bear Valley Sprints (fig. 26A). From this plot no isochron or initial ratio is readily apparent. Both the Dunlap Meadow and Bear Valley Springs bodies are similar physically and chemically and during early stages of mapping were considered correlative. Their ages may or may not be the same. Several U-Pb determinations on zircon from the Bear Valley Springs unit gave an average of 100 ma (Sams, 1986), within the range of the age interpretation of the Dunlap Meadow pluton (91.4±11.3 Ma). However, these similar tonalites have much different Rb-Sr signatures. The Bear Valley Springs unit covers a much larger area, however, and may be composite, accounting for some of the variability in fig. 26A. Nevertheless, the supposition that each pluton has a distinct initial strontium ratio does not seem to hold true for the Bear Valley Springs body, nor for several other plutons in the southern Sierra Nevada.

Granite of Little Lake. The Little Lake granitic body east of the Sierra Nevada fault was not examined during my reconnaissance of the southern Sierra Nevada, but a sample was collected near the west edge of the body for Rb/Sr and K/Ar age determinations (Kistler and Peterman, 1978). It is not known whether the sample is representative of the body. The sample has been described as "foliated porphyritic biotite quartz monzonite (granite by the new IUGS classification) outcropping on the east side of U. S. Highway 395 at the Little Lake turnoff on the road to the Lower Little Lake Ranch, Kistler and Peterman, 1978)." Close proximity to the large mass of the Sacatar unit to the west suggests possible similarity, but neither the sample description nor the chemical analysis is similar to the Sacatar.

The physical description and especially the chemical analysis are much like the Jurassic Paiute Monument Quartz Monzonite (IUGS = granite) Ross (1969) described in the Inyo Mountains to the north. The Little Lake chemical analysis is almost identical with an average of

two chemical analyses from the Paiute Monument mass (Table 5). Granite presumably correlative with the Paiute Monument mass also crops out between Little Lake and the Inyo Mountains in the Darwin area (Hall and MacKevett, 1962).

Cataclasis

Distribution of cataclasis in the southern Sierra Nevada. Cataclasis in the southern Sierra Nevada ranges from minor granulation to highly developed mylonite and ultramylonite. Cataclasis was noted in the course of reconnaissance geologic mapping and mostly in later petrographic studies, and a systematic search for cataclastic rocks was only pursued along the Kern Canyon-Breckenridge-White Wolf fault zone (Ross, 1986).

Even in this largely random collection of cataclastic data it became apparent that there were certain linear zones along which cataclasis was concentrated (fig. 27). Not surprisingly, these concentrations were largely along previously known faults such as the Kern Canyon-Breckenridge-White Wolf fault zone, the Sierra Nevada fault, and the north branch of the Garlock fault.

Another linear zone became apparent as the study proceeded. A somewhat sinuous north-south alignment of, in part, strongly mylonitized rocks, extends from the Kern Canyon fault at the latitude of Isabella Lake south to the Garlock fault. A bifurcation in the north part of this alignment is suggested both by the distribution of cataclastic rocks and the matching of similar-appearing metamorphic rocks. The "split" is apparently caused by the intrusion of the intervening younger granitic rocks. Near its south end, the north-south zone appears to bulge out to the west. Here strongly mylonitized tonalites form a mappable cataclastic envelope around a metasedimentary pendant (Ross, 1989c). Saleeby and Busby-Spera (1986) have referred to at least the northern part of the north-south zone as the "proto-Kern Canyon fault." The structure and the rock type distribution suggest that this north-south zone is a fundamental crustal feature in the southern Sierra Nevada. It marks a contact between largely tonalite on the west with largely granodiorite and granite on the east.

Saleeby and Busby-Spera (1986) further suggest that major basement movement on the Kern Canyon Faults continues only as far south as the Isabella Lake area where major basement movement is "transferred" to their proto-Kern Canyon fault (the north-south zone-2 on fig. 27). Basement offset of 10-20 kilometers in a right-lateral sense continues south almost to the latitude of Caliente (Ross, 1986), but further south the magnitude of the offset on the Kern Canyon-Breckenridge-White Wolf fault zone is problematical, and outcrops of cataclastically deformed rocks were not seen.

In addition to the general linear belts of cataclasis, there are abundant cataclastic rocks throughout the mafic gneiss complex north of the Garlock fault in the east-west-trending southernmost tip of the Sierra Nevada.

In the main bulk of the southern Sierra Nevada basement west of the Kern Canyon-Breckenridge-White Wolf fault zone and east of the north-south zone (on fig. 27) the basement appears to be largely undeformed on any major scale.

Quartz vs feldspar remnants in strongly fluxion-textured rocks. Just north of Isabella Lake some metavolcanic rocks have a strong fluxion texture and in the field were called "mylonite." Subsequent thin-section showed the common preservation of angular quartz fragments in these rocks, suggesting that they are volcanic tuffs, most commonly ash-flow tuffs, and not mylonite, where quartz is generally selectively milled down and rarely, if ever, preserved in angular fragments larger than those in the groundmass.

Janecke and Evans (1988) have suggested that, in southeast Arizona, temperature and pressure conditions were such that massive granitic rocks were deformed and transformed into "quartz-mica phyllonite" where quartz was preserved as augens in a matrix of strongly deformed and altered feldspar. Thus, in some conditions, quartz can apparently be selectively preserved in a strongly deformed cataclastic rock.

In the southern Sierra Nevada, quartz is not selectively preserved in mylonitic rocks

derived from undoubted granitic rocks; larger augen and other lozenge-shaped remnants are invariably feldspar. This suggests metamorphic conditions leading to widespread production of mylonite in the southern Sierra Nevada probably also applied to cataclasis of the associated volcanic rocks and that selective preservation of quartz would not be expected. Yet Saleeby and Busby-Spera (1986) refer to some of the metavolcanic rocks north of Isabella Lake as "phyllonites"; and I have been perplexed by some thin zones of fluxion textured rocks in the quartz diorite of Cyrus Flat that preserve small quartz clasts giving the rock the appearance of tuff, but the protolith of these rocks was almost surely granitic rock.

Preservation of coarser quartz clasts in fluxion-textured rocks does not prove that such rocks are not cataclastic, and consequently careful work is needed to sort out the origin and derivation of fluxion-textured rocks in the southern Sierra Nevada.

Miscellaneous

Distribution of aluminosilicates. One notable characteristic of the southern Sierra Nevada is the widespread occurrence of coarser prismatic sillimanite across the entire width of the range (fig. 28). Sillimanite is conspicuously absent from the mafic gneiss complex, however. Undoubtedly this is at least in part due to the lack of suitable aluminous metasedimentary rocks in the complex; but rather quartz-rich rocks elsewhere in the area are hosts for sillimanite, and similar lithologies are also a minor part of the mafic gneiss complex. In the Tejon Creek pendant just east of the complex, sillimanite is abundant, and sillimanite is also present just east of the complex south of Mountain Park. The rather abrupt appearance of sillimanite just east of the complex suggests possibly that metamorphic grade, or some other factor rather than lack of suitable host rocks, is the main reason for the absence of sillimanite in the mafic gneiss complex.

The aluminosilicates sillimanite and andalusite are both widely distributed in the southern Sierra Nevada, and in many samples these two aluminosilicates coexist. Cordierite has only been positively identified near lat 35°45'N and long 118°00'W, but suspicious crystals and "pinitic" alternations are found at several places, but are largely limited to the north half of the map area.

Coexisting sillimanite and andalusite are particularly common in the Long Canyon Formation. The Pampa Schist, on the west margin of the Sierra Nevada, also hosts abundant sillimanite and andalusite. Particularly well developed are coarse chiastolitic andalusite crystals in dark fine-grained pelitic rocks atypical of the southern Sierra Nevada. The only other common occurrence of such dark pelitic chiastolite rocks is in the Bean Canyon Formation south of the Garlock fault.

South of the Garlock fault only andalusite is present in the framework metamorphic rocks (Bean Canyon Formation) of the granodiorite of Gato-Montes, whereas only sillimanite is present south of the Pastoria fault in the wall rocks (Salt Creek Formation) of the granodiorite of Lebec, a presumed correlative of the Gato-Montes mass. The framework formations of these two granodiorites are different lithologically and also may be different in matamorphic grade. The dark-colored fine-grained graphite-bearing layers of the Bean Canyon Formation are ideal hosts for andalusite and suggest lower metamorphic grade than the coarser sillimanite-and-garnet-bearing schists of the Salt Creek Formation.

Magnetic susceptibility pattern of area shown on Plate 1. Magnetic susceptibility patterns for the granitic rocks of the southern Sierra Nevada based on averages for each unit have been published by Ross (1989a). In the present report, the magnetic susceptibility values for individual samples of granitic rocks in the area of Plate 1 are contoured (fig. 29) without regard for plutonic contacts. The contour intervals are: 0-100, 100-1000, 1000-2000, 2000-3000, and all values above 3000 x 10^{-5} siu. The contours were somewhat generalized, some minor anomalies were omitted, but some scattered magnetic susceptibility values were retained that are significantly higher than most surrounding values. These are shown as "hot spots" on fig. 29. The anomalously high spots reflect local relative concentration of magnetite in some specimens, and are of no great significance. These spots, scattered throughout the map area, are perhaps more abundant in the granodiorite of Sacatar in the northeast part of the area, and in the western tonalites where their values of 2000 to 4000 x 10^{-5} siu contrasted strongly with the susceptibility background of 100 to 1000 x 10^{-5} siu. The gross distribution pattern of fig. 29 is somewhat

similar to that of the north part of fig. 1 in Ross (1989a), which is based on average values of plutons. Apparently, plotting either unit averages or individual sample values gives essentially the same magnetic susceptibility pattern.

Perhaps the most significant feature of fig. 29 is the paucity of values above 2000 x 10^{-5} siu west of the Kern Canyon fault, contrasted to the much greater extent of such values east of the fault. The higher values also extend much further south on the east side of the fault. Values below 100 x 10^{-5} siu (virtually non-magnetic) are conversely much better represented west of the Kern Canyon fault and extend further north, reflecting the right-lateral offset of basement rocks across that fault.

The "rib" of relatively high values (+3000 x 10^{-5} siu) east of, and parallel to, the Kern Canyon fault is controlled by only a relatively few samples of the granodiorite of Castle Rock, and its significance is not obvious. This example suggests caution in interpreting the significance of minor features on fig. 29. One major feature fig. 29 does reflect is the contrast between the low magnetic susceptibility values of the largely tonalitic terrane to the west and the higher values in the granite and granodiorite terrane to the east.

Summary statement on the mafic gneiss complex in the southernmost Sierra Nevada, California.

The mainly mafic orthogneisses of the mafic gneiss complex cover a large area extending from near the west end of the San Emidgio Mountains eastward to the vicinity of Tejon Creek and Comanche Point (Ross, 1987c). These rocks were first mapped by Wiese (1950) in the Neenach quadrangle where he called them chiefly diorite, gabbro, and gneiss. A reconnaissance of the complex by Ross (1980, 1983 a,b, 1985) grossly divided it into mafic gneiss to amphibolite, felsic gneiss--transitional zone between the gneisses and tonalite to the east, and a distinctive quartz diorite in the San Emigdio Mountains. In addition, scattered through the mafic gneiss in particular, were relatively homogeneous generally hornblende-rich quartz diorites that were considered a petrographic unit but were not mapped, as discrete bodies were hard to differentiate in the complex.

At about the same time, more detailed investigations were carried on in the eastern part of the complex by Sharry (1981) and Sams (1986). They differentiated several units in the complex (fig. 30). Their two maps have some general similarities, particularly in the distribution of their White Oak, Bison Peak, and Tunis Creek units. Nevertheless, except for the White Oak unit, there are significant differences in the unit distribution in the area common to the two maps. This is not meant as a criticism of either or both of the maps, but rather to point out that defining map units in this complex, where exposures are not always excellent, is a problem that these two maps exemplify.

The samples I collected from the mafic gneiss complex (Ross, 1983b) generally fall into three metamorphic types (amphibolite, tonalitic gneiss, and quartzofeldspathic gneiss). The distribution of these samples is shown on fig. 31. The pattern of the distribution of these three units does not show any ready segregation into map units, but rather points out the general "mixing" so characteristic of the complex. The location of these same samples is also superposed onto a generalized map of the area of Sams (1986). The result (fig. 32), not surprisingly, shows all three lithologies scattered throughout Sams' map units with no obvious correlation with specific map units.

Some general comparisons of the units of Sams (1986) and Ross (1980) are possible. The hypersthene tonalite of Bison Peak (Sams, 1986) is probably closely related to the tonalite of Bear Valley Springs (Ross, 1980). The Bison Peak unit is more deformed and contains more widespread hypersthene, but both deformed and hypersthene-bearing rocks are found in the Bear Valley Springs unit. Also both are essentially 100 Ma (Sams, 1986). The "transition unit" (Ross, 1980) in part corresponds to the Bison Peak unit. The diorite gneiss of White Oak (Sams, 1986), as well as most of the metagabbro of Tunis Creek, the metagabbro of Squirrel Spring, and part of the tonalitic gneiss of Tejon Creek are amphibolite to amphibolite gneiss and correspond somewhat to the "dark gneiss." Gneisses of the Tejon Creek unit of tonalitic composition also correspond to the "dark gneiss" (Ross, 1980). The quartzo-feldspathic gneiss of Pastoria Creek and the paragneiss of Comanche Point are gneisses generally of granodiorite and granite composition and correspond to the "felsic gneiss" (Ross, 1980).

The foregoing discussion indicates the difficulty of defining map units in this complex. Perhaps more viable units can be mapped in this complex with detailed work. My suspicion is that more detailed mapping may produce more, rather than less, evidence of the complicated relations between rock types. A large-scale map of a small, well-exposed (if possible) pilot area might be worth pursuing to see what can be determined. The major petrographic units in the mafic gneiss complex are generally well agreed upon by various workers (although commonly given different names), but the basic distribution pattern of various units remains enigmatic.

My overall impression from field work and petrographic examination of many samples suggests that "complex" fairly accurately describes this group of mostly mafic rocks and that attempts to date to subdivide it into mappable units (Wiese, 1950; Ross, 1980; Sharry, 1981; and Sams, 1986) are merely good starts. The frustrating problems of mapping units in the mafic gneiss complex in the field and later trying to sort out igneous from metamorphic textures in thin section study are probably best typified by a statement by Sams (1986) in which one of his field units is distinguished from its neighbors by its "uniform heterogeneity" -- somehow that seems to say it all.

REFERENCES CITED

Bartow, J.A., and Doukas, M.P., 1978, Preliminary geologic map of the southeastern border of the San Joaquin Valley, California: U.S. Geological Survey Miscellaneous Field Studies Map MF-944, scale 1:125,000.

Bateman, P.C., 1988, Constitution and genesis of the central part of the Sierra Nevada, California: U.S. Geological Survey Open-File Report 88-382, 188 p.

Bateman, P.C., and Dodge, F.C.W., 1970, Variations of major chemical constituents across the central Sierra Nevada batholith: Geological Society of America Bulletin, v. 81, p. 409-420.

Bergquist, J. R., and Nitkiewicz, A.M., 1982, Geologic map of the Domelands Wilderness and contiguous roadless areas, Kern and Tulare Counties, California: U.S. Geological Survey Miscellaneous Field Series Map, MF 1395-A, scale 1:48,000.

Best, M.G., and Weiss, L.E., 1964, Mineralogical relations in some pelitic hornfelses from the southern Sierra Nevada, California: American Mineralogist, v. 49, p. 1240-1266.

Bruce, J.L., 1981, Geology of the eastern portion of the Indian Wells Canyon mining district, Kern County, California (unpublished M.S. thesis): Reno, University of Nevada.

Busby-Spera, C.J., 1983, Paleogeographic reconstruction of a submarine volcanic center: Geochronology, volcanology, and sedimentology of the Mineral King roof pendant, Sierra Nevada, California (unpublished Ph.D. thesis): Princeton, Princeton University.

Chen, J.H., and Moore, J.G., 1979, Late Jurassic Independence Dike swarm in eastern California: Geology, v. 7, no. 3, p. 129-133.

Daly, R.A., 1933, Igneous rocks and the depths of the earth: New York, McGraw-Hill, 508 p.

Diggles, M.F., 1984, Peraluminous granite from the southern Sierra Nevada, California: Geological Society of America Abstracts with Programs, v. 16, no. 5, p. 278.

Diggles, M.F., Dellinger, D.A., and Conrad, J.E., 1987, Geologic map of the Owens Peak and Little Lake Canyon wilderness study areas: Inyo and Kern Counties, California: U.S. Geological Survey Miscellaneous Field Studies Map MF-1927-A, scale 1:48,000.

Dodge, F.C.W., 1972, Variation of ferrous-ferric ratios in the central Sierra Nevada batholith, U.S.A.: International Geologic Congress, 24, section 10, Proceedings, p. 12-19.

du Bray, E.A., and Dellinger, D.A., 1981, Geology of the Golden Trout Wilderness, California: U.S. Geological Survey Miscellaneous Field Studies Map MF-1231-A, scale 1:48,000.

Duffield, W.A., and Bacon, C.R., 1981, Geologic map of the Coso volcanic field and adjacent areas, Inyo County, California: U.S. Geological Survey Miscellaneous Investigation Series Map I-1200, scale 1:50,000.

Elan, Ron, 1985, High-grade contact metamorphism at the Lake Isabella north shore roof pendant, southern Sierra Nevada (M.S. thesis): Los Angeles, University of Southern California, 202 p.

Evernden, J.F., and Kistler, R.W., 1970, Chronology of emplacement of Mesozoic batholithic complexes in California and western Nevada: U.S. Geological Survey Professional Paper 623, 42 p.

Fox, L.K., 1981, Compositional variations and implications of petrogenesis of the Kernville pluton, southern Sierra Nevada, California (unpublished thesis): Princeton, Princeton

University, 77 p.

Geraci, Jeffrey; Fischer, Patrick, and Dunne, George, 1987, Indian Wells Canyon roof pendant, southeast Sierra Nevada, California: Another fragment of the Paleozoic Cordilleran eugeocline?: Geological Society of America Abstracts with Programs, v. 19, no. 6, p. 381.

Gilluly, James, 1954, Composition of the continental plates: Tschermaks mineralogische und petrographische mitteilungen, Band 4, Heft 1, s. 360-369.

Hall, W.E., and MacKevett, E.M., Jr., 1962, Geology and ore deposits of the Darwin quadrangle, Inyo County, California: U.S. Geological Survey Professional Paper 368, 87 p.

Harner, J.L., Chaffee, M.A., Seitz, J.F., and Capstick, D.O., 1983, Mineral resource potential of the Scodies roadless area, Kern County, California: U.S. Geological Survey Open-File Report 83-510, 14 p.

Janecke, S.U., and Evans, J.P., 1988, Feldspar-influenced rock rheologies: Geology, v. 16, no. 12, p. 1064-1067.

Jenkins, S.F., 1961, A structural study of a portion of the Kerville series (unpublished M.A. thesis): Berkeley, University of California, 83 p.

Kennedy, G.L., Chaffee, M.A., Seitz, J.F., Harner, J.L., and Capstick, D.O., 1983, Mineral resource potential of the Cypress roadless area, southern Sierra Nevada, California: U.S. Geological Survey Miscellaneous Field Studies Map MF-1532-A, scale 1:24,000, 7 p.

Kistler, R.W., in press, Two different lithosphere types in the Sierra Nevada, California, in Anderson, J.L., ed., Cordilleran magmatism: Geological Society of America Special Paper.

Kistler, R.W., and Peterman, Z.E., 1973, Variations in Sr, Rb, K, Na, and initial Sr^{87}/Sr^{86} in Mesozoic granitic rocks and intruded wall rocks in central California: Geological Society of America Bulletin, v. 84, no. 11, p. 3489-3512.

_____1978, Reconstruction of crustal blocks of California on the basis of initial strontium isotopic compositions of Mesozoic granitic rocks: U.S. Geological Survey Professional Paper 1071, 17 p.

Kistler, R.W., and Ross, D.C., in press, A strontium isotopic study of plutons and associated rocks of the southern Sierra Nevada and vicinity: U.S. Geological Survey Bulletin __, ___ p.

Kuenen, P.H., 1941, Geochemical calculations concerning the total mass of sediments in the earth: American Journal of Science, v. 239, p. 161-190.

Lawson, A.C., 1906, The geomorphic features of the Middle Kern: University of California Publications in Geological Sciences, v. 4, no. 16, p. 397-409.

MacKevett, E.M., Jr., 1960, Geology and ore deposits of the Kern River uranium area, California: U.S. Geological Survey Bulletin 1087-F, p. 169-222.

Miller, W.J., and Webb, R.W., 1940, Descriptive geology of the Kernville [30'] quadrangle, California: California Journal of Mines and Geology, v. 36, p. 343-378.

Moore, J.G., and Hopson, C.A., 1961, The Independence dike swarm in eastern California: American Journal of Science, v. 259, p. 241-259.

Prout, J.W., Jr., 1940, Geology of the Big Blue group of mines, Kernville, California: California Journal of Mines and Geology, v. 36, no. 4, p. 379-421.

Ross, D.C., 1969, Descriptive petrography of three large granitic bodies in the Inyo Mountains, California: U.S. Geological Survey Professional Paper 601, 47 p.

_____1980, Reconnaissance geologic map of basement rocks of the southernmost Sierra Nevada (north to 35°30'N): U.S. Geological Survey Open-File Report, 80-307, scale 1:125,000, 22 p.

_____1983a, Hornblende-rich, high-grade metamorphic terranes in the southernmost Sierra Nevada, California, and implications for crustal depths and batholith roots: U.S. Geological Survey Open-File Report 83-465, 51 p.

_____1983b, Petrographic (thin section) notes on selected samples from hornblende-rich metamorphic terranes in the southernmost Sierra Nevada, California: U.S. Geological Survey Open-File Report 83-587, 36 p.

_____1985, Mafic complex (batholithic root?) in the southernmost Sierra Nevada, California: Geology, v. 13, no. 4, p. 288-291.

_____1986, Basement-rock correlations across the White Wolf-Breckenridge-Southern Kern Canyon fault zone, southern Sierra Nevada, California: U.S. Geological Survey Bulletin 1651, 25 p.

_____1987a, Metamorphic framework rocks of the southern Sierra Nevada, California: U.S. Geological Survey Open-File Report 87-81, 74 p.

_____1987b, Mafic plutonic rocks of the southern Sierra Nevada, California: U.S. Geological Survey Open-file Report 87-275, 42 p.

_____1987c, Generalized geologic map of the basement rocks of the southern Sierra Nevada, California: U. S. Geological Survey Open-File Report 87-276, scale 1:250,000, 28 p.

_____1987d, Granitic rock modal data from the southern Sierra Nevada, California: U.S. Geological Survey Open-File Report 87-373, 276 p.

_____1988a, Specific gravity data from granitic rocks of the southern Sierra Nevada, California: U.S. Geological Survey Open-File Report 88-72, 32 p.

_____1988b, Chemical traits and trends of the granitic rocks of the southern Sierra Nevada, California: U.S. Geological Survey Open-File Report 88-374, 119 p.

_____1989a, Magnetic susceptibilities of modally analyzed granitic rocks from the southern Sierra Nevada, California: U.S. Geological Survey Open-File Report 89-204, 53 p.

_____1989b, Air photo lineaments, southern Sierra Nevada, California: U.S. Geological Survey Open-File Report 89-365, 23 p.

_____1989c, Metamorphic and plutonic rocks of the southernmost Sierra Nevada, California, and their tectonic framework: U.S. Geological Survey Professional Paper 1381, 159 p.

Saleeby, J.B., and Busby-Spera, Cathy, 1986, Field trip guide to the metamorphic framework rocks of the Lake Isabella area, southern Sierra Nevada, California, in Dunne, G.C., compiler, Mesozoic and Cenozoic structural evolution of selected areas, east-central California: Cordilleran Section of the Geological Society of America, 82nd Annual Meeting, Guidebook, p. 81-94.

Saleeby, J.B., Goodin, S.E., Sharp, W.D., and Busby, C.J., 1978, Early Mesozoic paleotectonic-paleographic reconstruction of the southern Sierra Nevada region, in Howell, D.G., and

McDougall, K.A., eds., Mesozoic paleogeography of the western United States: Pacific Coast Paleogeography Symposium 2: Los Angeles, Society of Economic Paleontologists and Mineralogists, Pacific Section, p. 311-336.

Saleeby, J.B., and Sharp, W.D., 1980, Chronology of the structural and petrologic development of the southwest Sierra Nevada foothills, California: Geological Society of America Bulletin, v. 91, pt. 1, p. 317-320; v. 91, pt. 2, p. 1416-1535.

Sams, D.B., 1986, U/Pb geochronology, petrology, and structural geology of the crystalline rocks of the southernmost Sierra Nevada and Tehachapi Mountains, Kern County, California (Ph.D. thesis): Pasadena, California, Institute of Technology, 315 p.

Sharry, John, 1981, The geology of the western Tehachapi mountains, California (Ph.D. thesis): Cambridge, Massachusetts Institute of Technology, 215 p.

Smith, A.R. (compiler), 1965, Bakersfield sheet of the Geologic Map of California (Olaf P. Jenkins edition): California Division of Mines and Geology, scale 1:250,000.

Taylor, G.C., Loyd, R.C., Alfors, J.T., Burnett, J.L., Stinson, M.C., Chapman, R.H., Silva, M.A., Bacon, C.E., Bushnell, M.M., and Anderson, T.P., 1986, Mineral resource potential of the Rockhouse Basin Wilderness study area, Kern and Tulare Counties, California: California Division of Mines and Geology Special Report 157, 75 p.

Treasher, R.A., (compiler), 1948, Definite project report, Isabella project, Kern River, California, Part IV - Dam and appurtenances, Appendix A (unpublished administrative report): Sacramento District, U.S. Corps of Engineers, 51 p.

Vogt, J.H.L., 1931, The average composition of the earth's crust: Oslo, Skr. Norske Vidensk.-Akad., K1:I, no. 7, 48 p.

Webb, R.W., 1936, Kern Canyon fault, southern Sierra Nevada: Journal of Geology, v. 44, p. 631-638.

_____1946, Geomorphology of the middle Kern River basin, southern Sierra Nevada, California: Geological Society of America Bulletin, v. 57, p. 355-382.

_____1955, Kern Canyon lineament, in Oakeshott, G.B., ed., Earthquakes in Kern County, California during 1952: California Division of Mines and Geology Bulletin 171, p. 35-36.

Wiese, J.H., 1950, Geology and mineral deposits of the Neenach quadrangle, California: California Division of Mines and Geology Bulletin 153, 53 p.

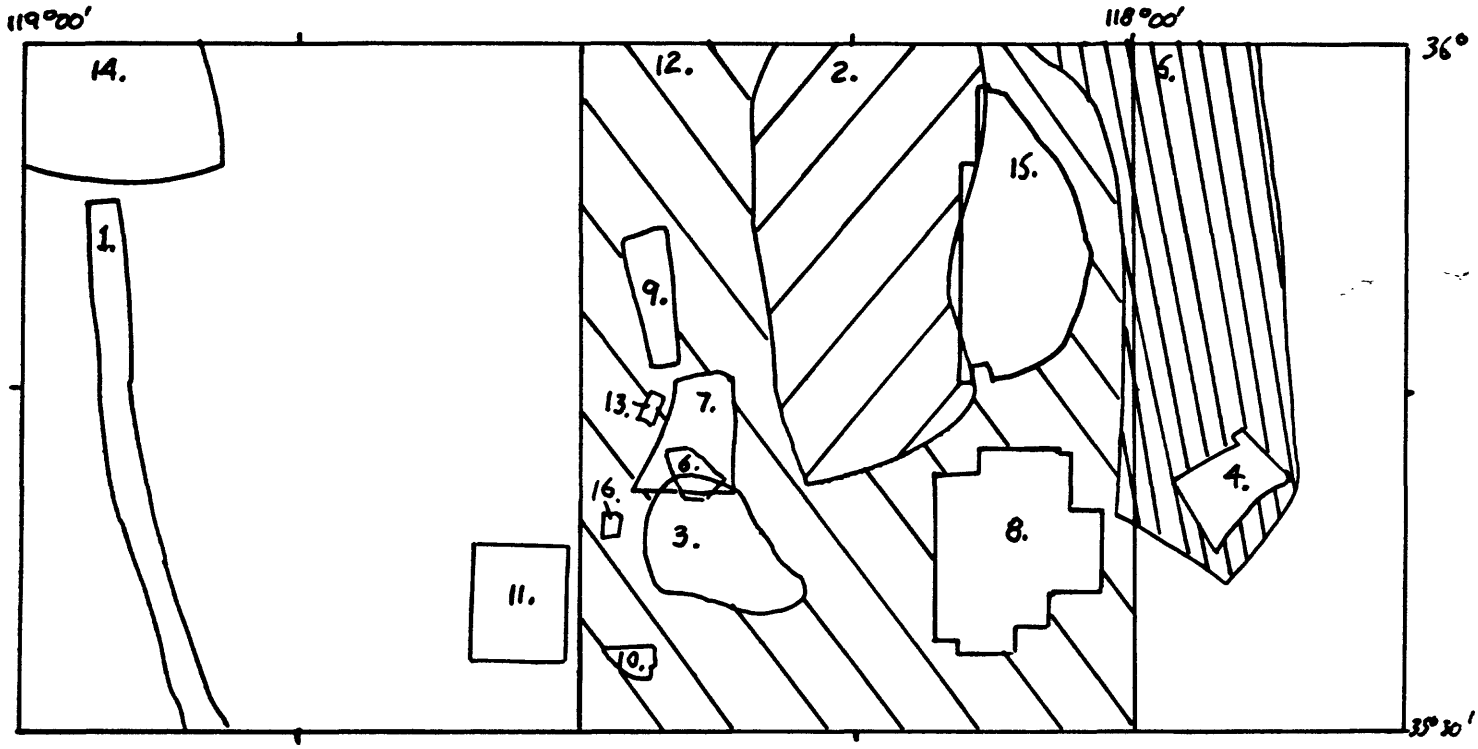

Figure 1.

Index to previous studies that supplied data for the present regional map of the southern Sierra Nevada between lat 35°30' and 36°00' N. (see text for explanation: p. 2-4)

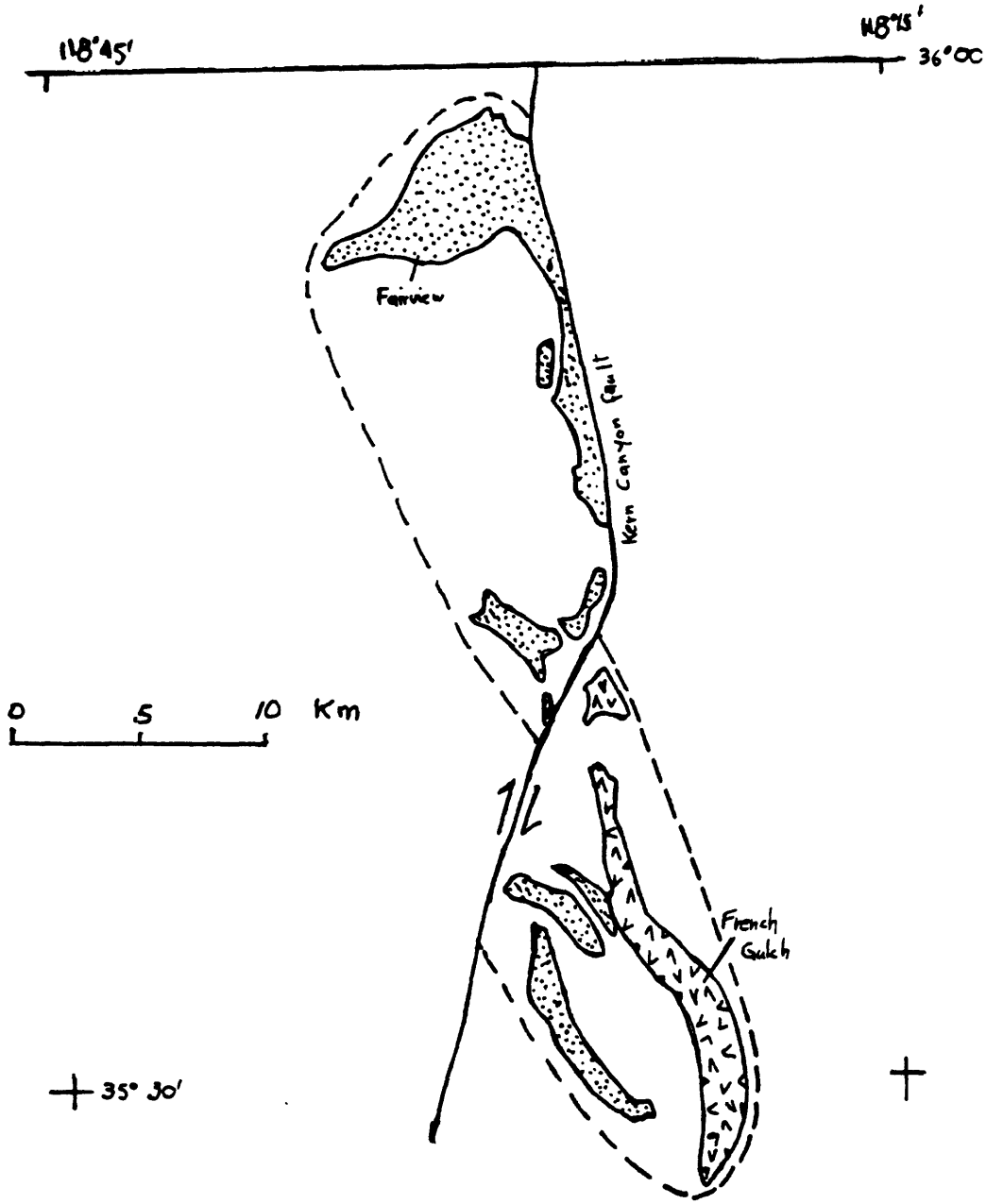

Figure 2. Lens-like (?) distribution of the Fairview pendant and related quartzitic rocks and the French Gulch pendant of metavolcanic rocks.

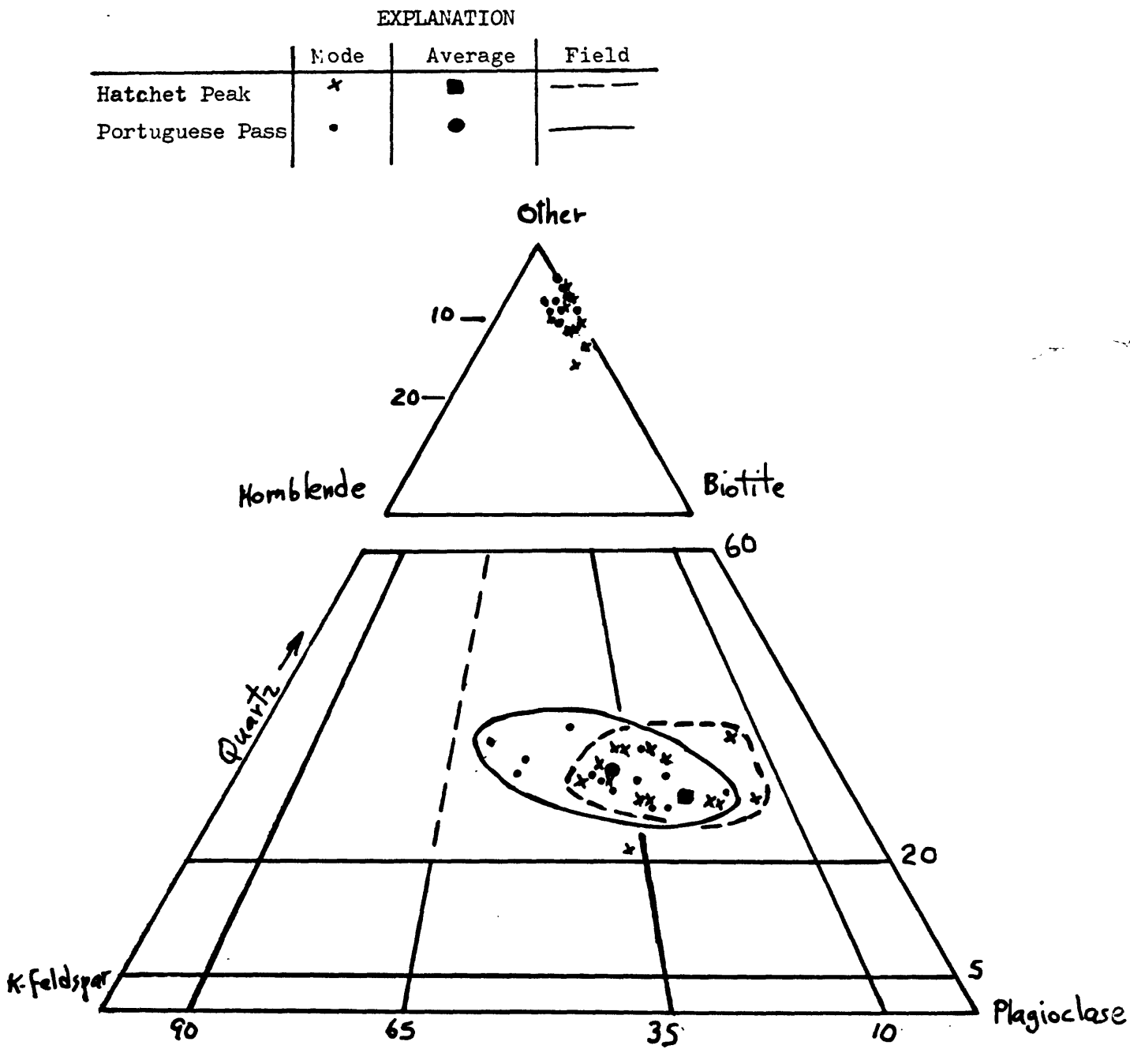

Figure 3. Modal comparison of the granodiorite of Hatchet Peak and the granite of Portuguese Pass.

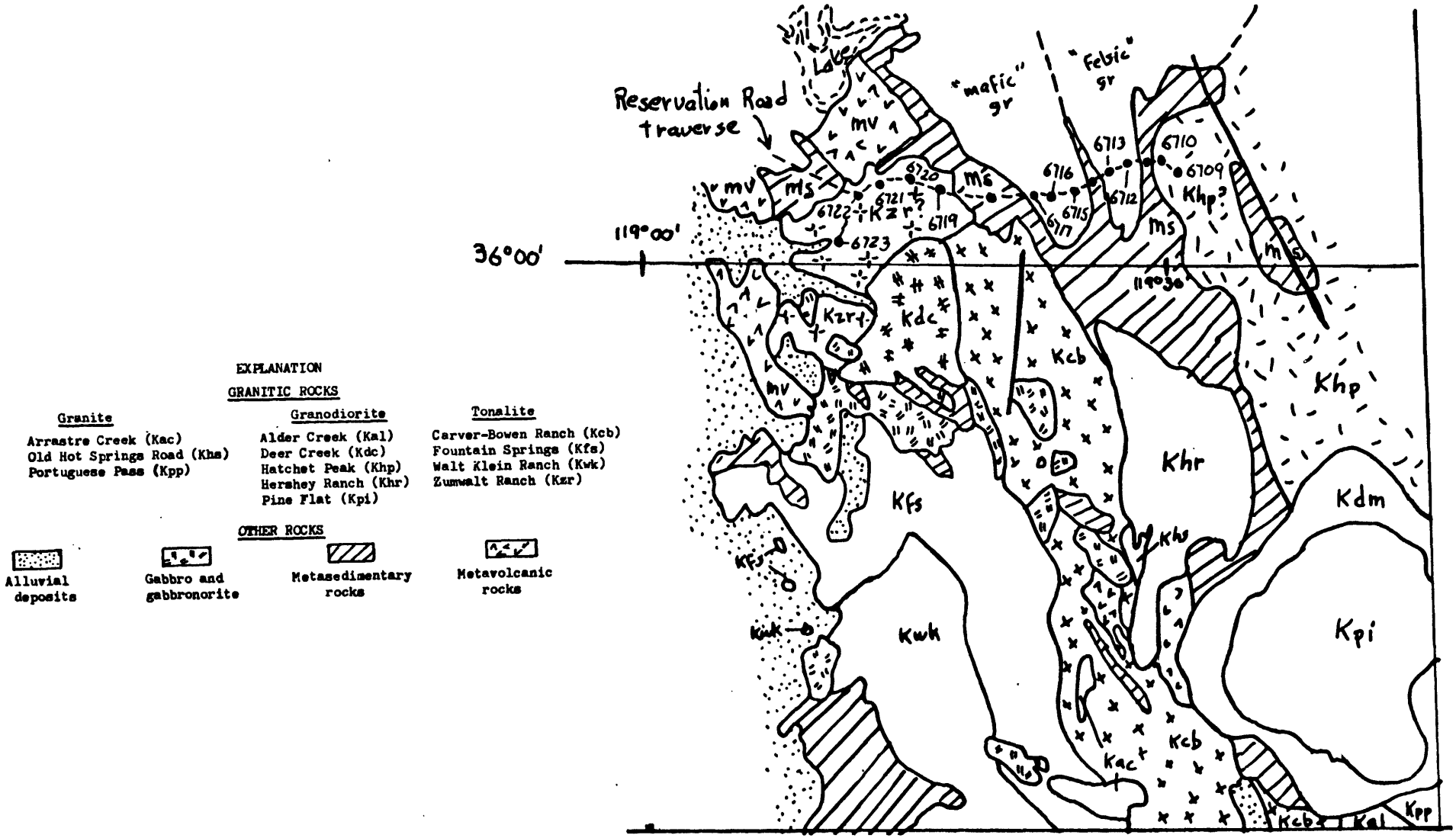

Figure 4. Location of Reservation Road samples (large numbered black dots) relative to northwest corner of map area, and showing probable continuation north beyond lat 36° 00' N of the Zumwalt Ranch, Deer Creek, Carver-Bowen, and Hatchet Peak granitic units.

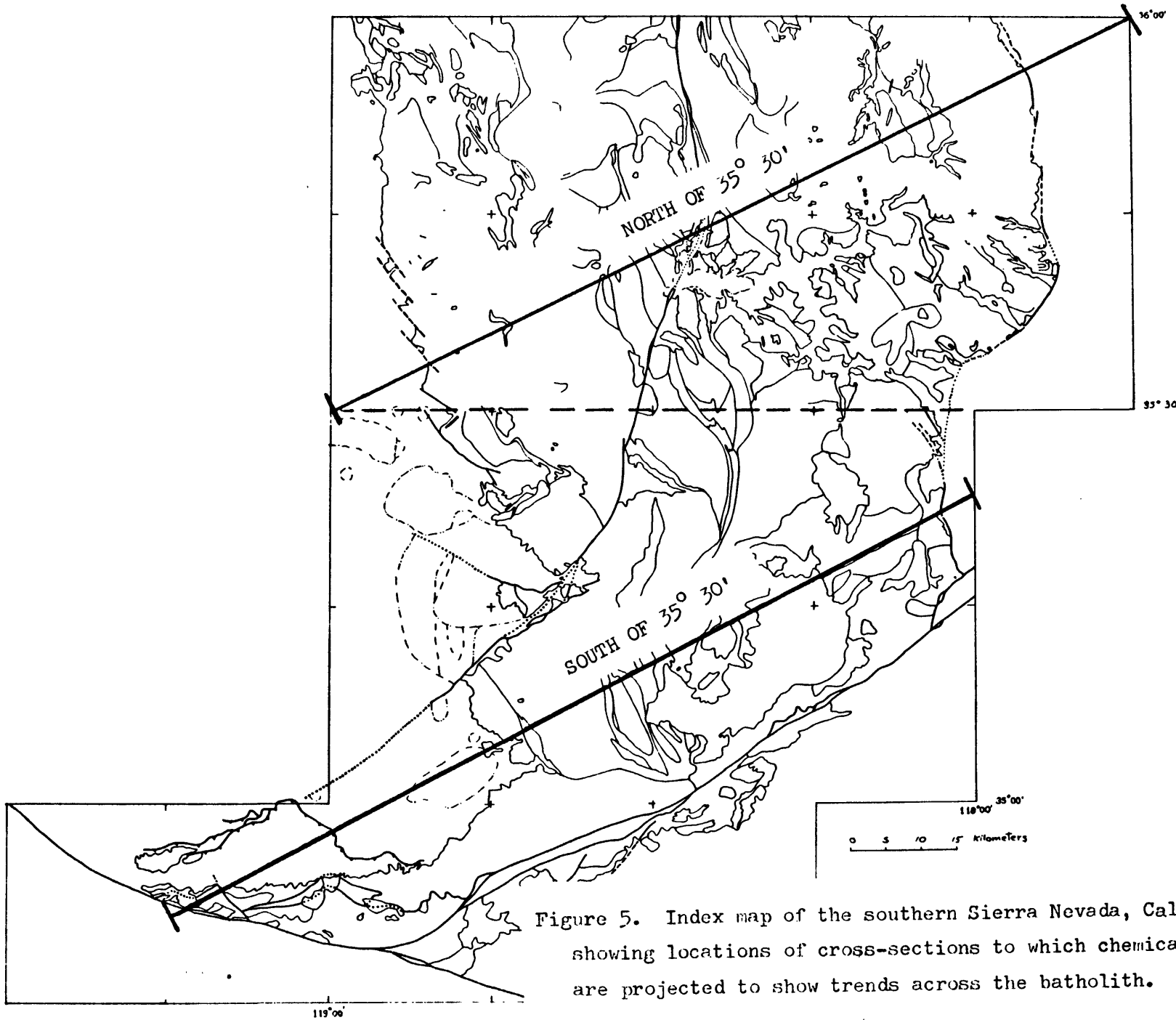

Figure 5. Index map of the southern Sierra Nevada, California showing locations of cross-sections to which chemical data are projected to show trends across the batholith.

Figure 6. Variation of oxidation ratio across the southern part of the Sierra Nevada batholith.

A. Cross-section north of lat 35° 30' N.
B. Cross-section south of lat 35° 30' N.
C. Composite of the two cross-sections.
D. Modified composite plot.
E. Oxidation ratio against magnetic susceptibility

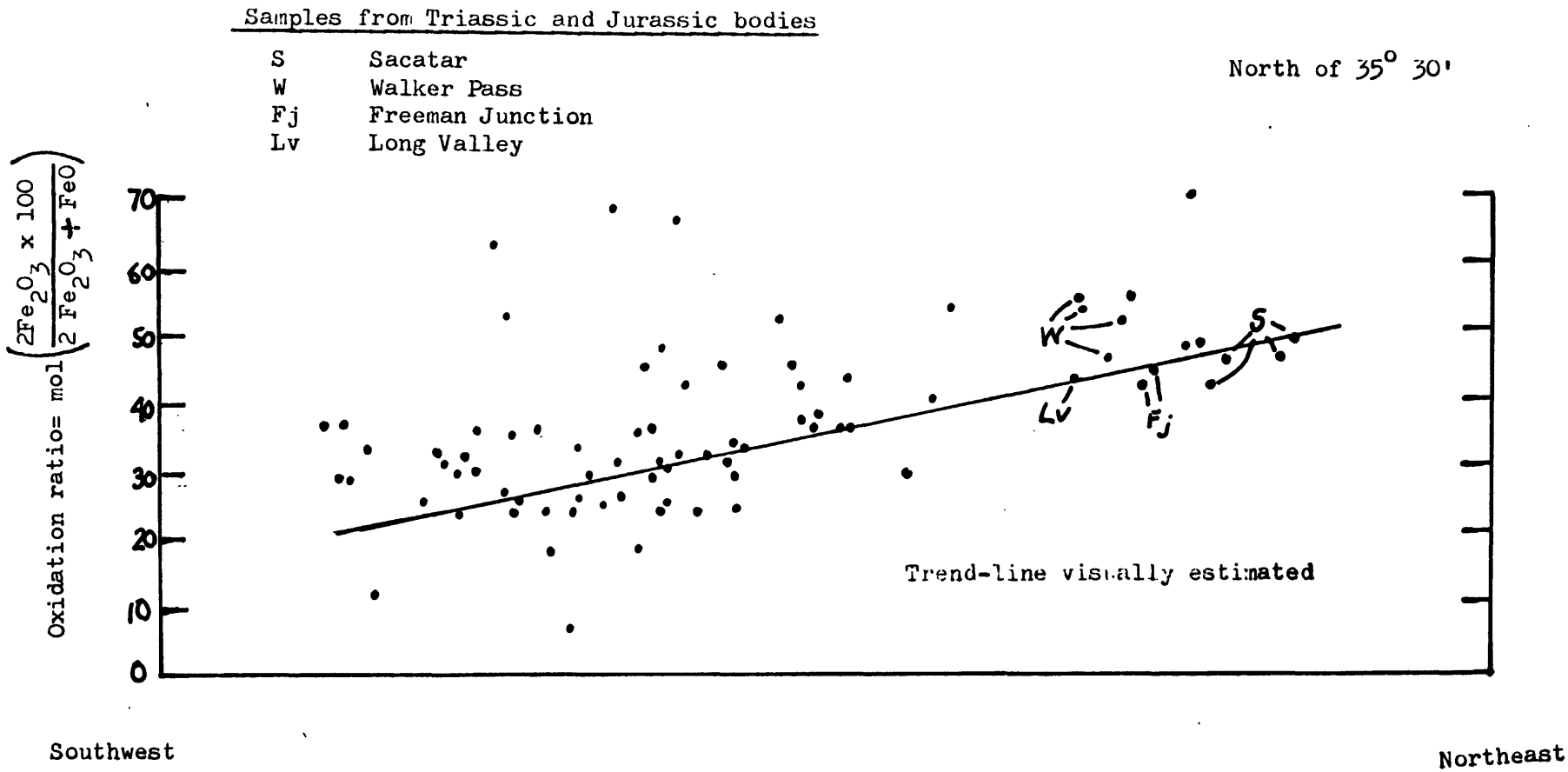
Samples from Triassic and Jurassic bodies
S Sacatar
W Walker Pass
Fj Freeman Junction
Lv Long Valley
North of 35° 30'
Oxidation ratio= mol $\left(\frac{2Fe_2O_3 \times 100}{2Fe_2O_3 + FeO}\right)$
70
60
50
40
30
20
10
0
W
S
Lv
Fj
Trend-line visually estimated
Southwest
Northeast

Figure 6 A.

South of 35° 30'

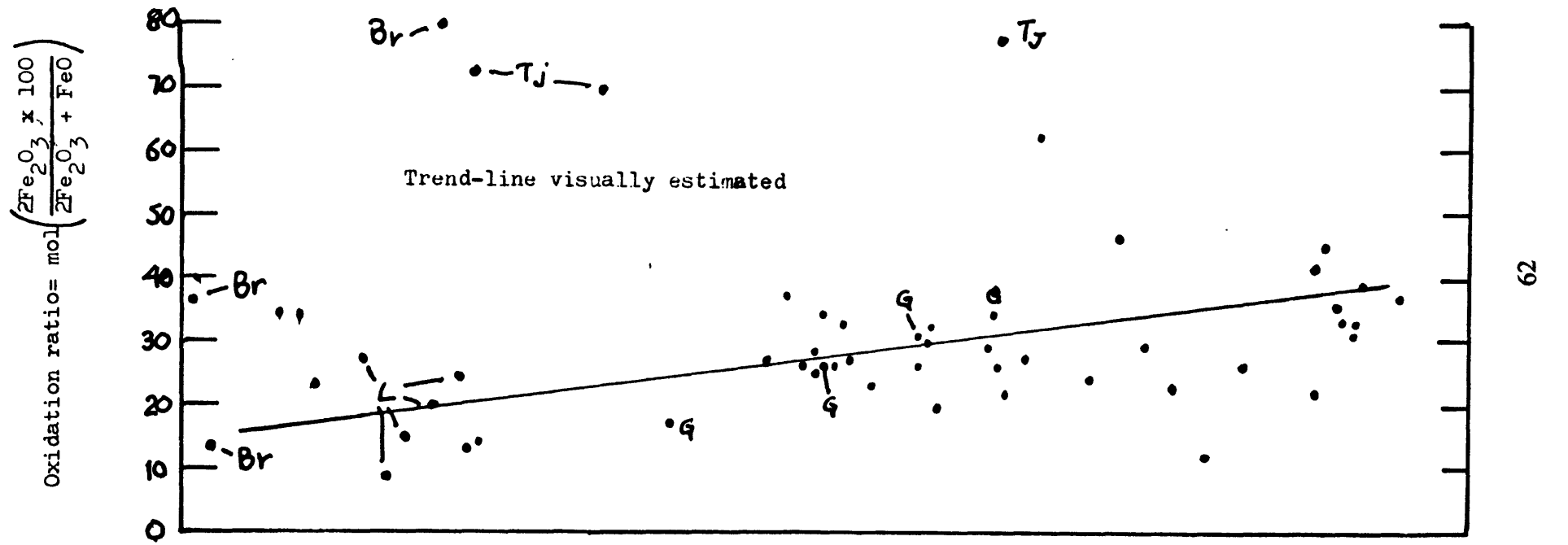

Samples from south of the Garlock and Pastoria faults

Br	Brush Mountain
Tj	Tejon Lookout
L	Lebec
G	Gato-Montes

Figure 6 B.

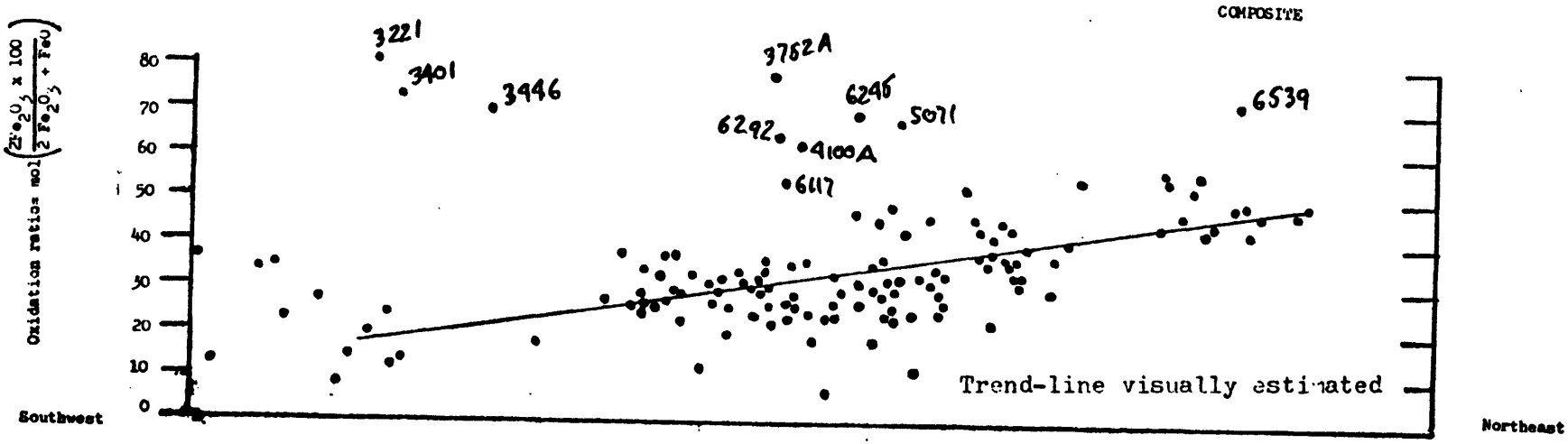

Figure 6C.

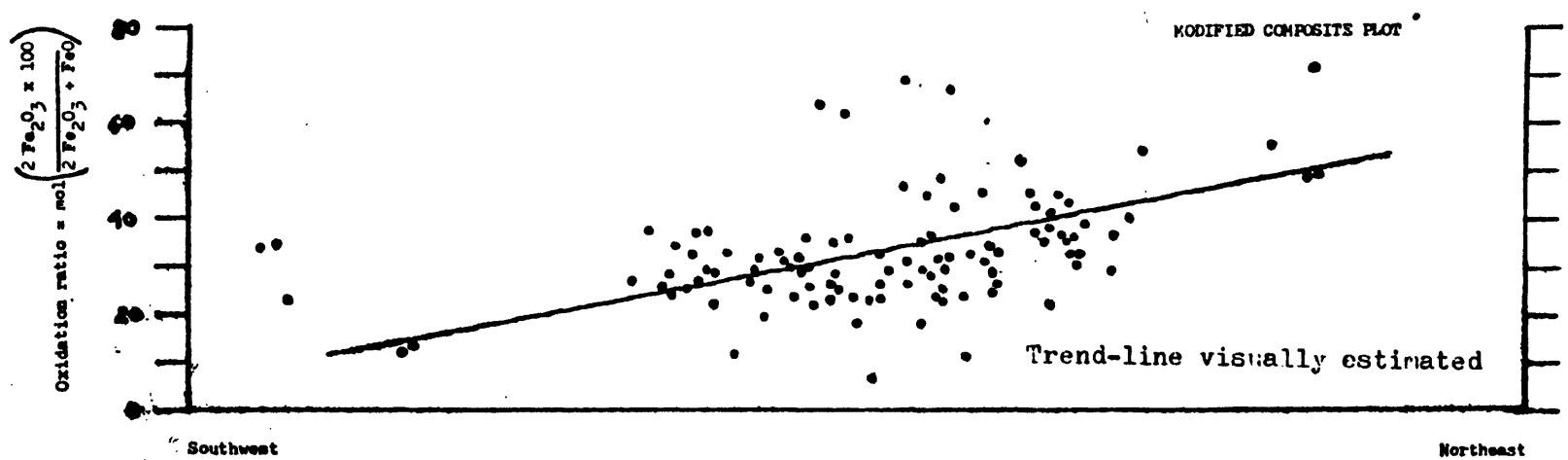

Figure 6D.

*/ Samples labeled on north and south cross-sections omitted

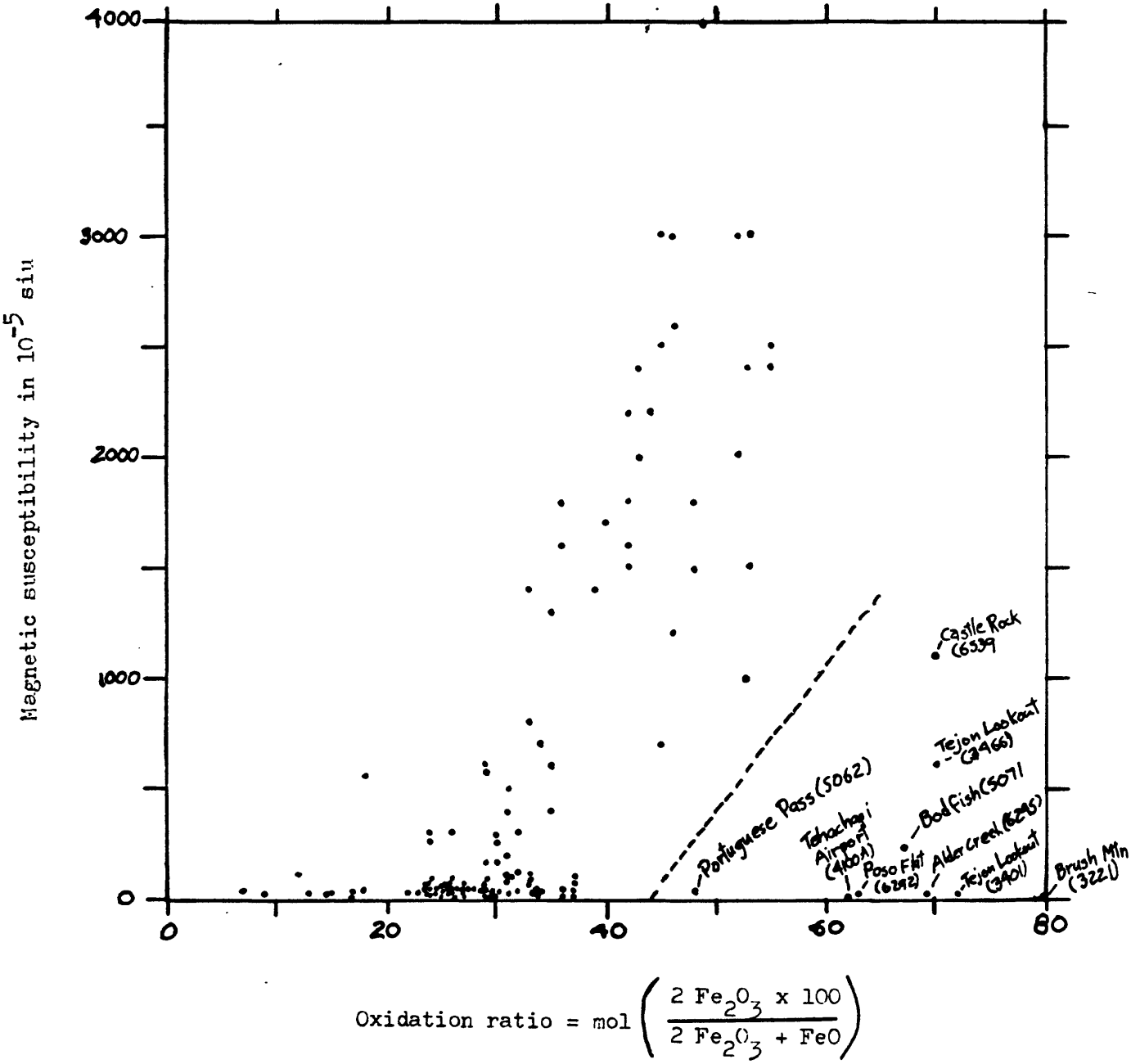

Figure 6E. Plot of oxidation ratio against magnetic susceptibility for chemically analyzed granitic rocks, southern Sierra Nevada, California. Dashed line separates altered and unaltered samples.

Figure 7. Variation in SiO_2 across the southern part of the Sierra Nevada batholith.

A. Cross-section north of lat 35° 30' N.
B. Cross-section south of lat 35° 30' N.
C. Composite of two cross-sections
D. Modified composite plot

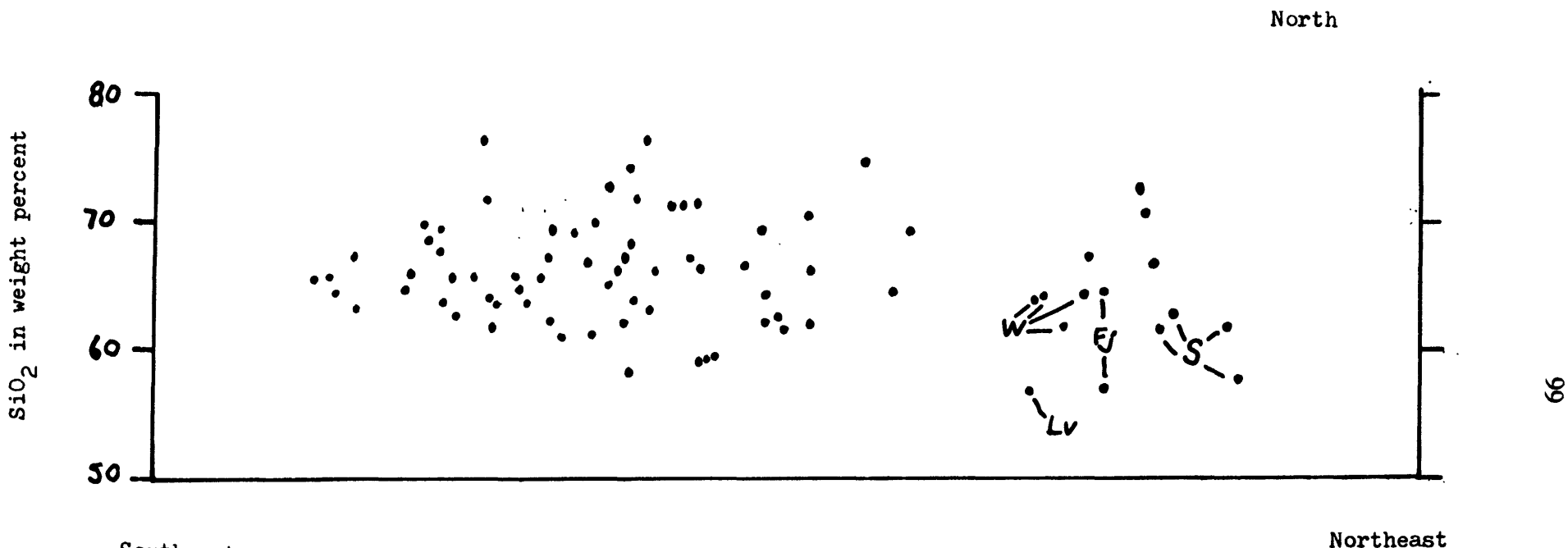

Samples from Triassic and Jurassic bodies

S Sacatar
W Walker Pass
Fj Freeman Junction
Lv Long Valley

Figure 7 A.

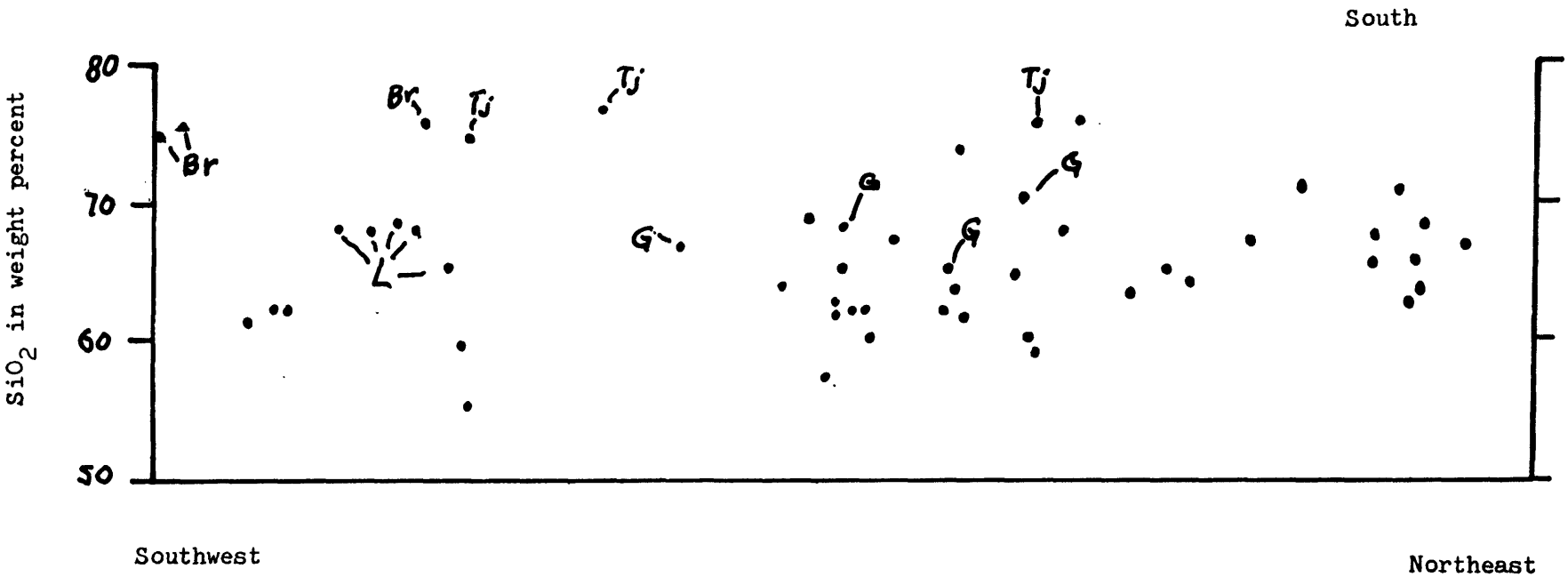

Samples from bodies south of the Garlock and Pastoria faults

L Lebec
G Gato-Montes
Tj Tejon Lookout
Br Brush Mountain

Figure 7 B.

Figure 7C.

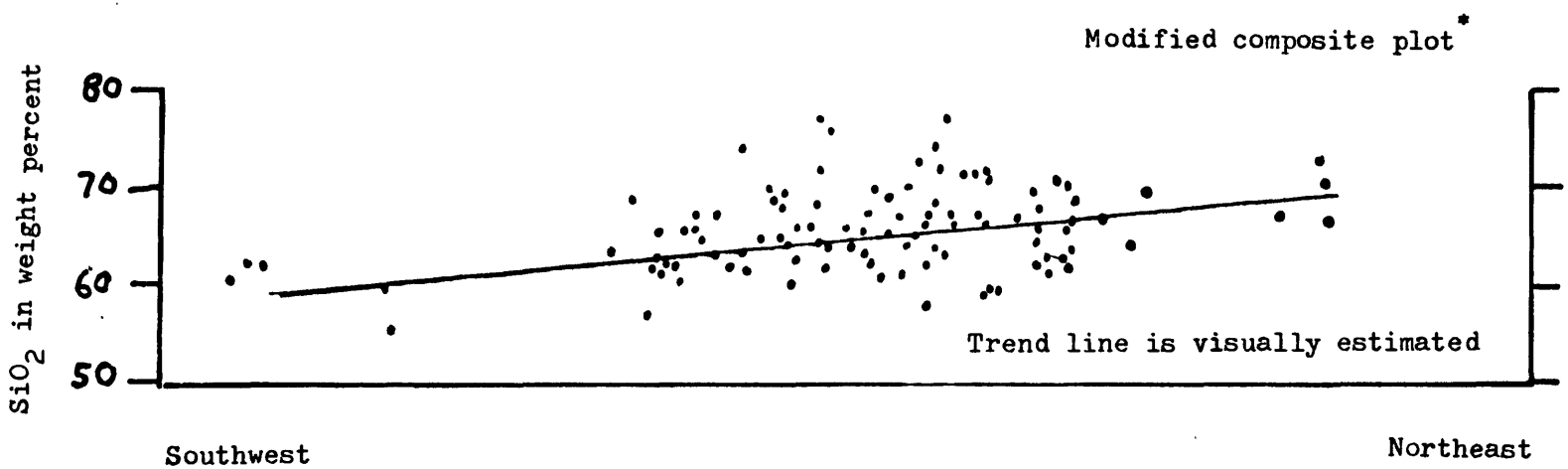

*/ Labeled samples from north and south sections omitted

Figure 7D.

Figure 8. Variation of Al_2O_3 across the southern part of the Sierra Nevada batholith.

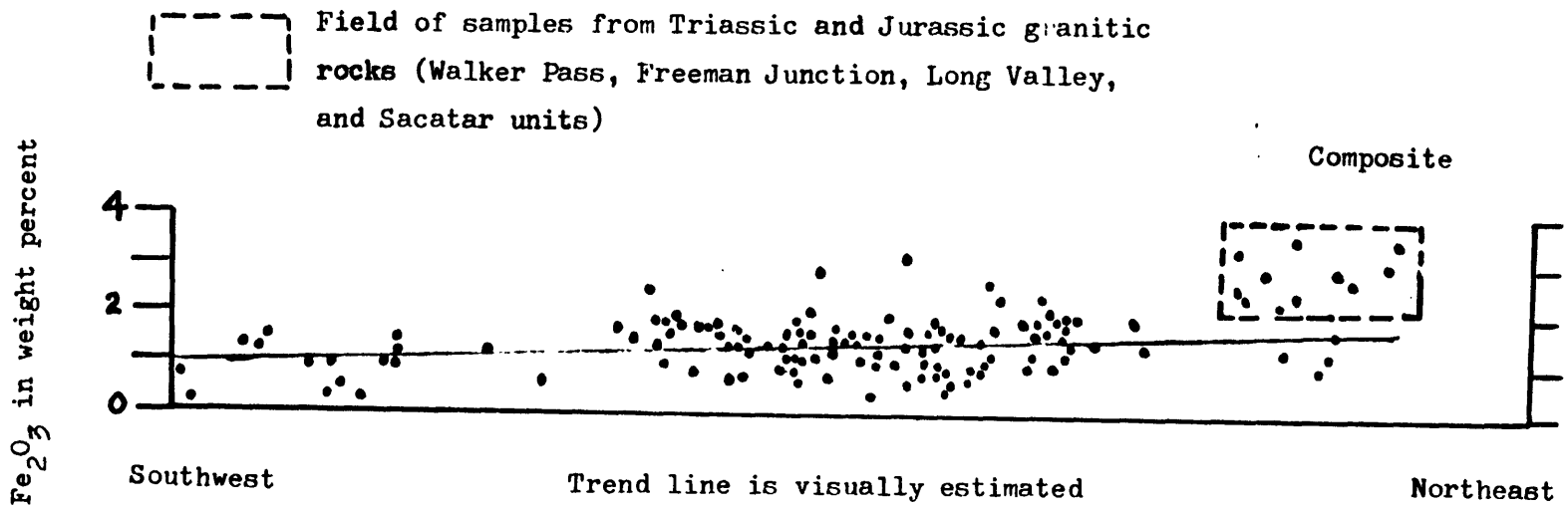

Figure 9A.

Figure 9. Variation in Fe_2O_3 across the southern part of the Sierra Nevada batholith.

A. Composite cross-section

B. Cross-section north of lat 35° 30' N.

C. Cross-section south of lat 35° 30' N.

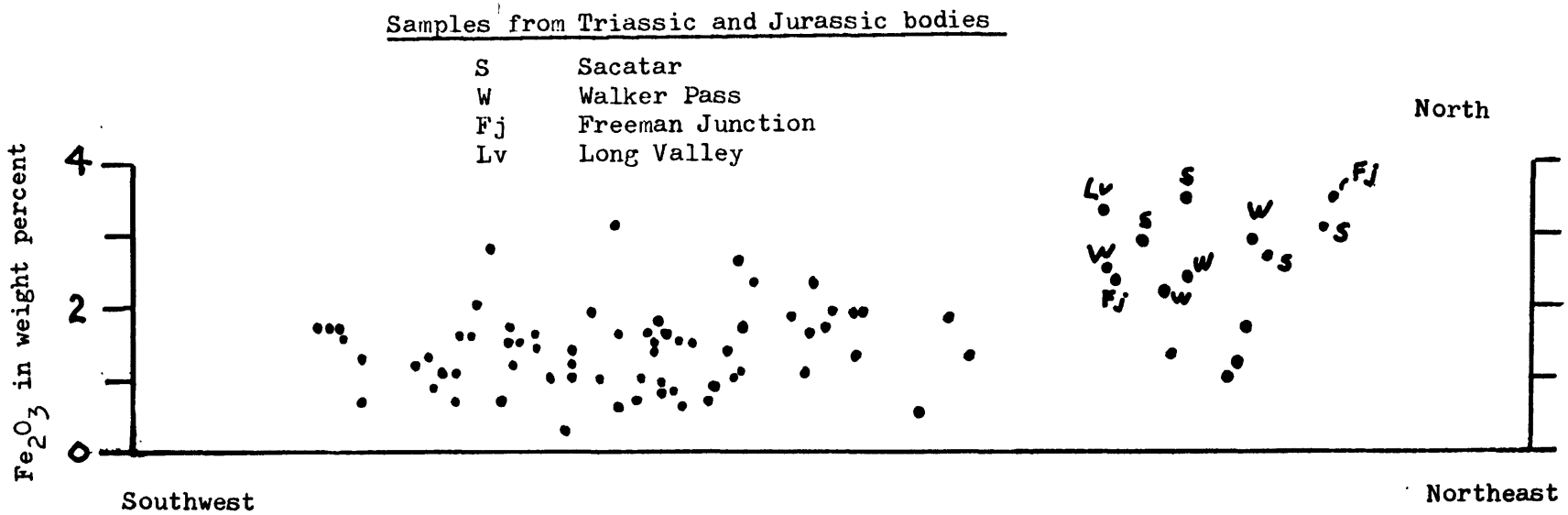

Figure 9 B.

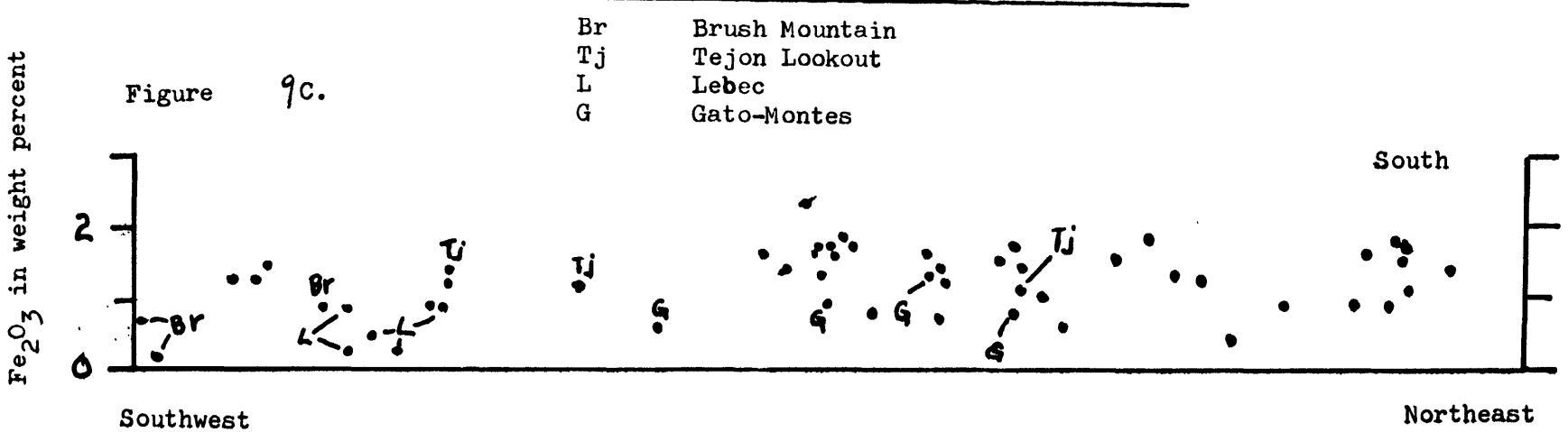

Figure 9C.

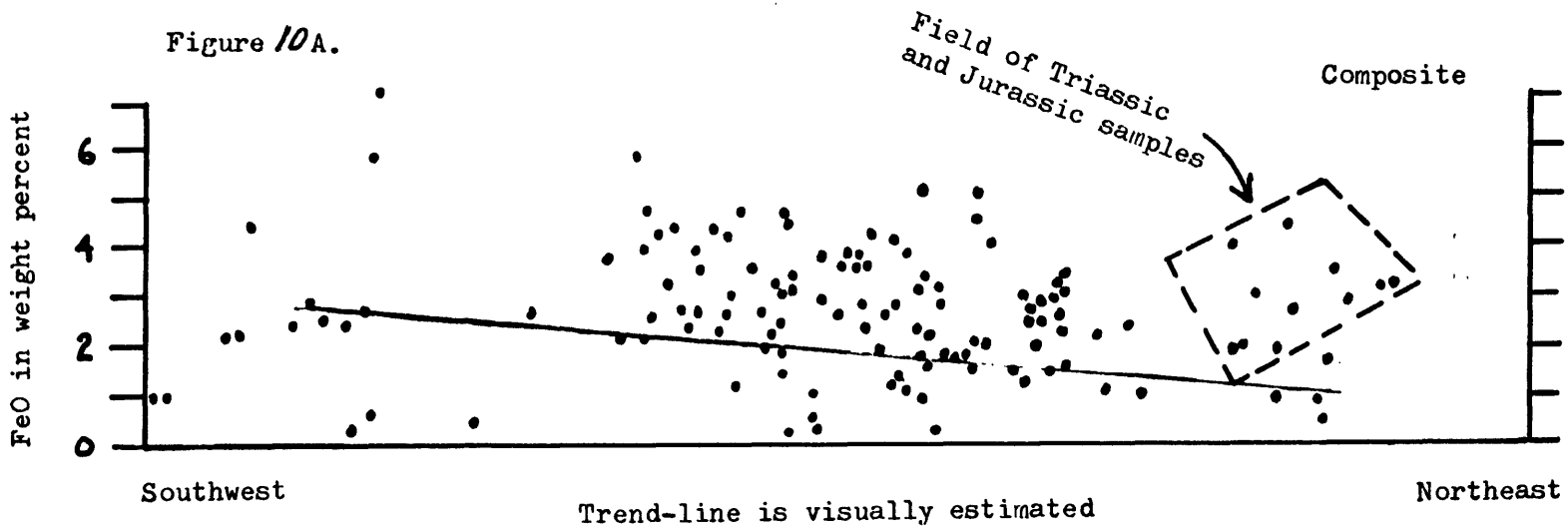

Figure 10. Variation in FeO across the southern part of the Sierra Nevada batholith.

A. Composite cross-section

B. Cross-section north of lat 35° 30' N.

C. Cross-section south of lat 35° 30'N .

Samples from Triassic and Jurassic bodies

S Sacatar
W Walker Pass
Fj Freeman Junction
Lv Long Valley

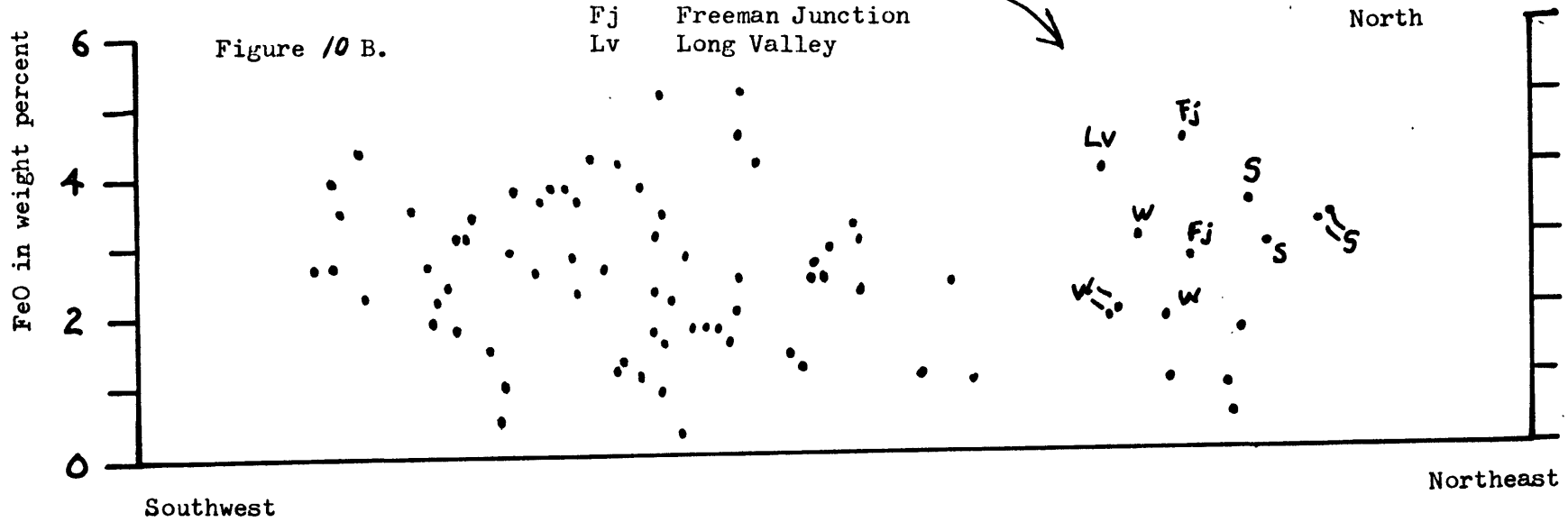

Figure 10 B.

Samples south of the Garlock and Pastoria faults

Br Brush Mountain
Tj Tejon Lookout
L Lebec
G Gato-Montes

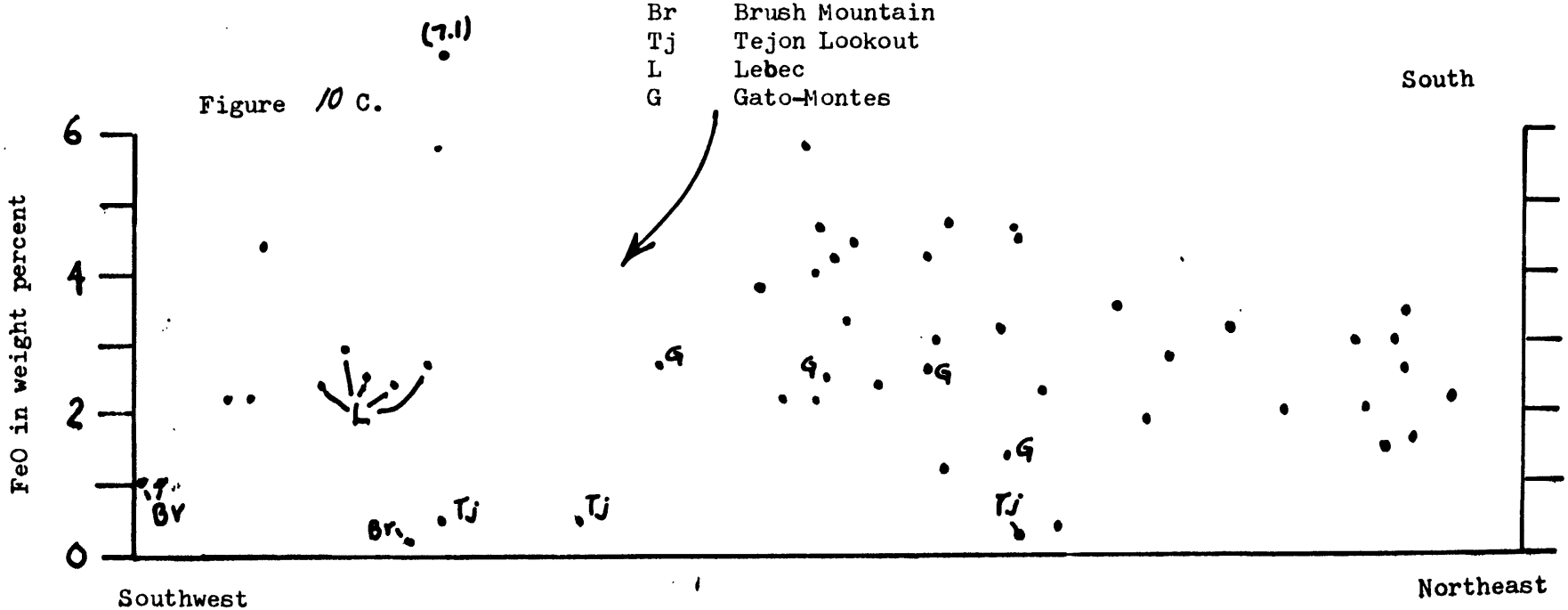

Figure 10 C.

Figure 11. Variation of total iron oxide (Fe_2O_3 + FeO) across the southern part of the Sierra Nevada batholith.

A. Cross-section north of lat 35° 30' N.
B. Cross-section south of lat 35° 30' N.
C. Composite of upper two cross sections.
D. Modified composite plot

Figure 11 A.

Samples from Triassic and Jurassic bodies

S Sacatar
W Walker Pass
Fj Freeman Junction
Lv Long Valley

North of 35° 30'

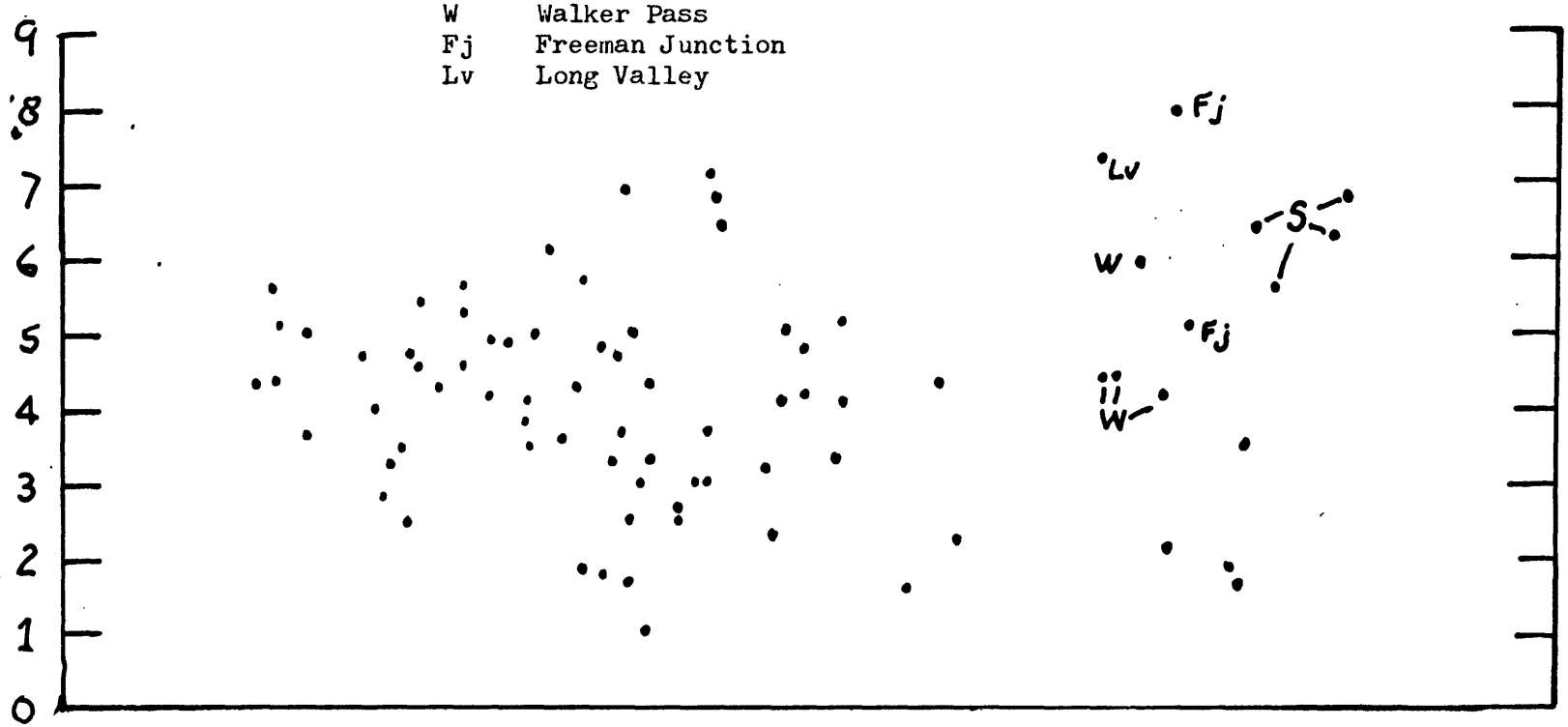

Southwest

Northeast

Samples south of the Garlock and Pastoria faults

Figure 11 B.

Br	Brush Mountain
Tj	Tejon Lookout
L	Lebec
G	Gato-Montes

South of 35° 30'

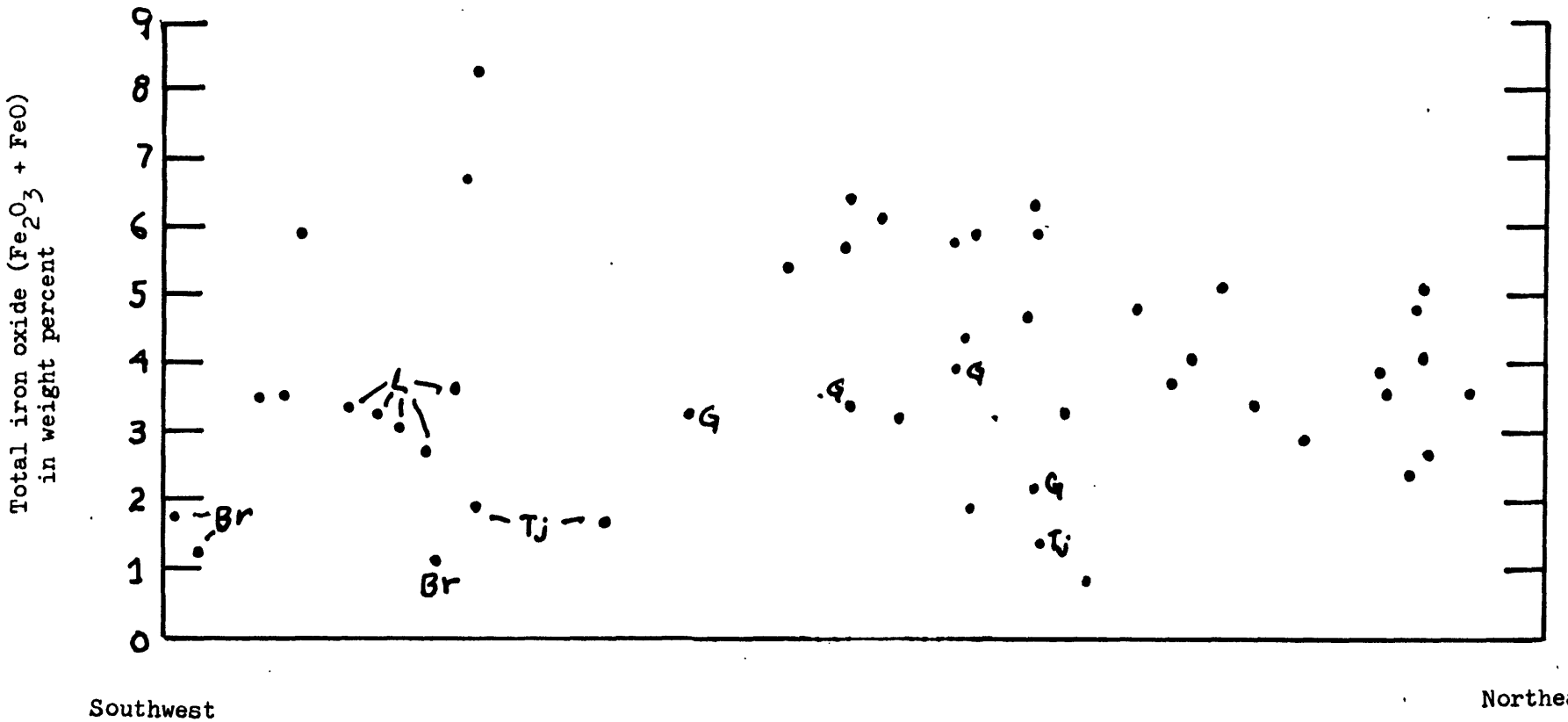

Figure II C.

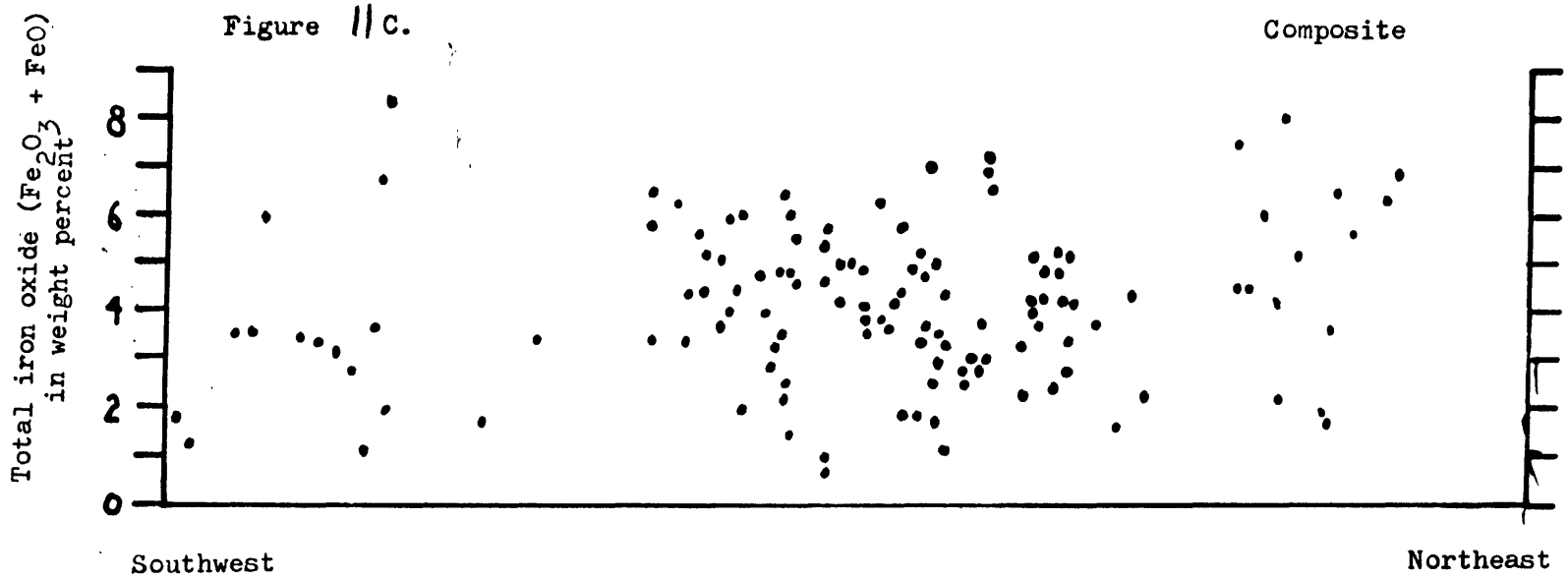

Figure II D.

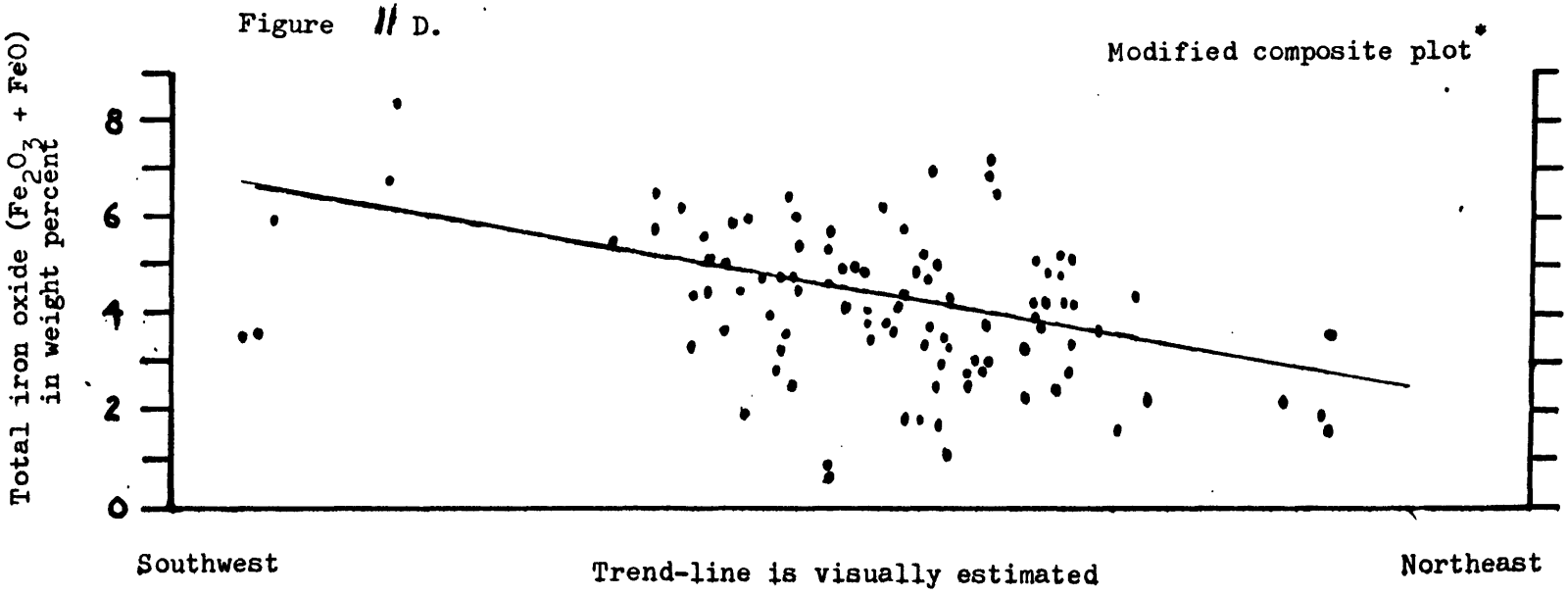

*/ Labeled samples from north and south sections omitted

Figure 12. Variation of MgO across the southern part of the Sierra Nevada batholith.

A. Cross-section north of lat 35° 30' N.
B. Cross-section south of lat 35° 30' N.
C. Composite of upper two cross-sections.
D. Modified composite plot.

Samples from Triassic and Jurassic bodies

S Sacatar
W Walker Pass
Fj Freeman Junction
Lv Long Valley

Figure 12 A.

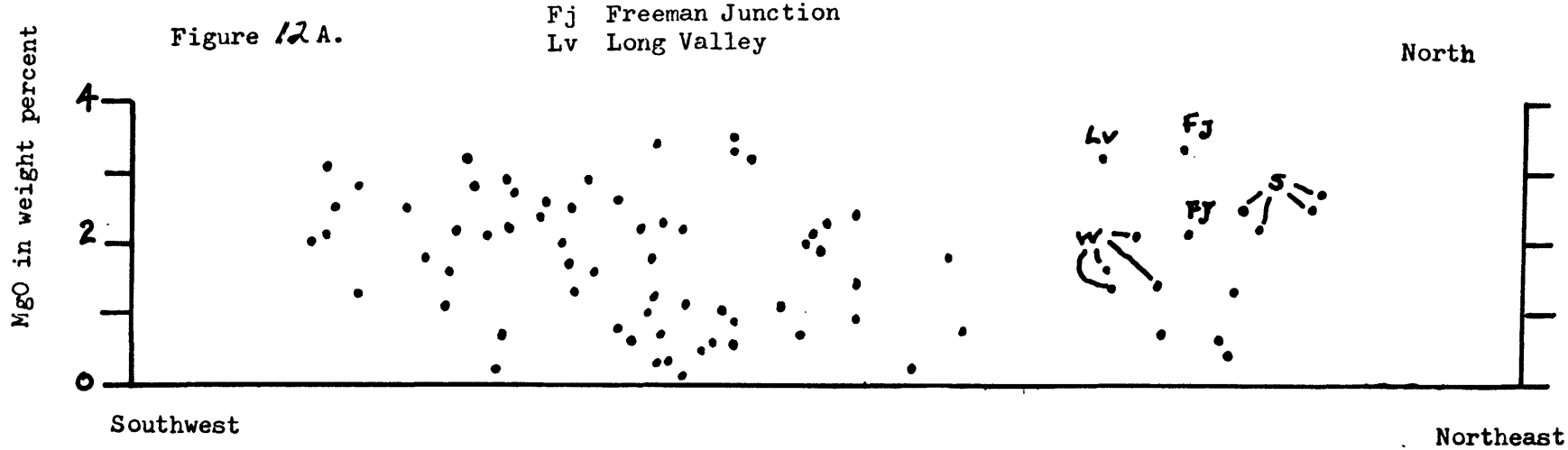

Samples south of the Garlock and Pastoria faults

Br Brush Mountain
Tj Tejon Lookout
L Lebec
G Gato-Montes

Figure 12 B.

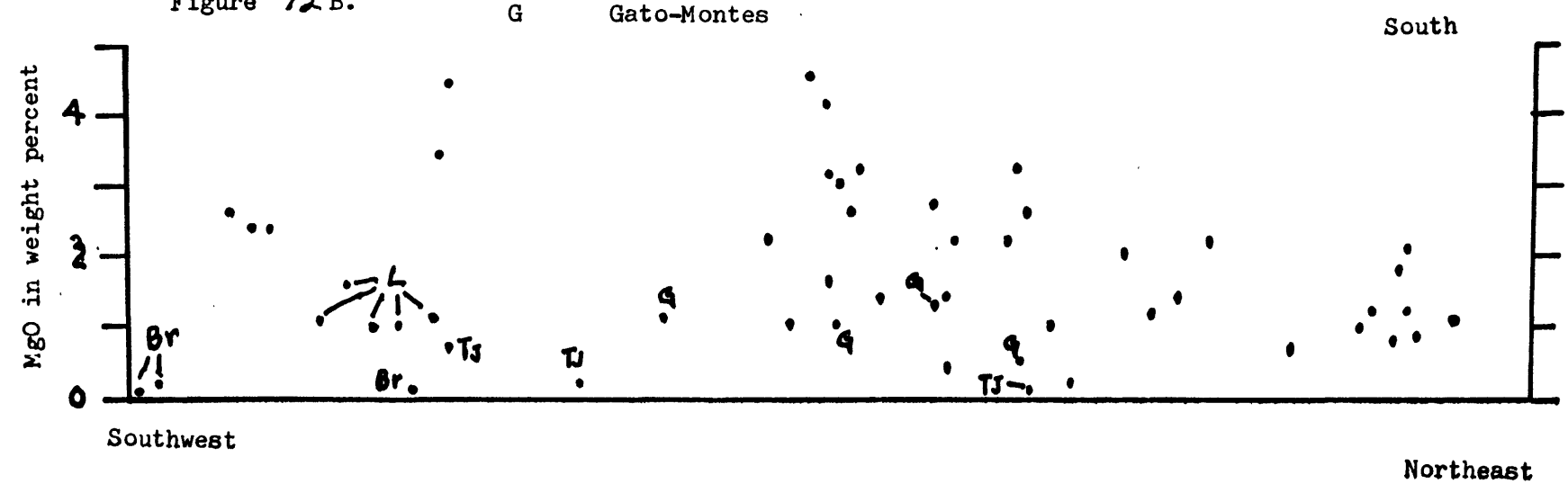

Figure 12 C.

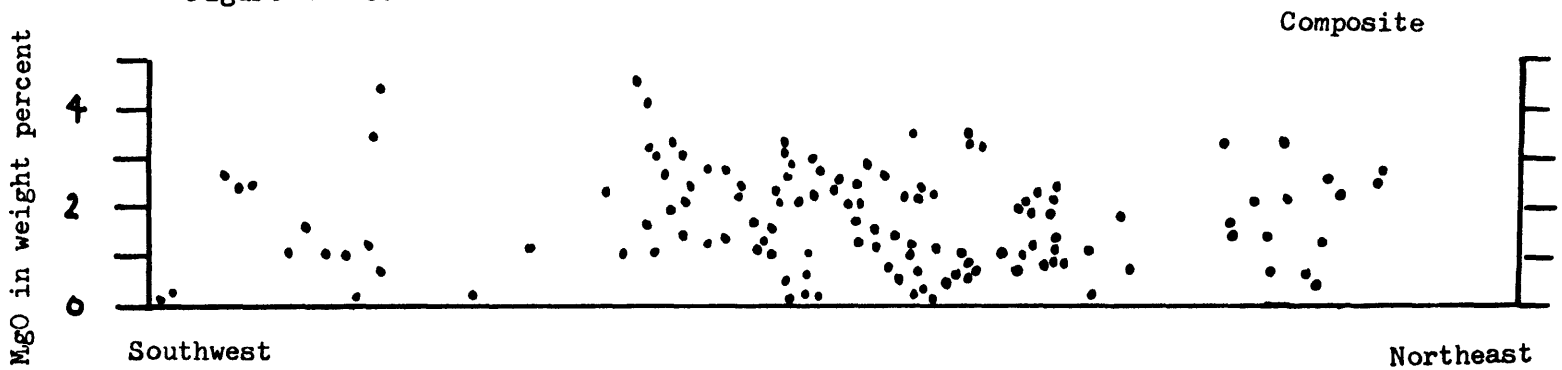

Figure 12 D.

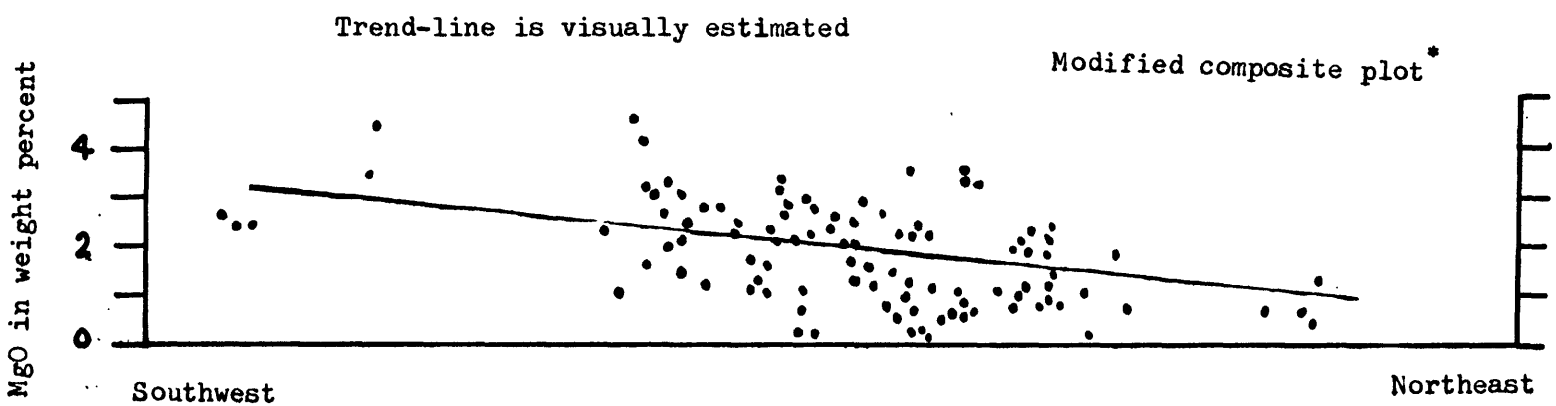

*/ Labeled samples from north and south cross-sections omitted

Figure 13. Variation of CaO across the southern part of the Sierra Nevada batholith.

A. Cross-section north of lat 35° 00' N.
B. Cross-section south of lat 35° 30' N.
C. Composite of upper two cross-sections.
D. Modified composite plot.

Samples from Triassic and Jurassic bodies

S	Sacatar
W	Walker Pass
Fj	Freeman Junction
Lv	Long Valley

Figure 13A.

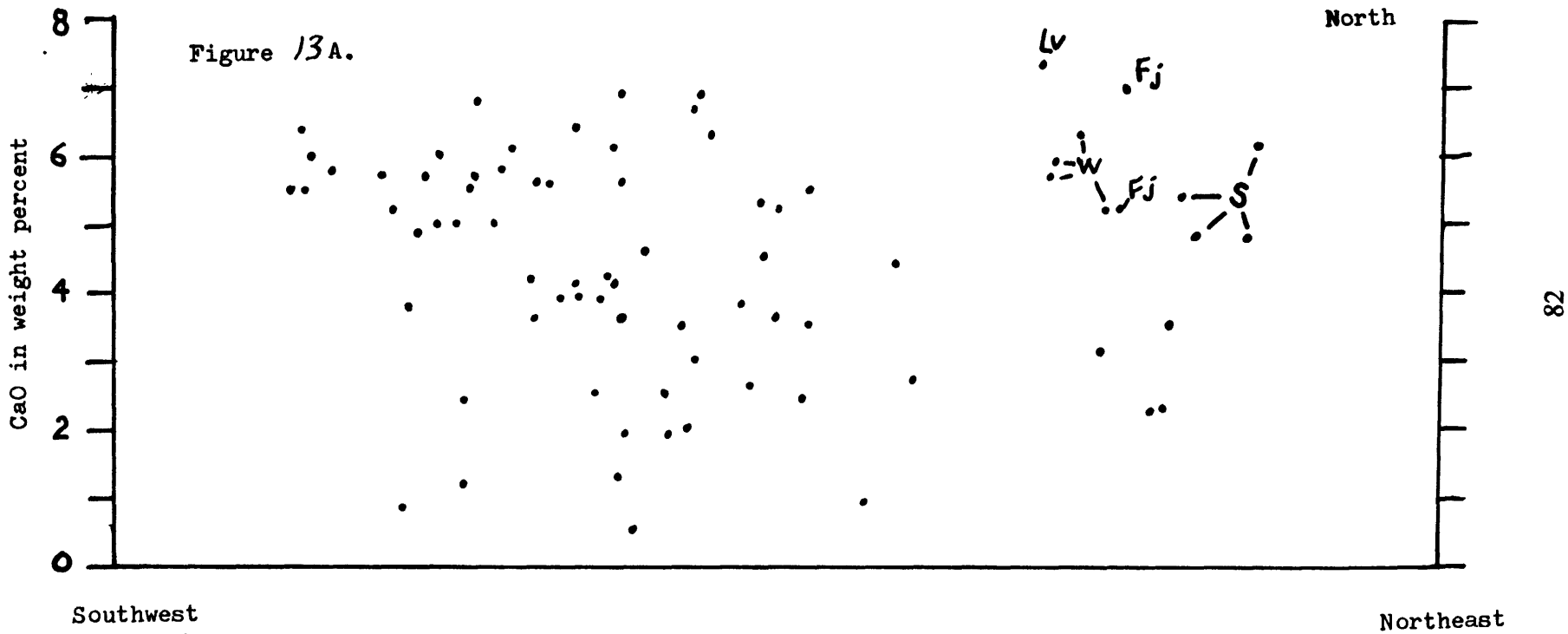

Samples south of the Garlock and P^{a}storia faults

Br Brush Mountain
Tj Tejon Lookout
L Lebec
G Gato-Montes

Figure 13 B.

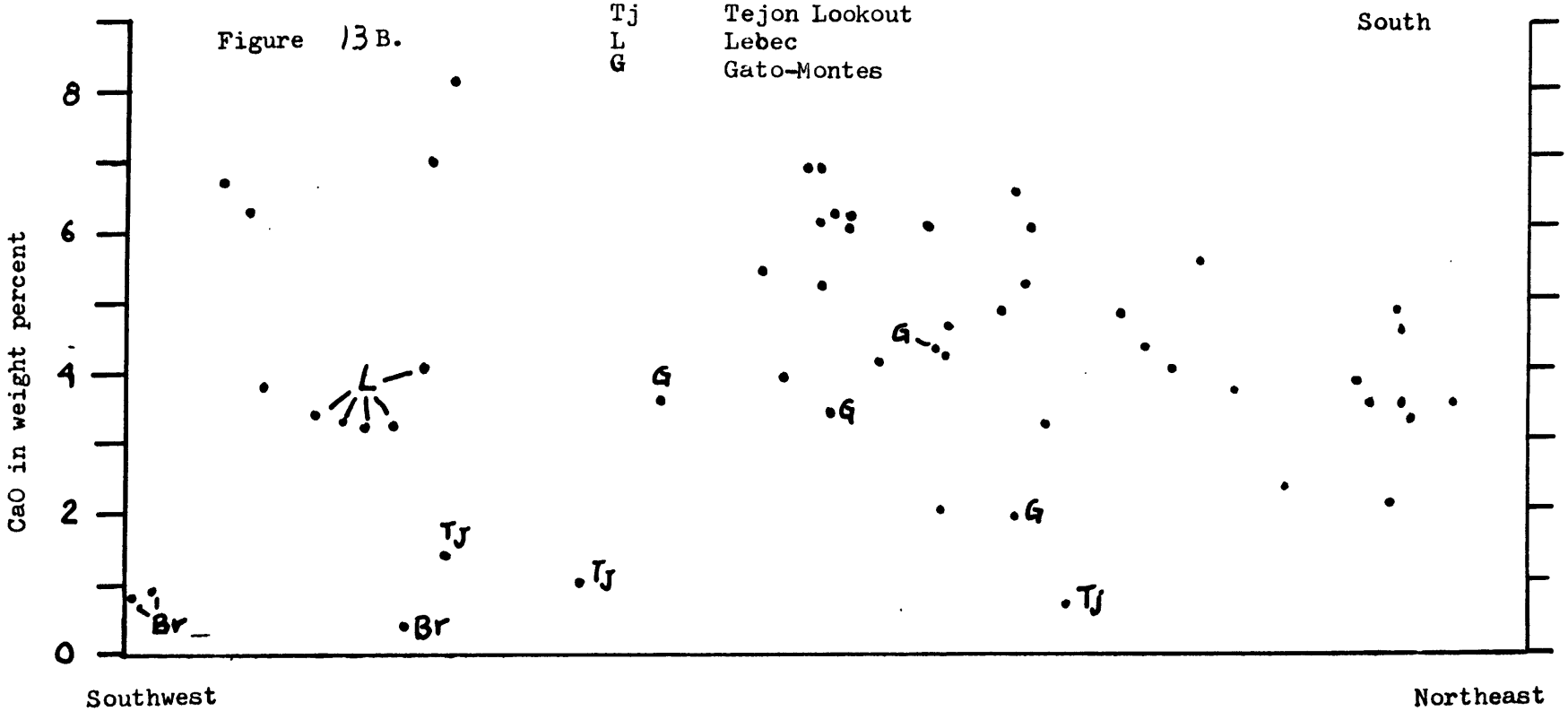

Figure 13C.

Figure 13D.

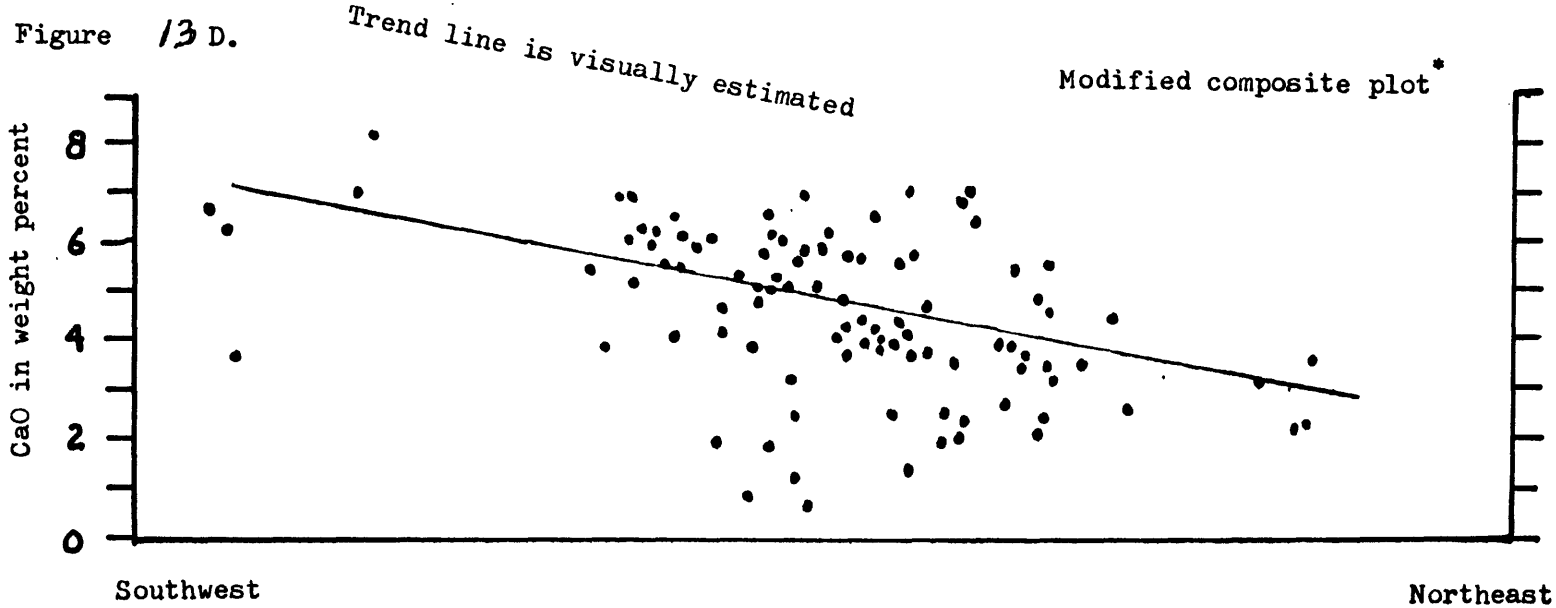

*/ Labeled samples from north and south cross-sections omitted

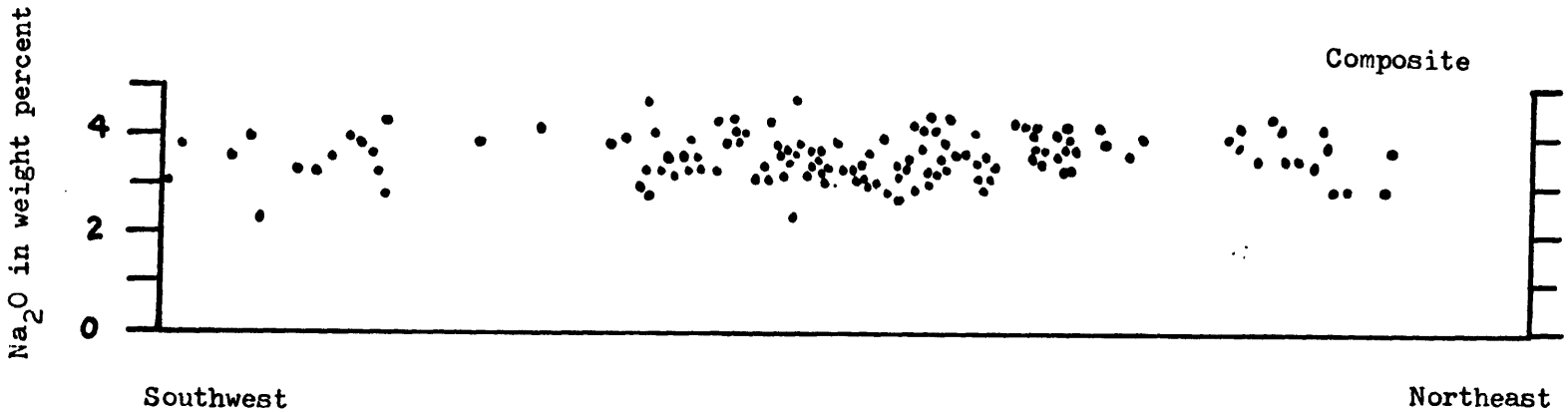

Figure 14. Variation in Na_2O across the southern part of the Sierra Nevada batholith. Composite section only as there is no visually apparent trend.

Figure 15. Variation of K_2O across the southern part of the Sierra Nevada batholith.

A. Cross-section north of lat 35° 30' N.
B. Cross-section south of lat 35° 30' N.
C. Composite of upper two cross-sections
D. Modified composite plot.

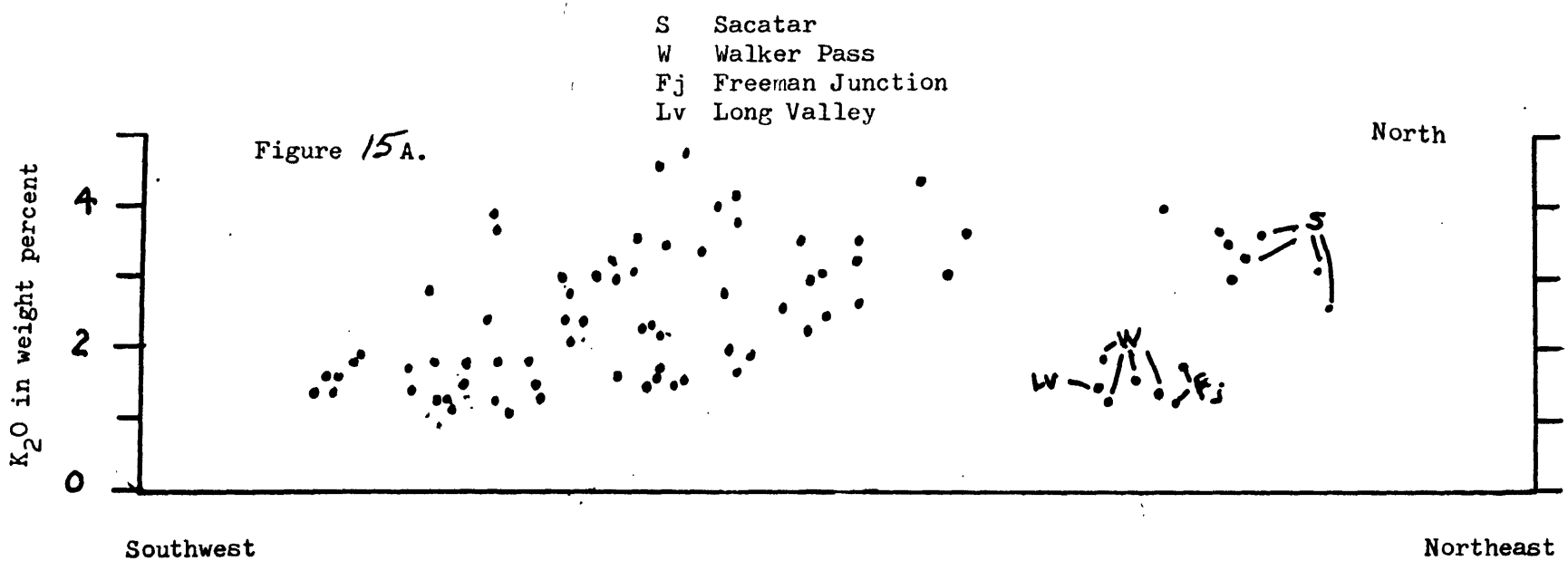

Figure 15A.

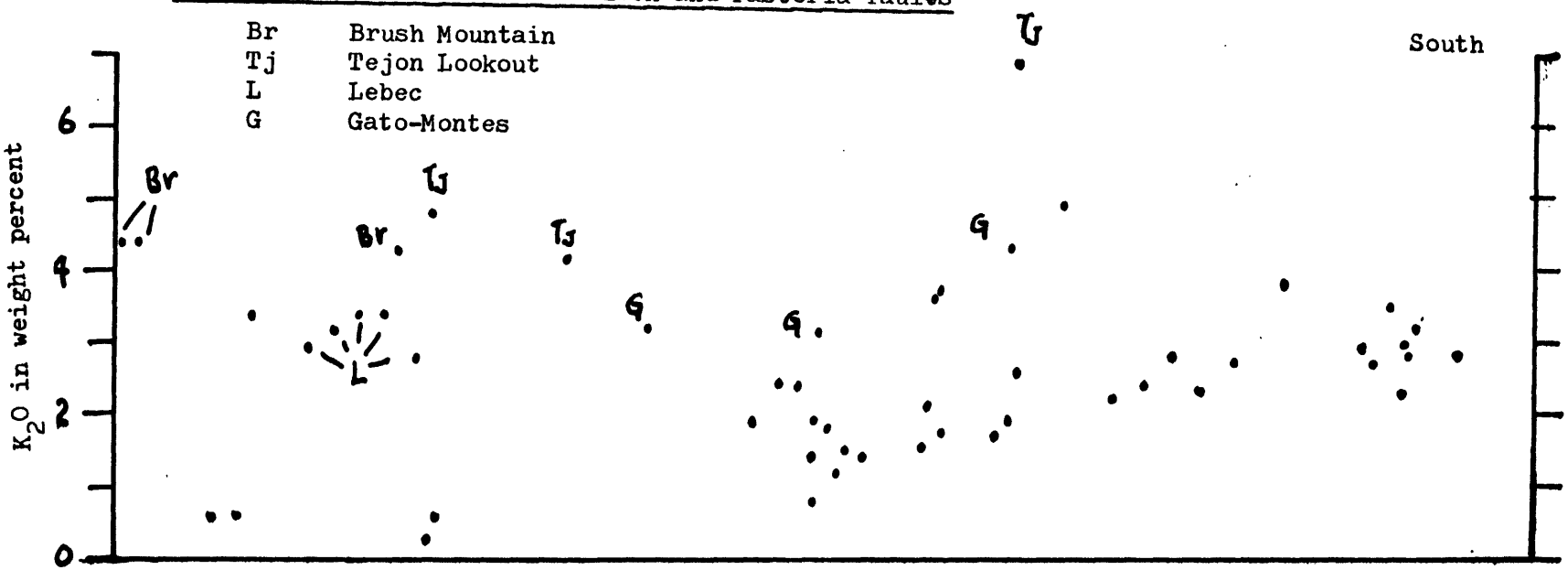

Figure 15 B.

Figure 15C.

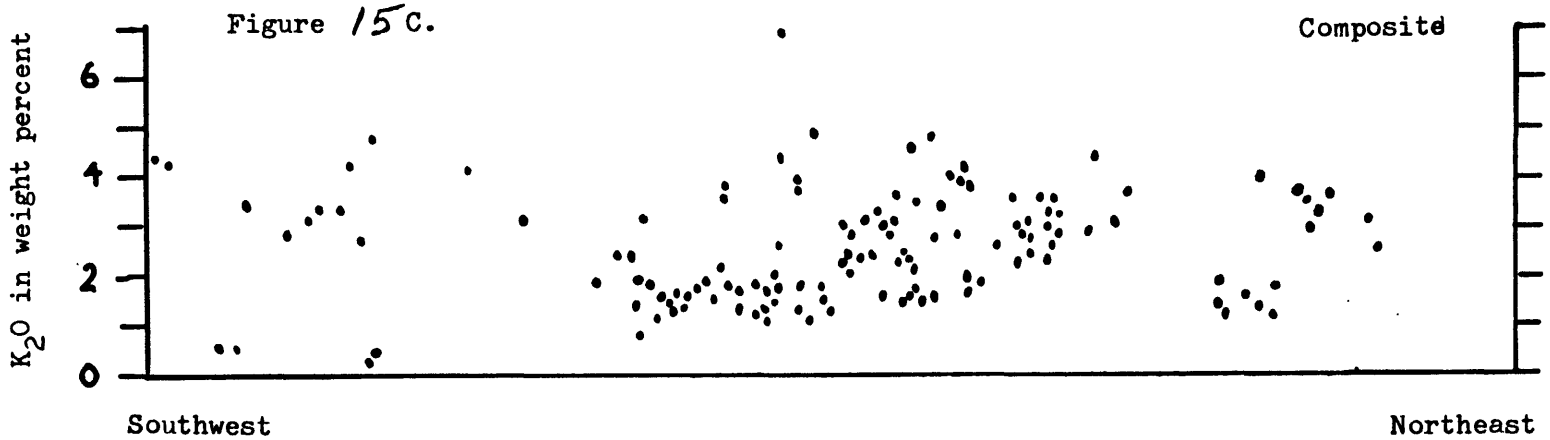

Figure 15D.

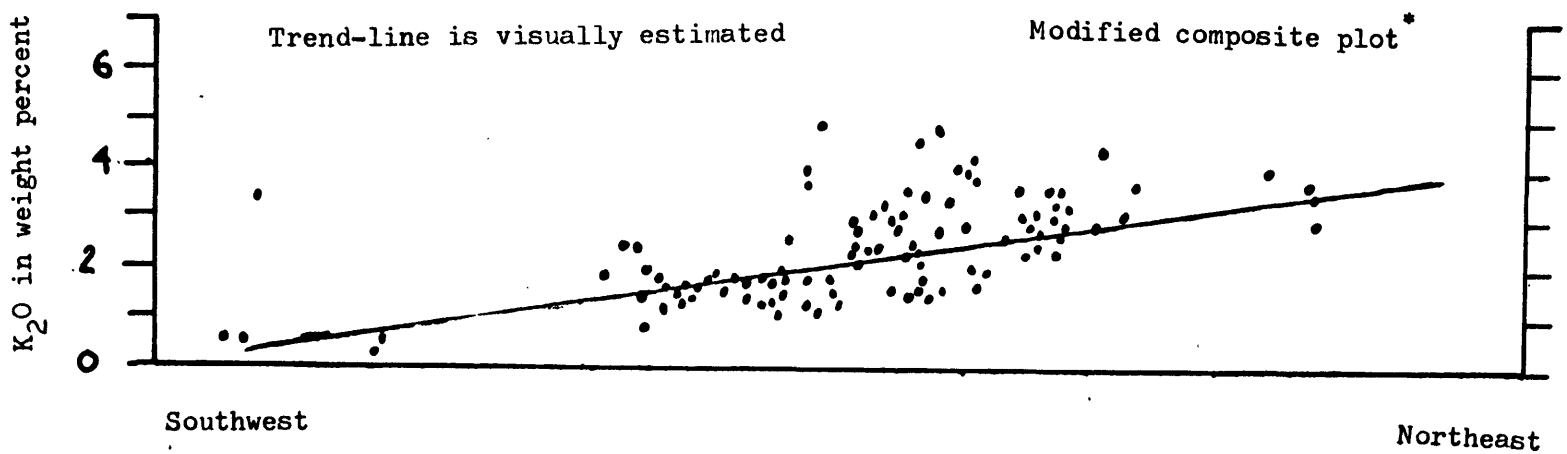

*/ Samples labeled on north and south cross sections omitted

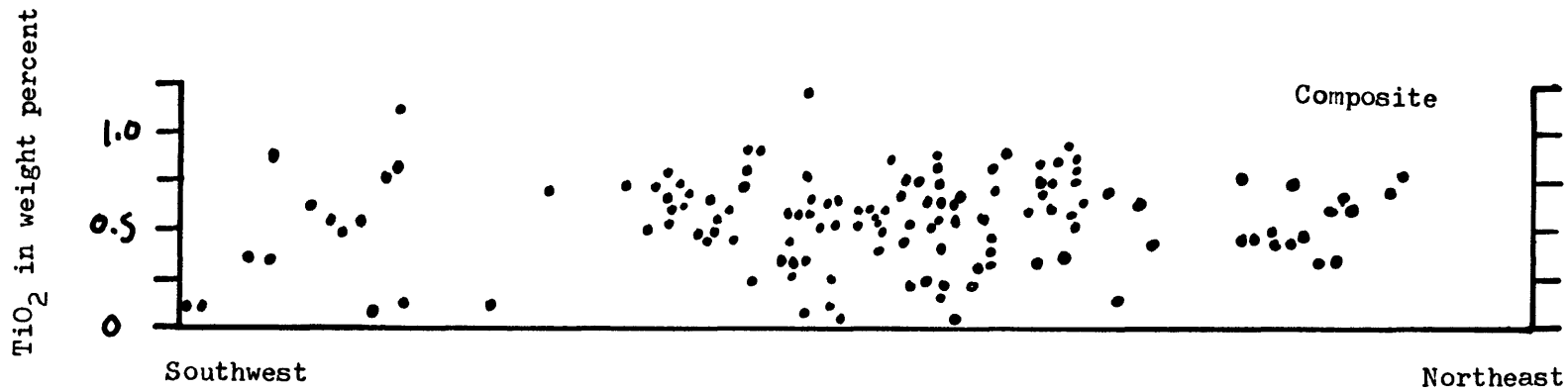

Figure 16. Variation in TiO_2 across the southern part of the Sierra Nevada batholith. Composite section only as there is no visually apparent trend.

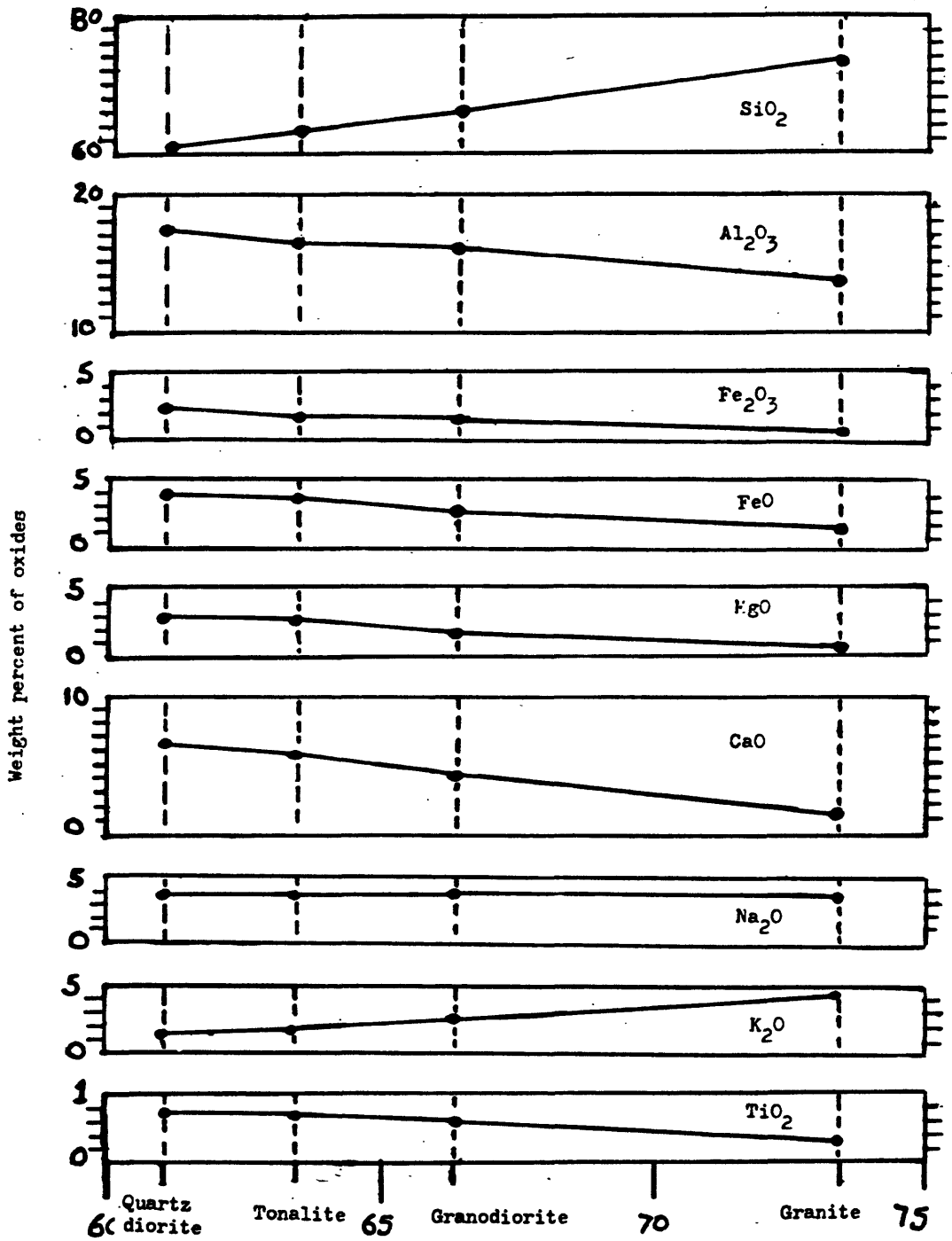

Figure 17. Silica variation ("Harker") diagrams for average compositions of major rock types (quartz diorite, tonalite, granodiorite, and granite), southern Sierra Nevada, California

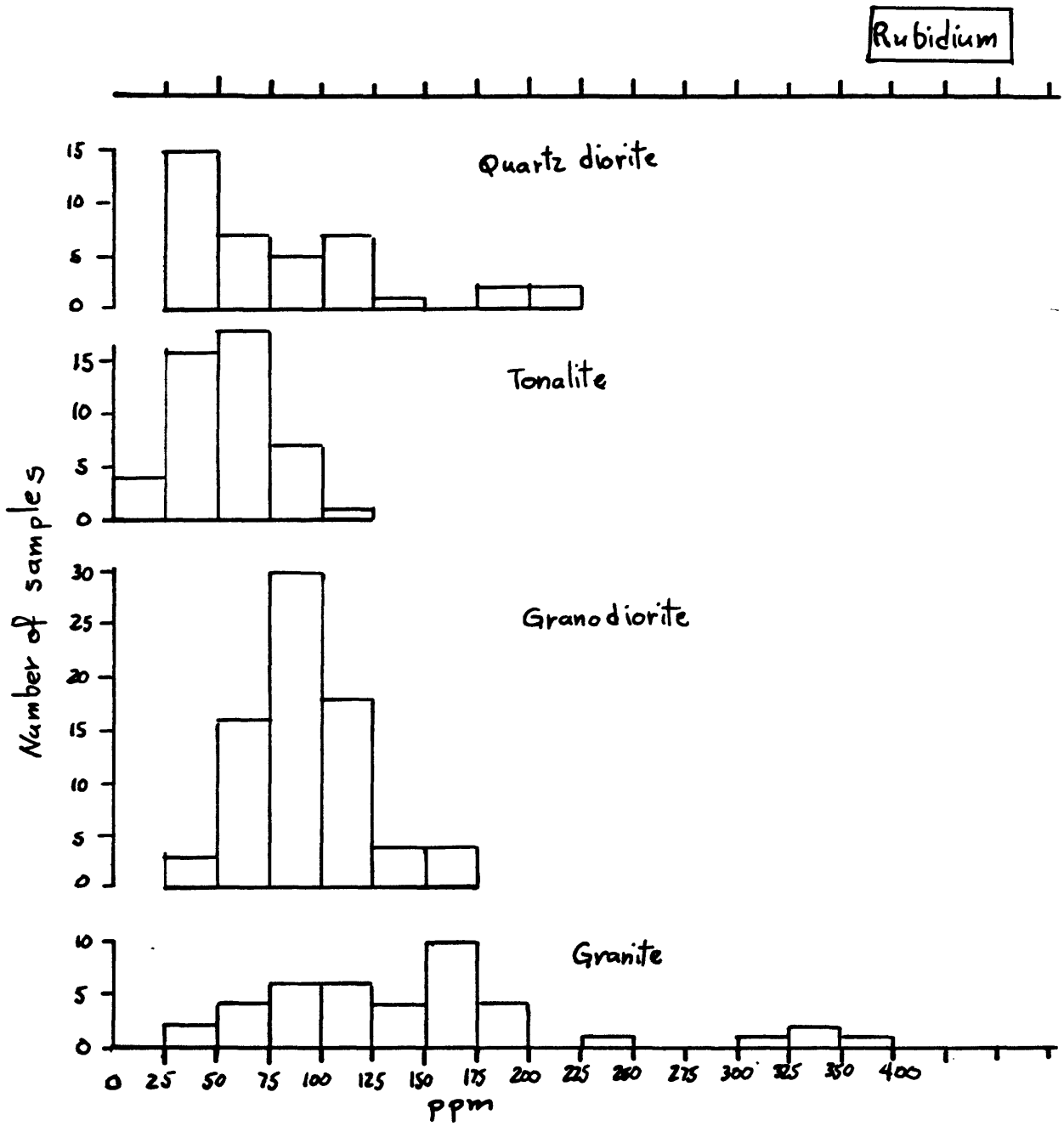

Figure 18. Histograms showing distribution of rubidium (in ppm) by rock type.

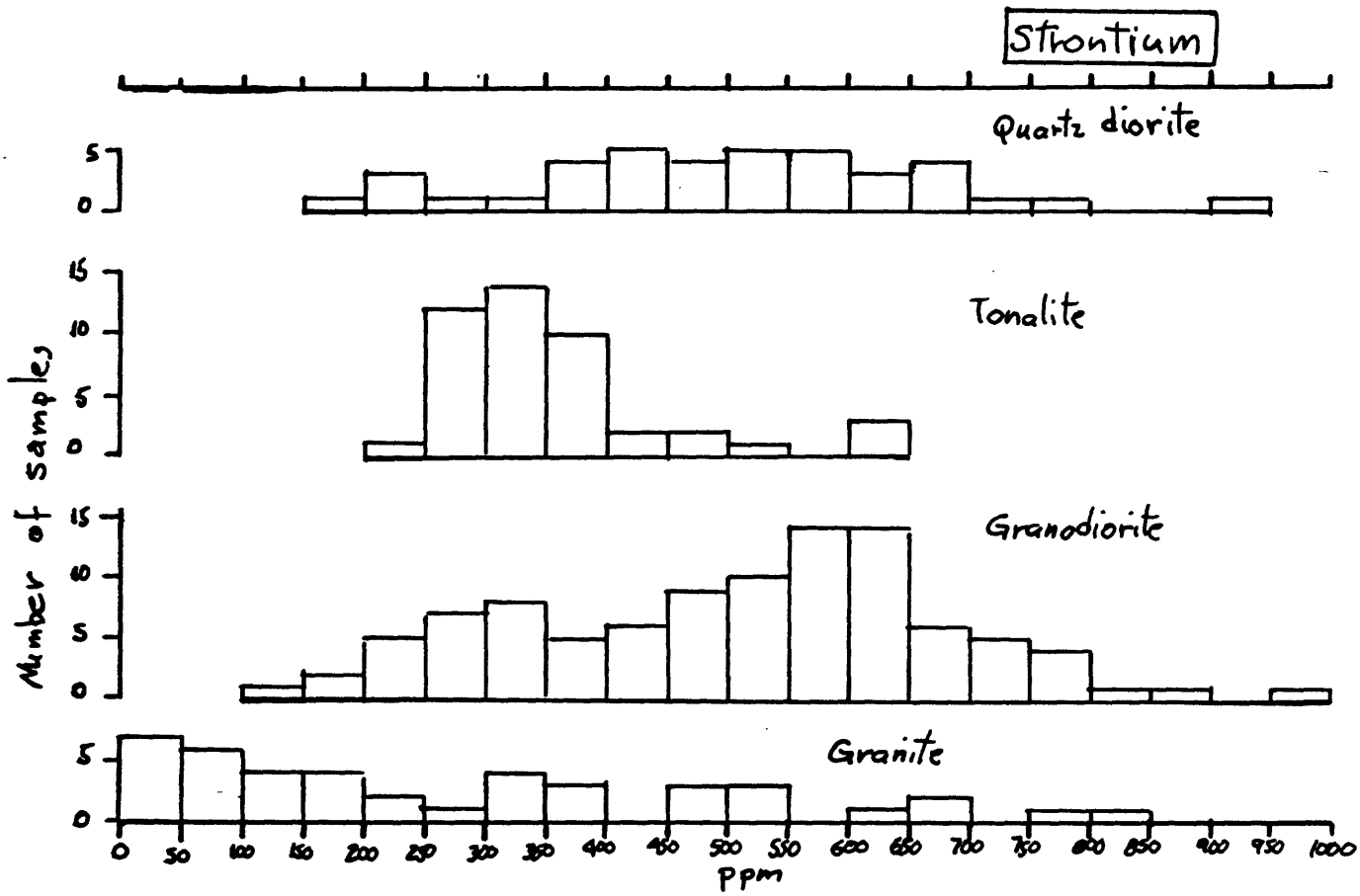

Figure 19. Histograms showing distribution of strontium (in ppm) by rock type.

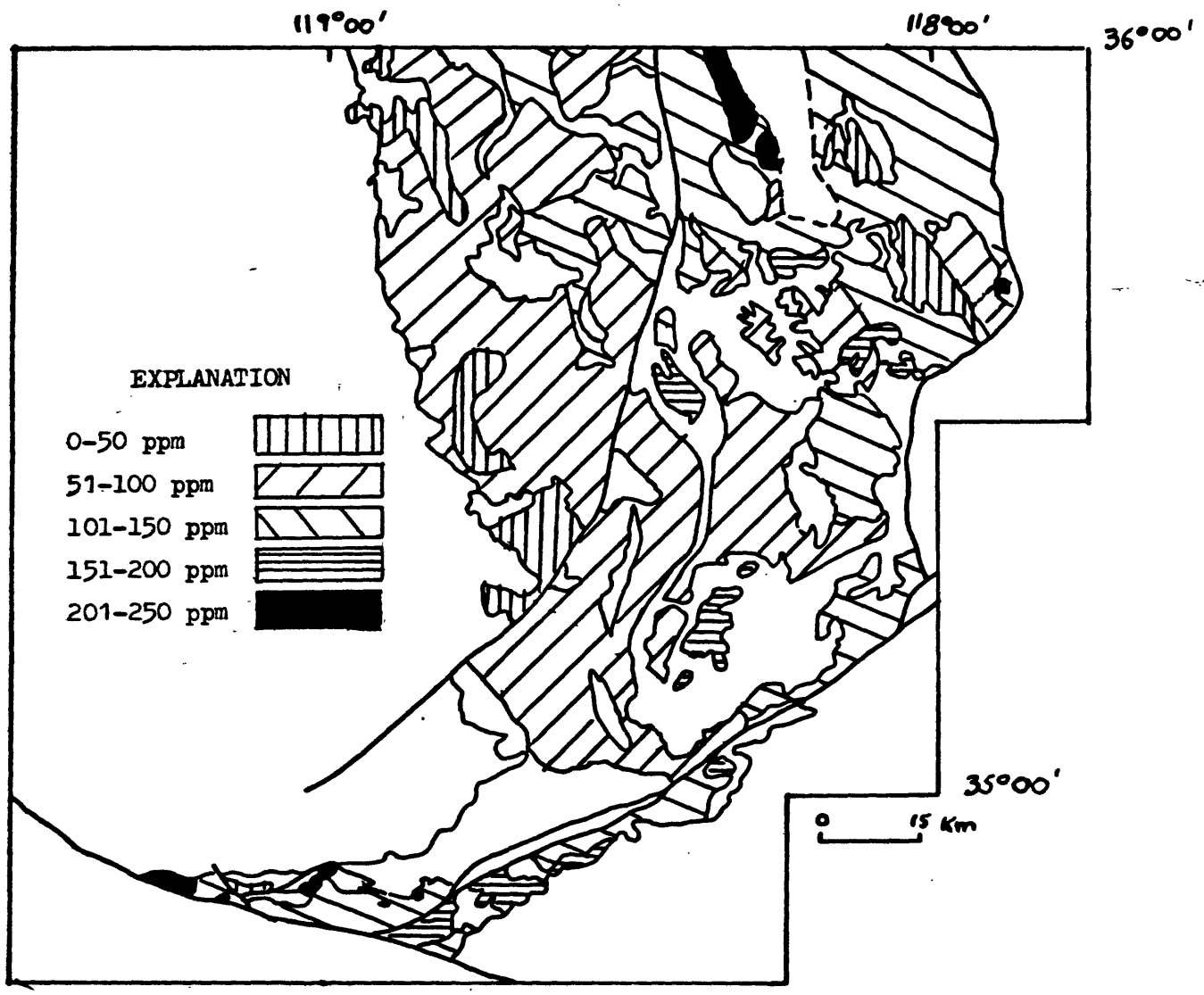

Figure 20. Index map of the southern Sierra Nevada showing distribution of rubidium in ppm based on pluton averages from Table 3.

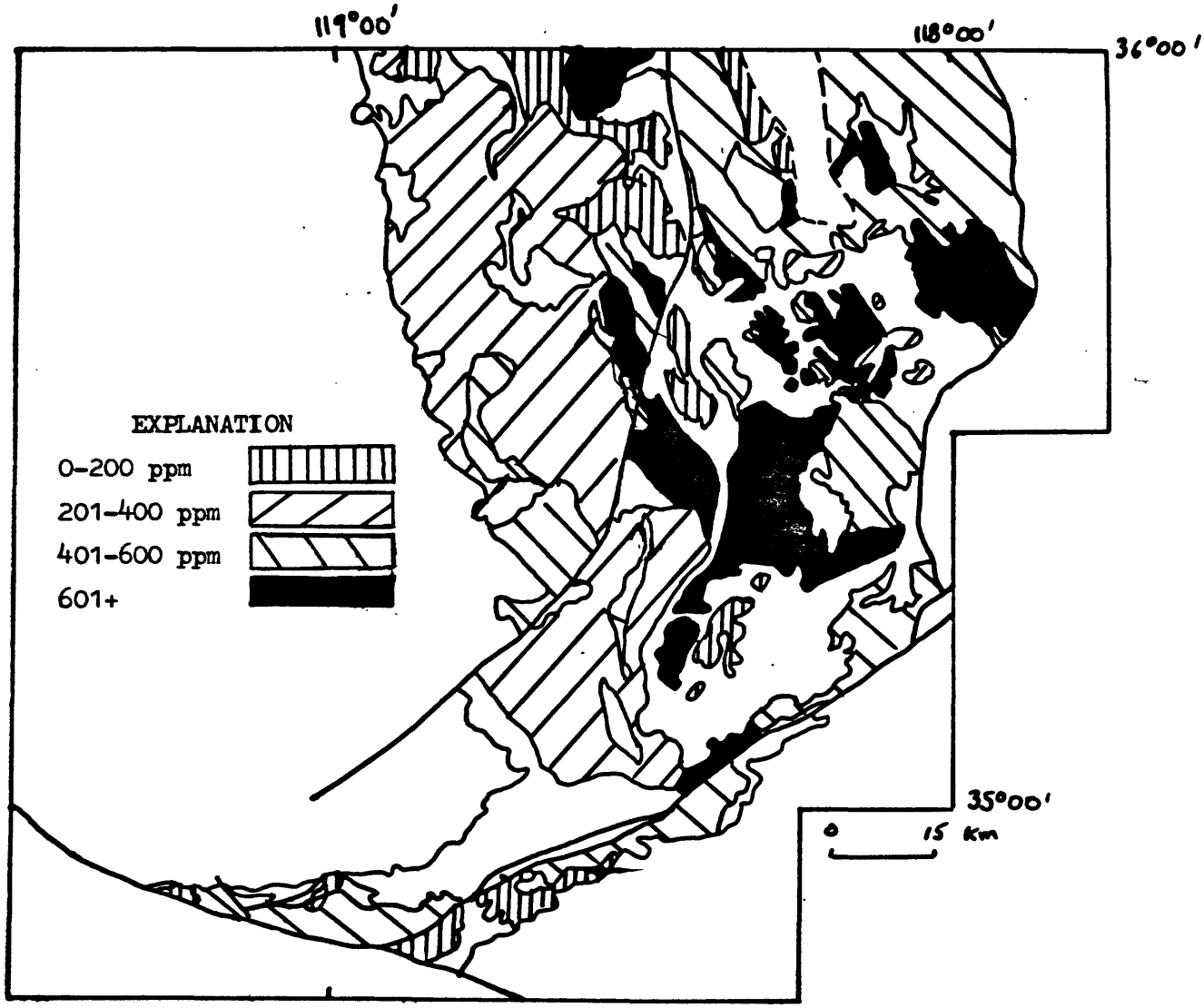

Figure 21. Index map of the southern Sierra Nevada showing distribution of strontium in ppm based on pluton averages from Table 3.

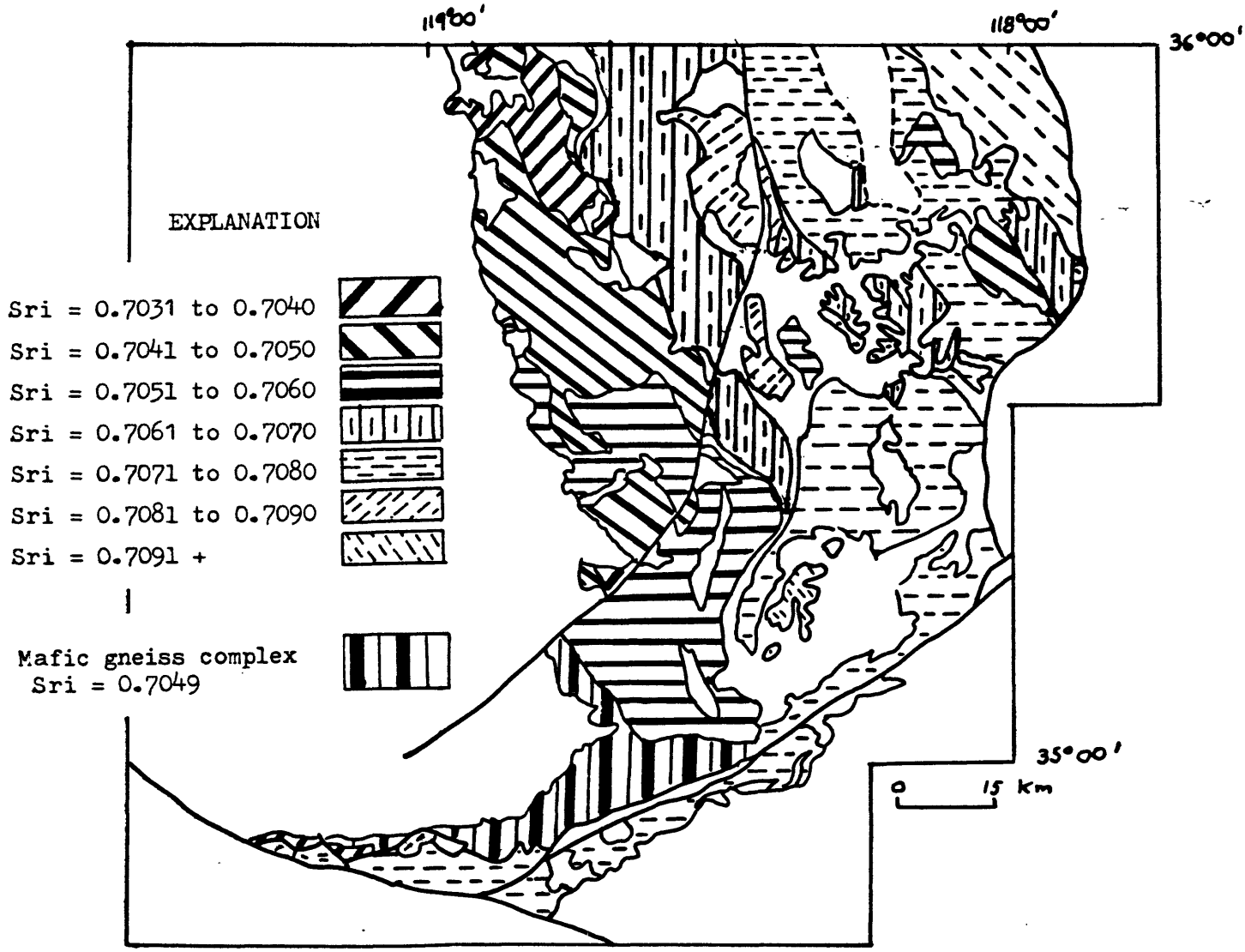

Figure 22. Index map of the southern Sierra Nevada showing distribution of initial strontium ratio (Sri) based on pluton averages from Table 3.

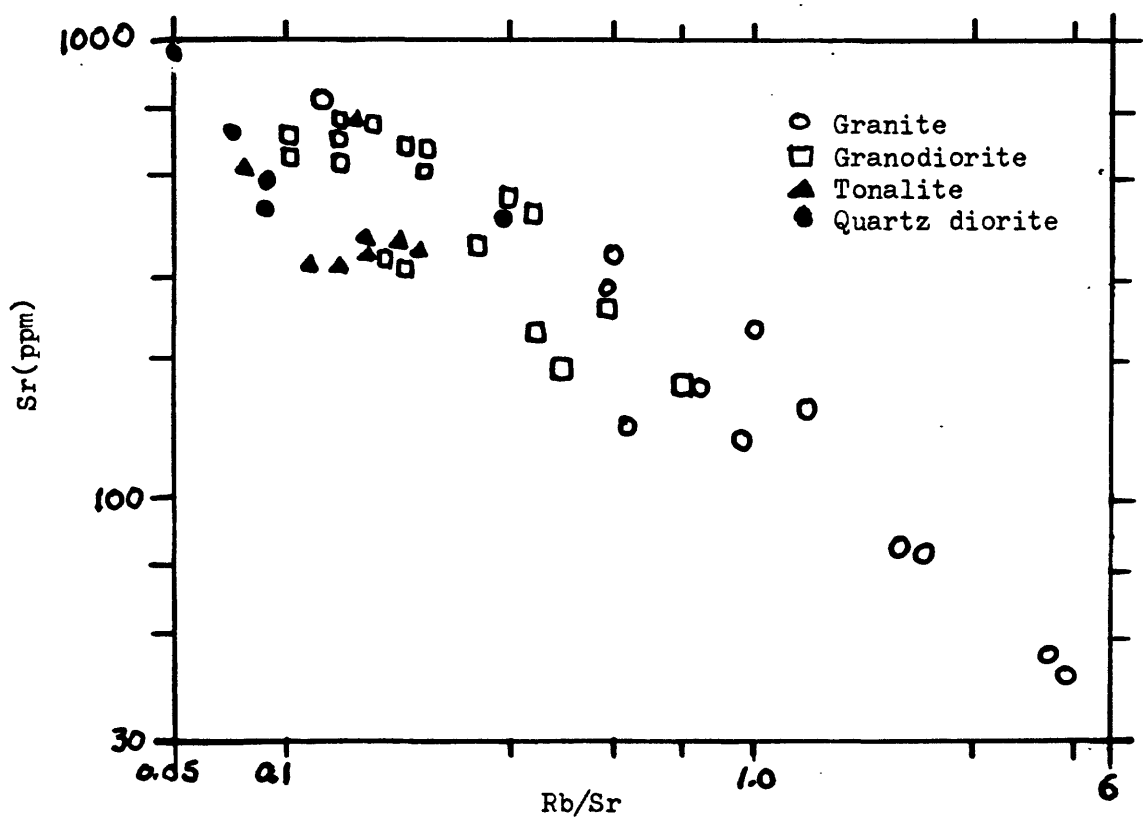

Figure 23. Rb/Sr-Sr variation diagram

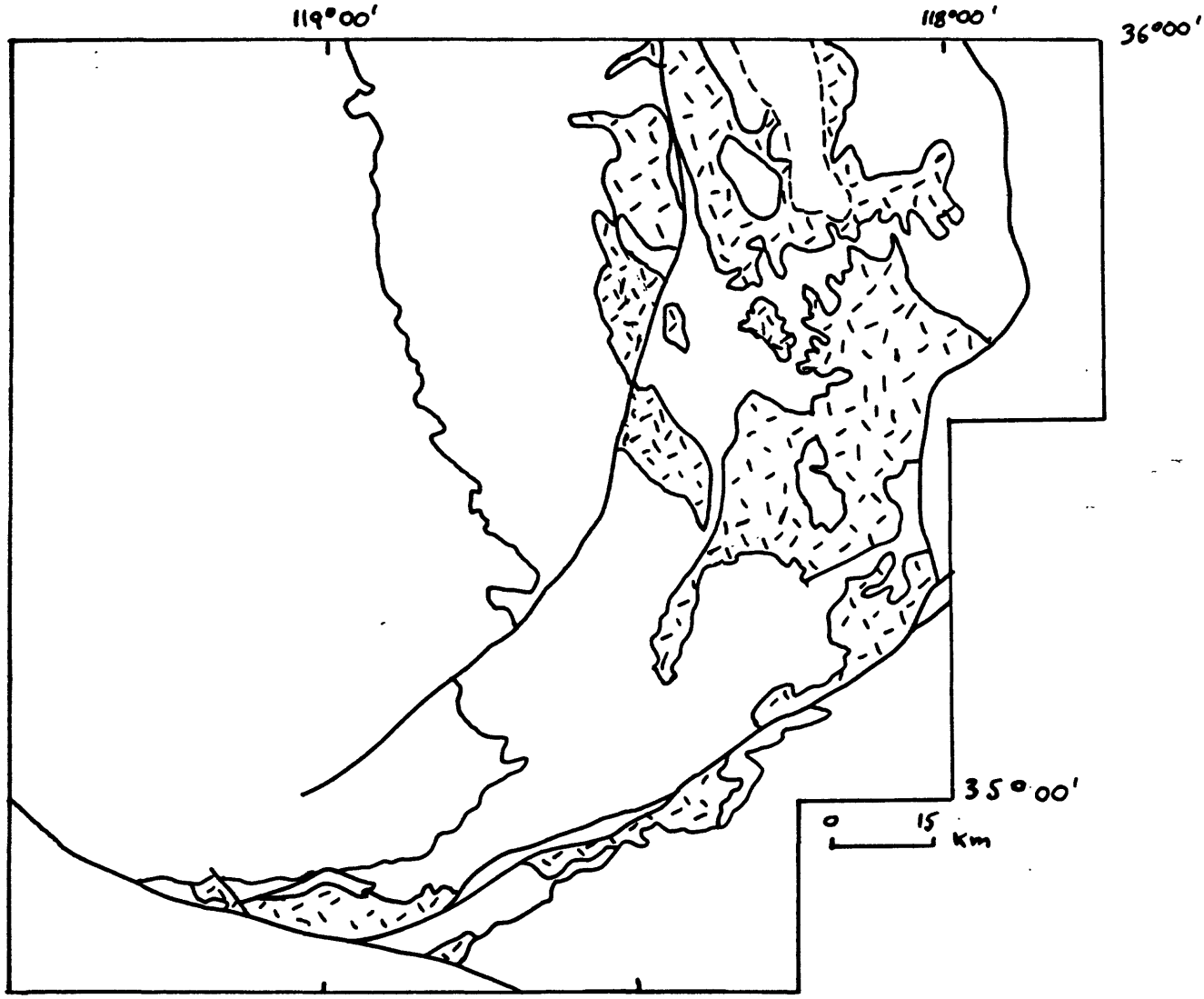

Figure 24. Distribution of granitic rocks that have $\delta^{18}O$ of greater than +9 per mil SMOW and also have Sr_i greater than 0.706

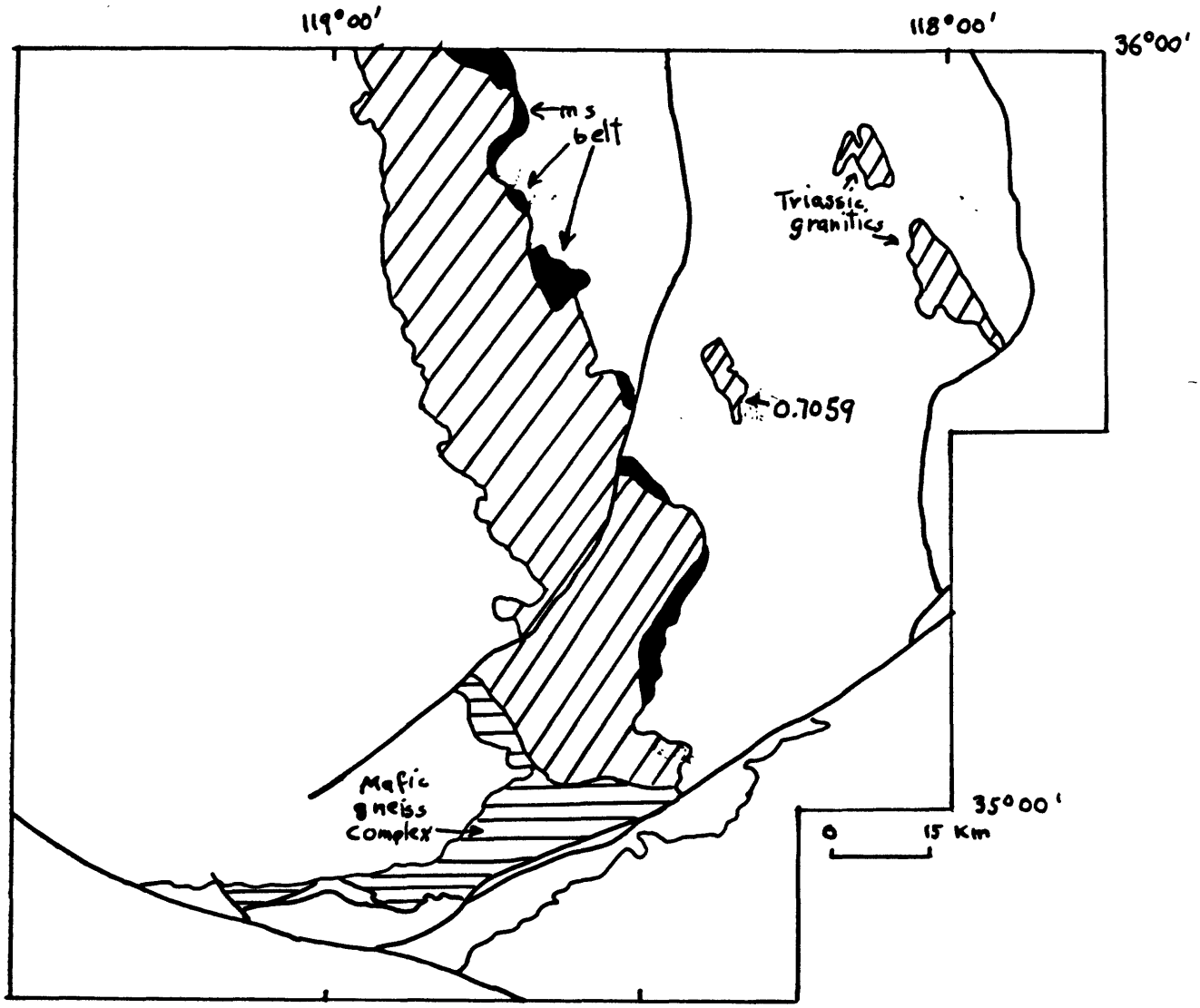

Figure 25. Distribution of granitic rocks (slant bar pattern) and orthogneiss and quartz diorite in the mafic gneiss complex (horizontal bar pattern) with Rb of less than 100 ppm and Sri less than 0.706.

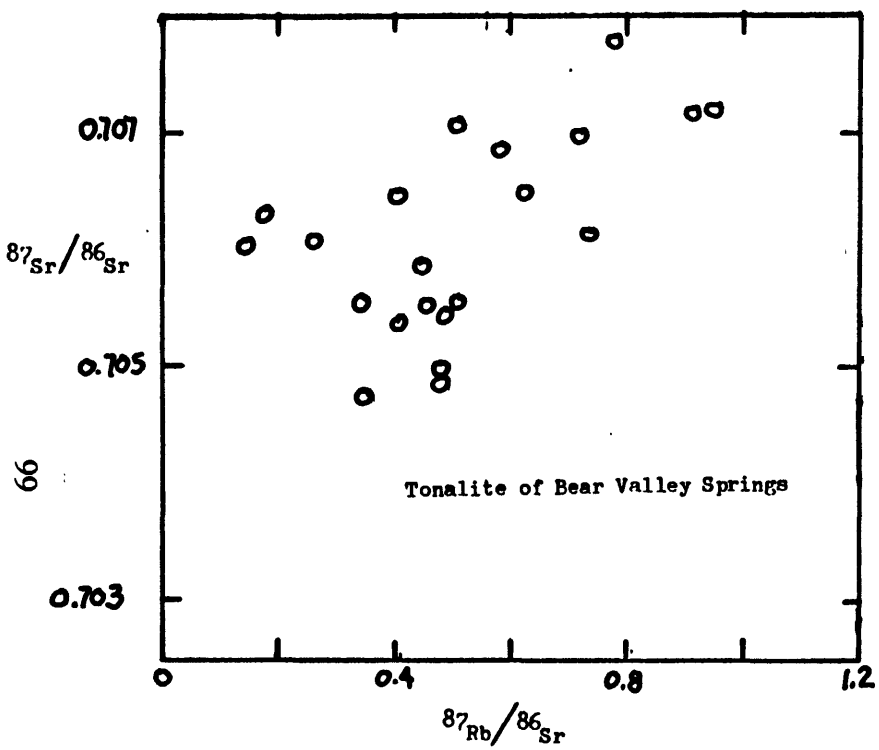

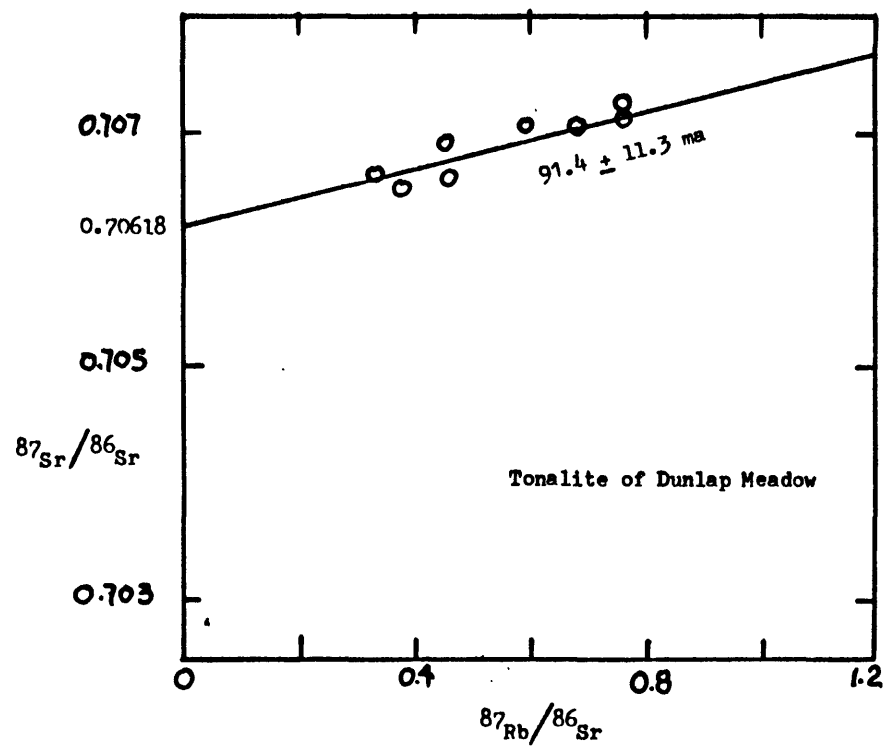

Figure 26. Example of contrast in evolution diagram patterns in similar tonalites.

EXPLANATION

▲

Strong fluxion structure
(protomylonite, mylonite, ultramylonite)

●

Modest fluxion structure (or none)
(slivered granulated, and brecciated rocks;
includes some augen gneiss)

//////

Linear zones of concentrated cataclasis

1. Kern Canyon-Breckenridge-White Wolf fault zone
2. North-south zone (proto-Kern Canyon fault?)
   (bifurcated by younger granitic
   intrusives at north end)
3. Sierra Nevada fault zone
4. North branch of Garlock fault zone

Figure 27. Simplified index map of the southern Sierra Nevada showing location of petrographically examined cataclastic rocks.

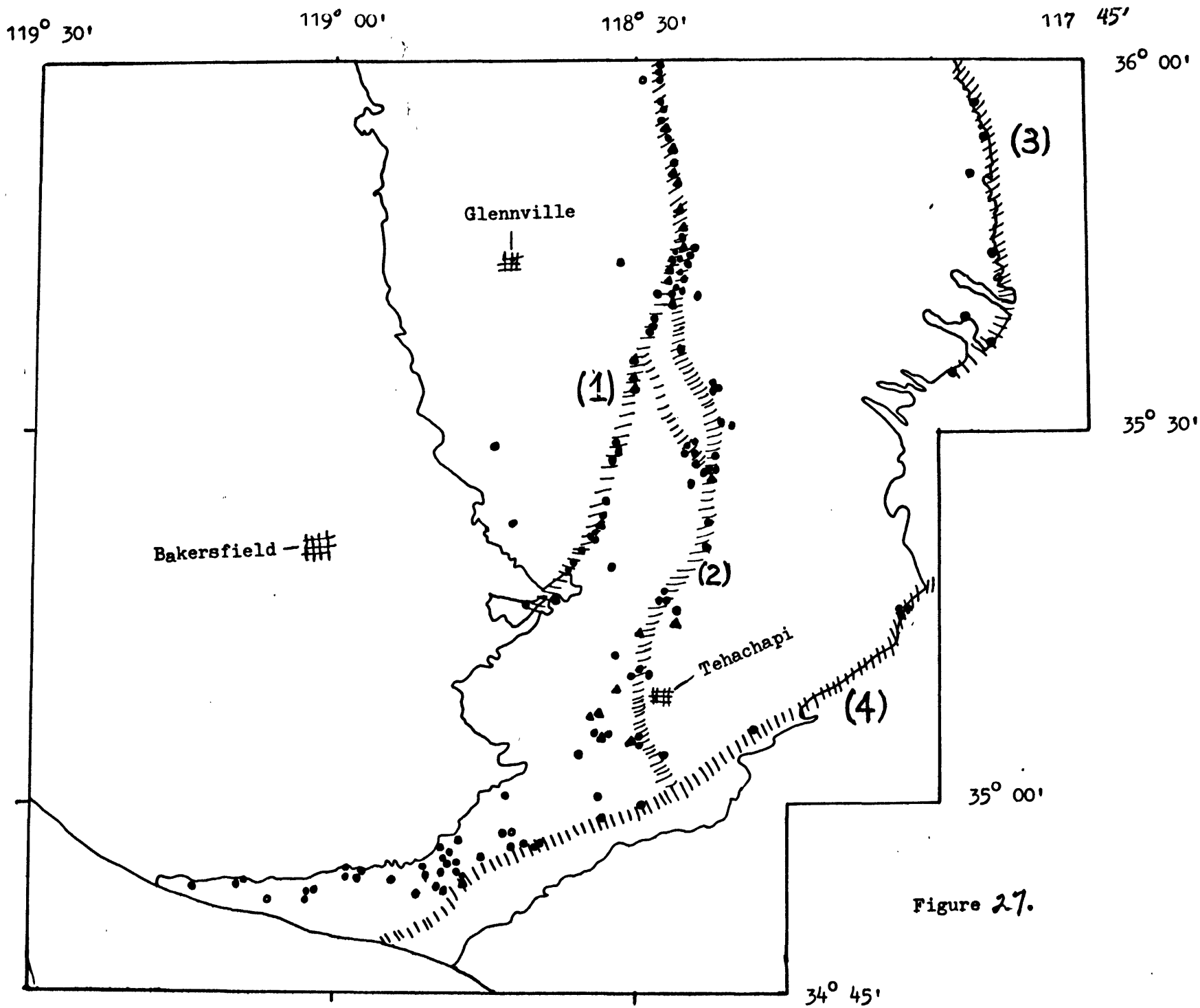
119° 30'
119° 00'
118° 30'
117 45'
36° 00'
35° 30'
35° 00'
34° 45'
Glennville
Bakersfield
Tehachapi
(1)
(2)
(3)
(4)

Figure 27.

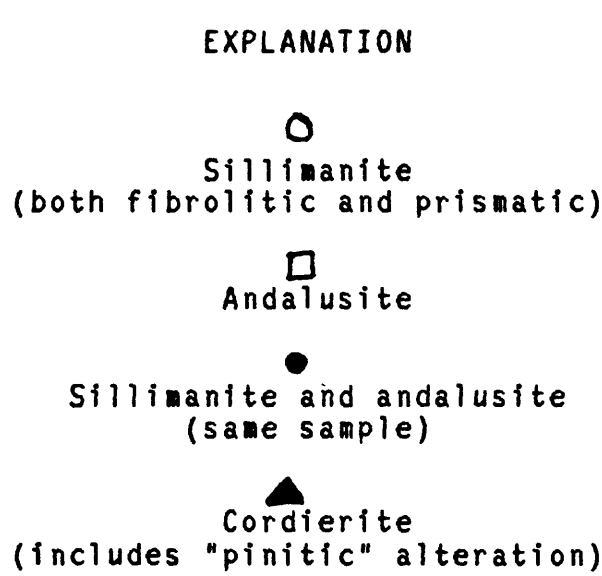

Figure 28. Index map showing location of thin section identified aluminosilicates in the southern Sierra Nevada, California

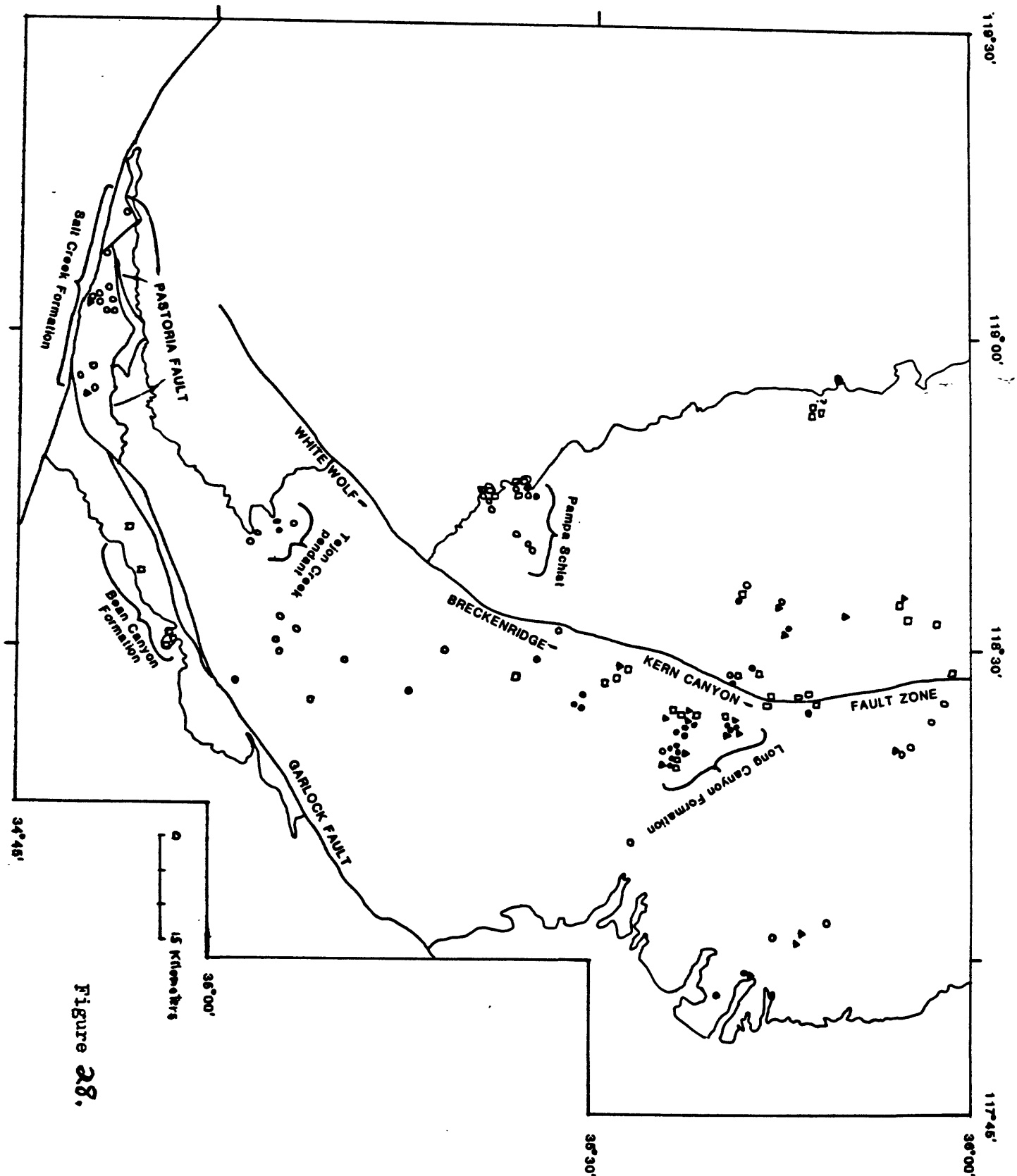
Sall Creek Formation
PASTORIA FAULT
WHITE WOLF
Teion Creek pendant
Bean Canyon Formation
Pampa Schist
BRECKENRIDGE
KERN CANYON
FAULT ZONE
Long Canyon Formation
GARLOCK FAULT
15 Kilometers
119°30'
119°00'
118°30'
117°45'
35°30'
35°00'
34°45'
36°00'

Figure 28.

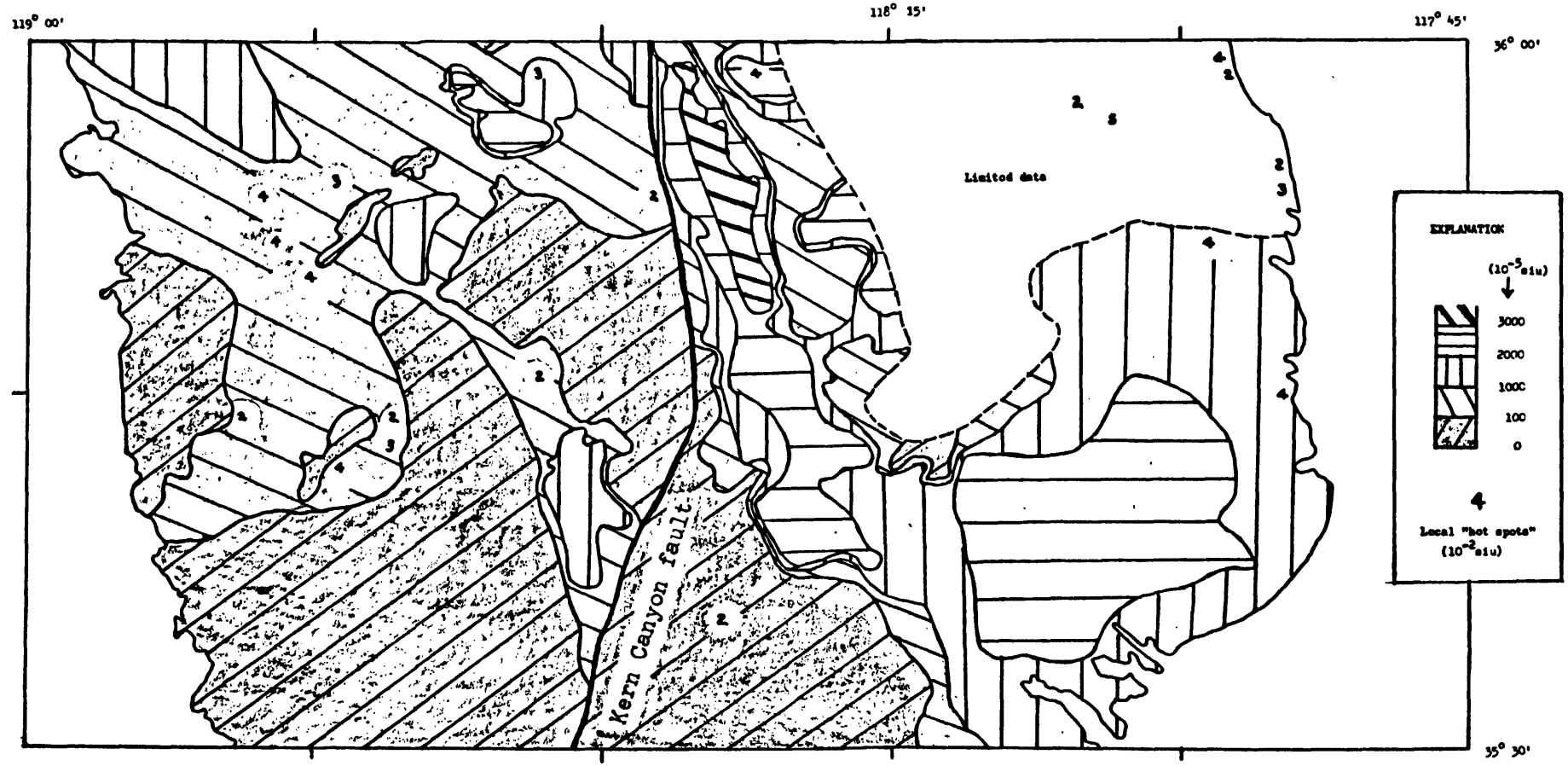

Figure 29. Magnetic susceptibility pattern in area of Plate 1.

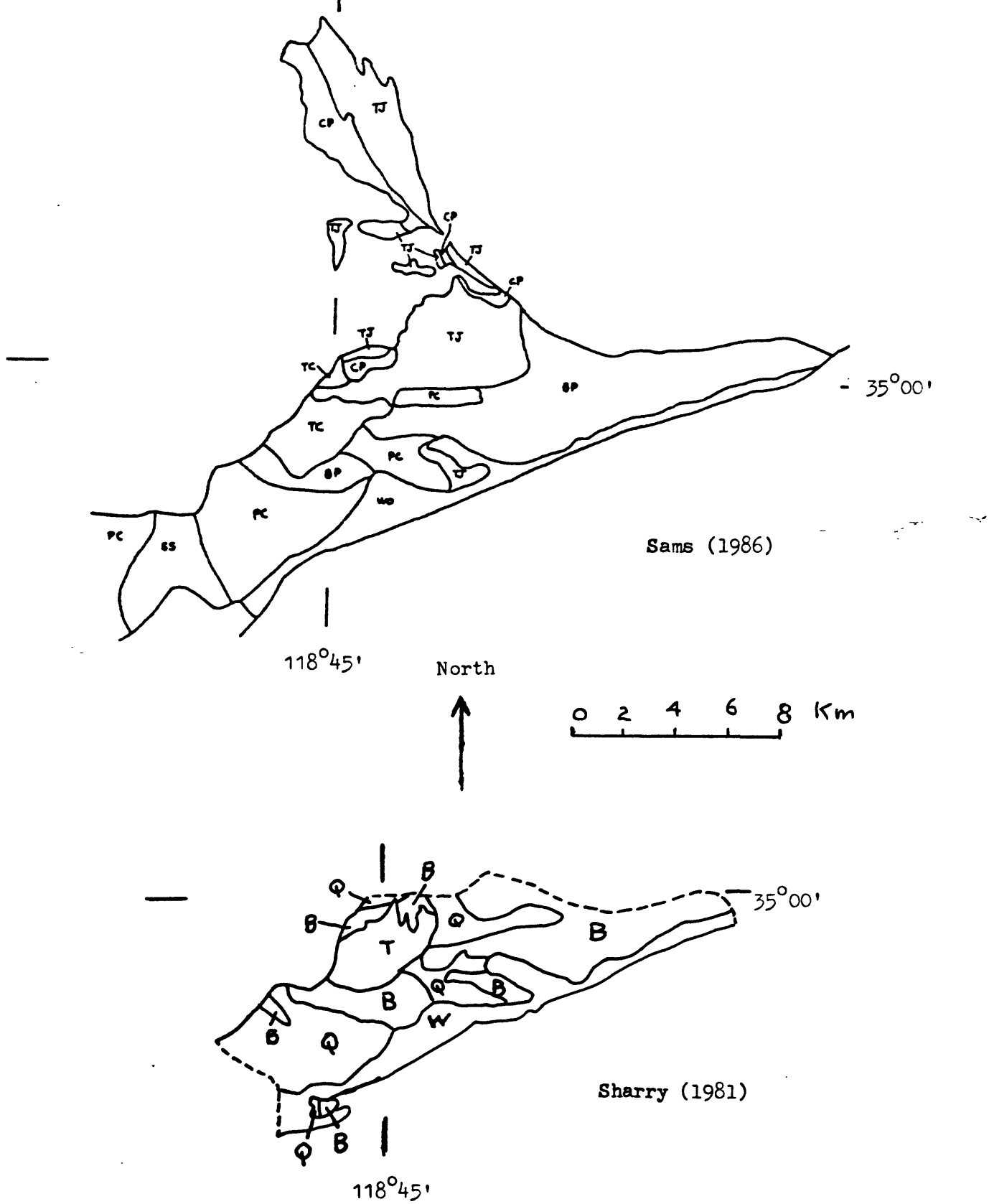

Figure 30. Comparison of geologic maps of Sams (1986) and Sharry (1981) for part of the mafic gneiss complex showing distribution of map units. Both maps at same scale (~1:200,000)

EXPLANATION

(for Fig. 30)

Map units
(mineral content)

BP Hypersthene tonalite of Bison Peak
(plag + qtz + biot + hbnd ± opx)

TC Metagabbro of Tunis Creek
(plag + hbnd ± cpx ± opx ± garnet ± qtz)

SS Metagabbro of Squirrel Spring
(plag + hbnd ± qtz)

TJ Tonalitic gneiss of Tejon Creek
(plag + qtz + biot + hbnd ± opx ± cpx ± garnet)

WO Dioritic gneiss of White Oak
(plag + hbnd ± qtz ± biot)

PC Quartzo-feldspathic gneiss of Pastoria Creek
(qtz + plag + biot ± hbnd ± cpx ± opx ± garnet)

CP Paragneiss of Comanche Point
(qtz + plag + biot ± K-fld ± garnet ± graphite ± musc ± cpx ± hbnd)

Sams (1986)

EXPLANATION (CONT.)

(for Fig. 30)

Map units
(mineral content)

Q Quartzo-feldspathic gneiss
(qtz + plag + biot ± hbnd ± opx ± K-feld)

B Bison Granulite
(plag + hbnd + qtz + biot ± op x ± cpx)

T Tunis Creek Garnet Granulite
(plag + hbnd ± opx ± garnet)

W White Oak Diorite $G_n$eiss
(plag + hbnd + minor qtz) (much shearing)

Sharry (1981)

Figure 31. Index maps showing location of petrographically examined samples from the major rock types of the mafic gneiss complex (Ross, 1983b), southern Sierra Nevada, California.

A. Amphibolite and amphibolite gneiss
(dominantly plag + hbnd)

B. Tonalitic gneiss and granofels*
(dominantly plag + qtz + biot + hbnd)

C. Quartzofeldspathic gneiss and granofels (generally relatively felsic) (dominantly plag + qtz + biot ± hbnd)

---

*/ Includes some relatively homogeneous tonalite-quartz diorite samples with hornblende > biotite (and generally hornblende >> biotite).

Figure 31A.

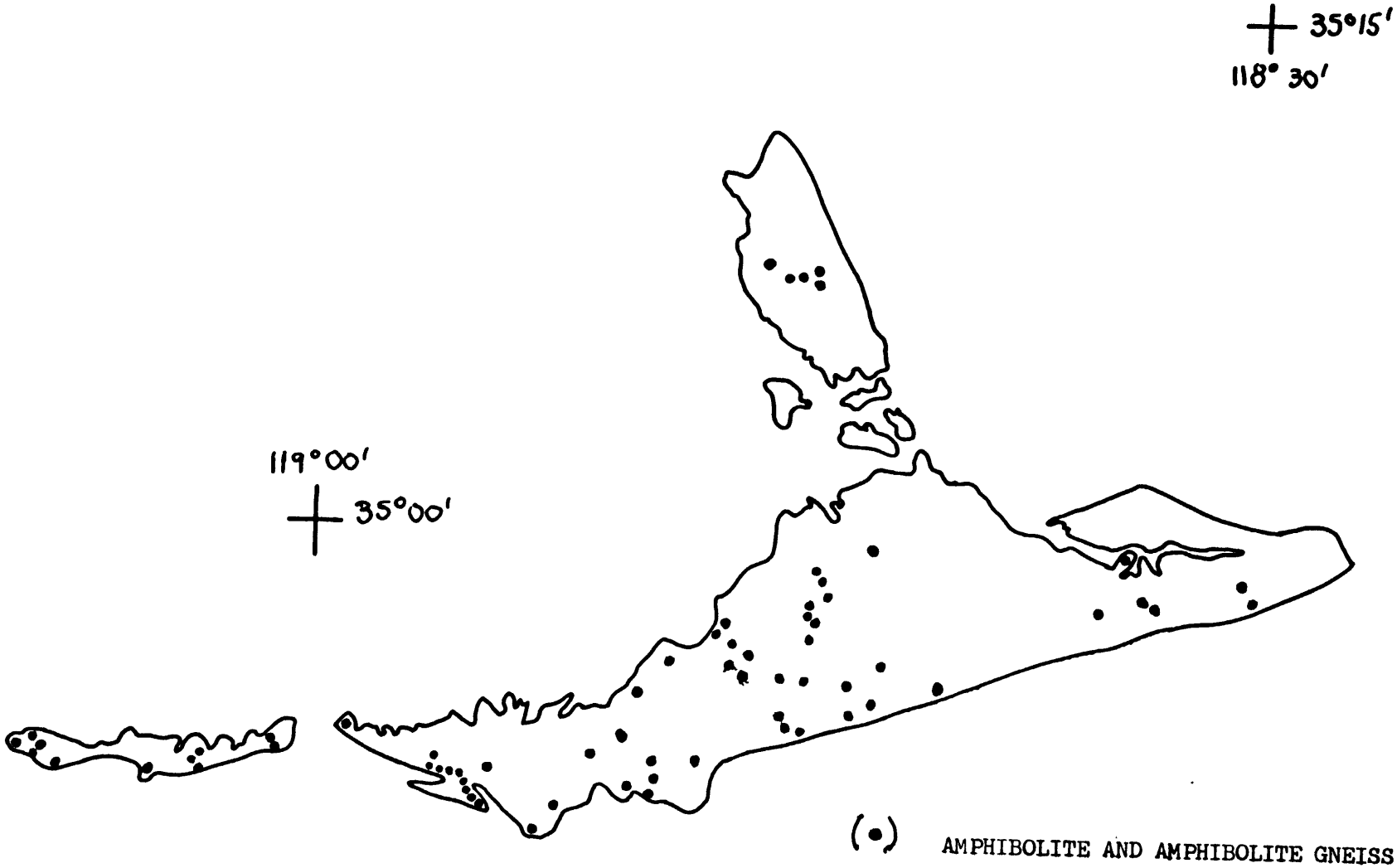

Figure 31 B.

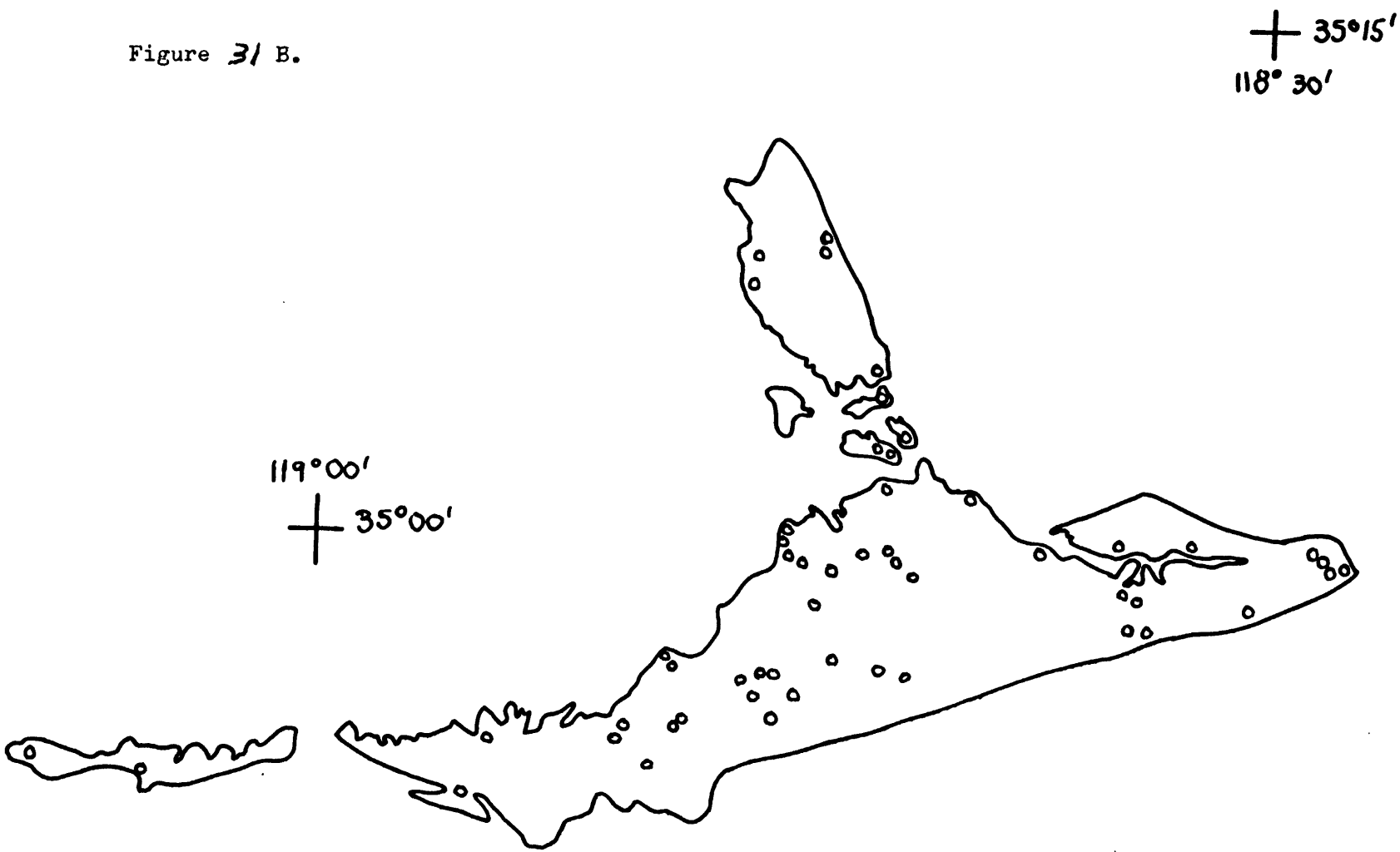

(o) TONALITIC GNEISS AND GRANOFELS

Figure 31 c.

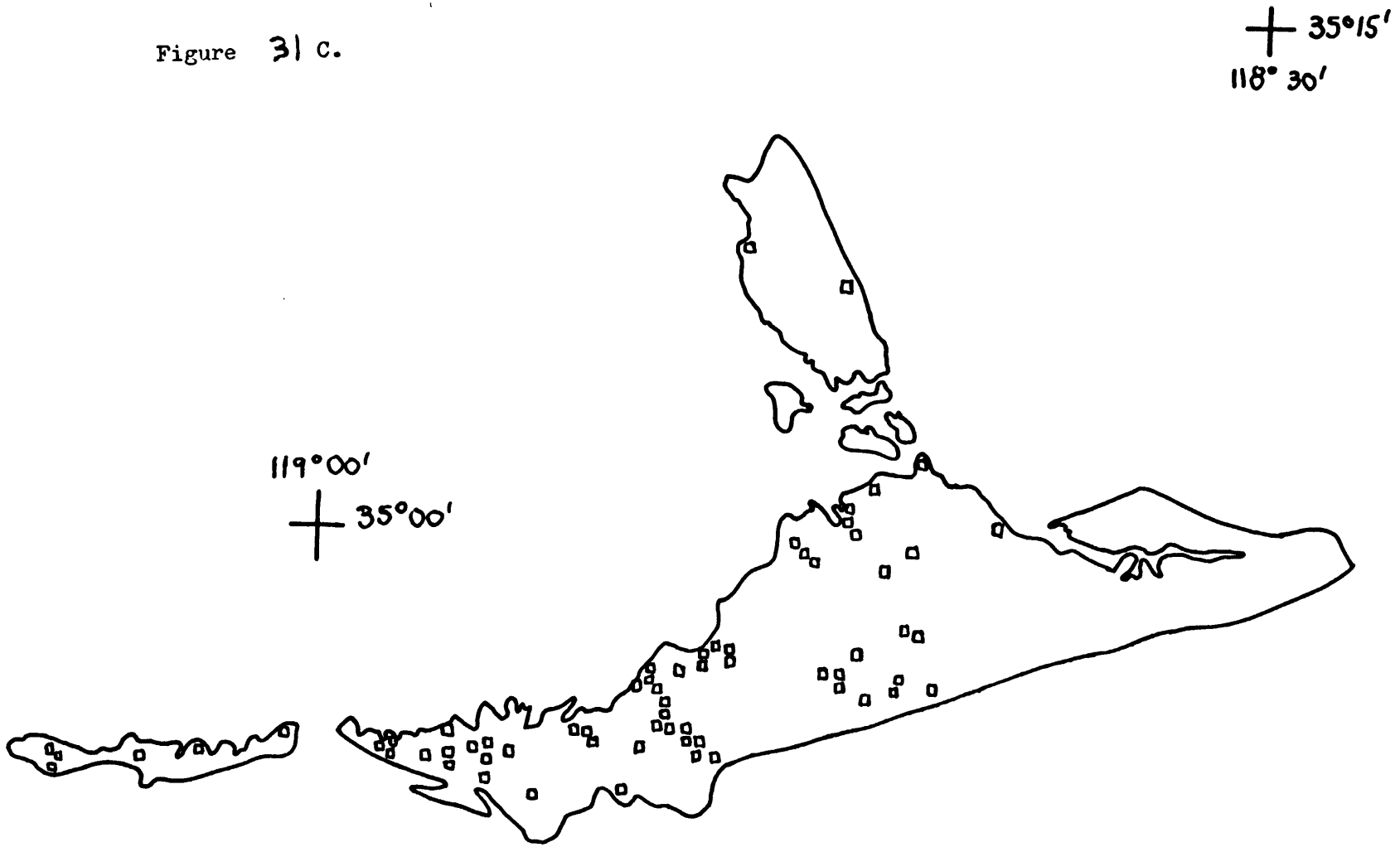

(□) QUARTZOFELDSPATHIC GNEISS AND GRANOFELS

Figure 32. Sample locations from figure 31 superposed on a simplified and generalized version of the geologic map of Sams (1986) for part of the mafic gneiss complex of the southern Sierra Nevada, California. (see fig. 30 for Sams' map units)

A. Amphibolite and amphibolite gneiss
B. Tonalitic gneiss and granofels
C. Quartzofeldspathic gneiss and granofels

Figure 32A.

(for explanation of map symbols see fig. 30)

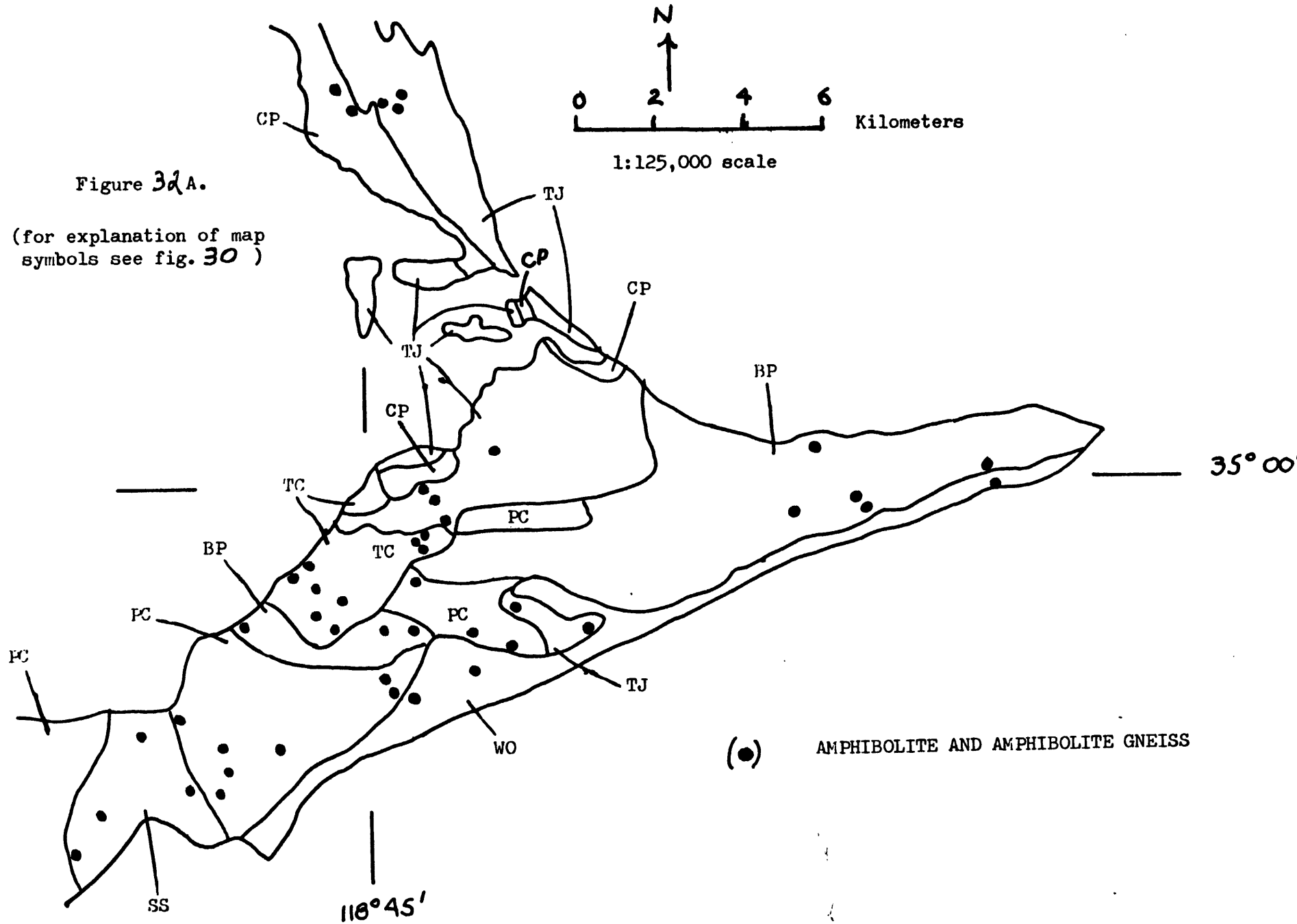

Figure 32B.

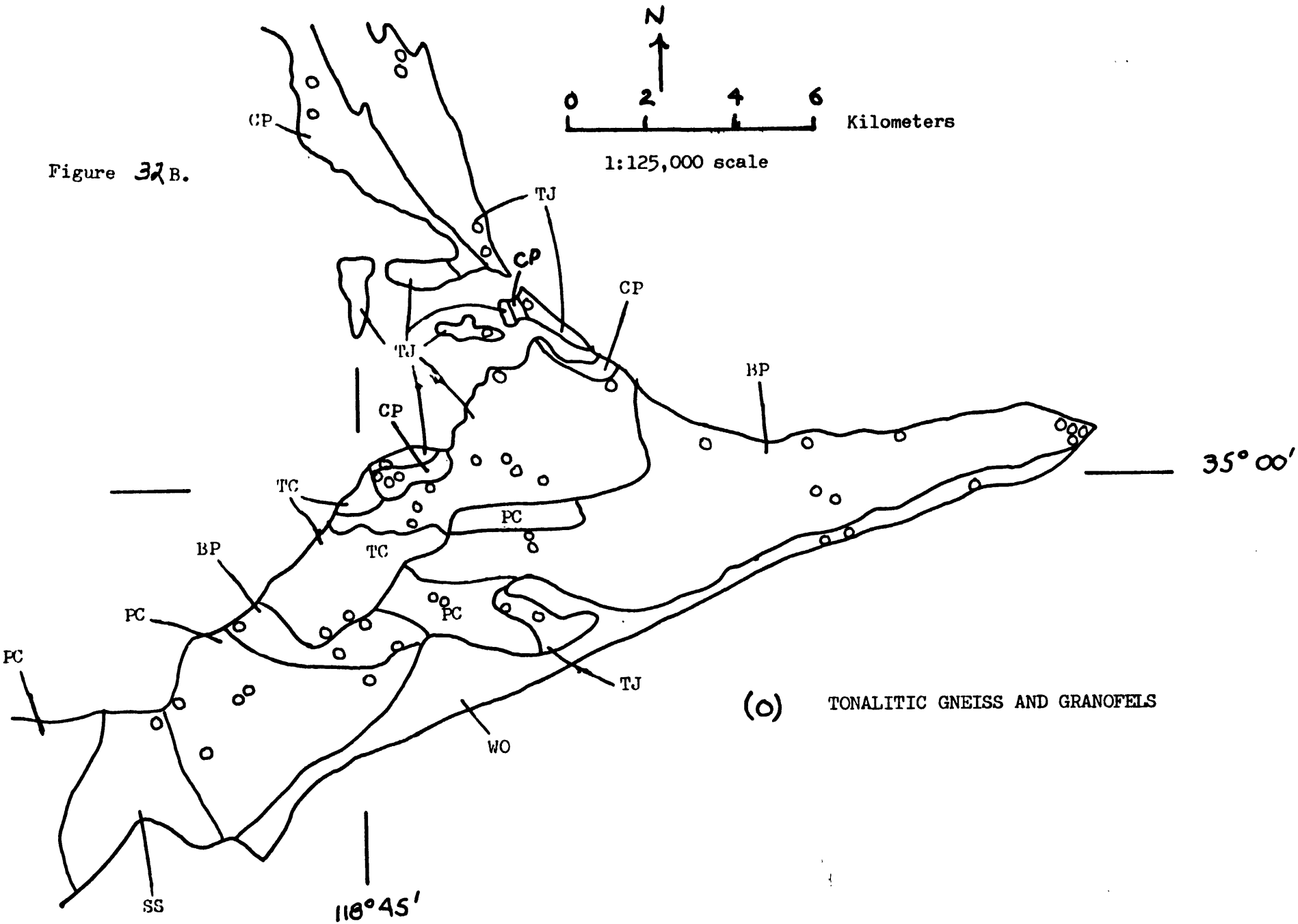
N
0 2 4 6
Kilometers
1:125,000 scale
CP
TJ
CP
CP
TJ
BP
CP
35° 00'
TC
PC
BP
TC
PC
PC
PC
TJ
WO
SS
118°45'
(o) TONALITIC GNEISS AND GRANOFELS

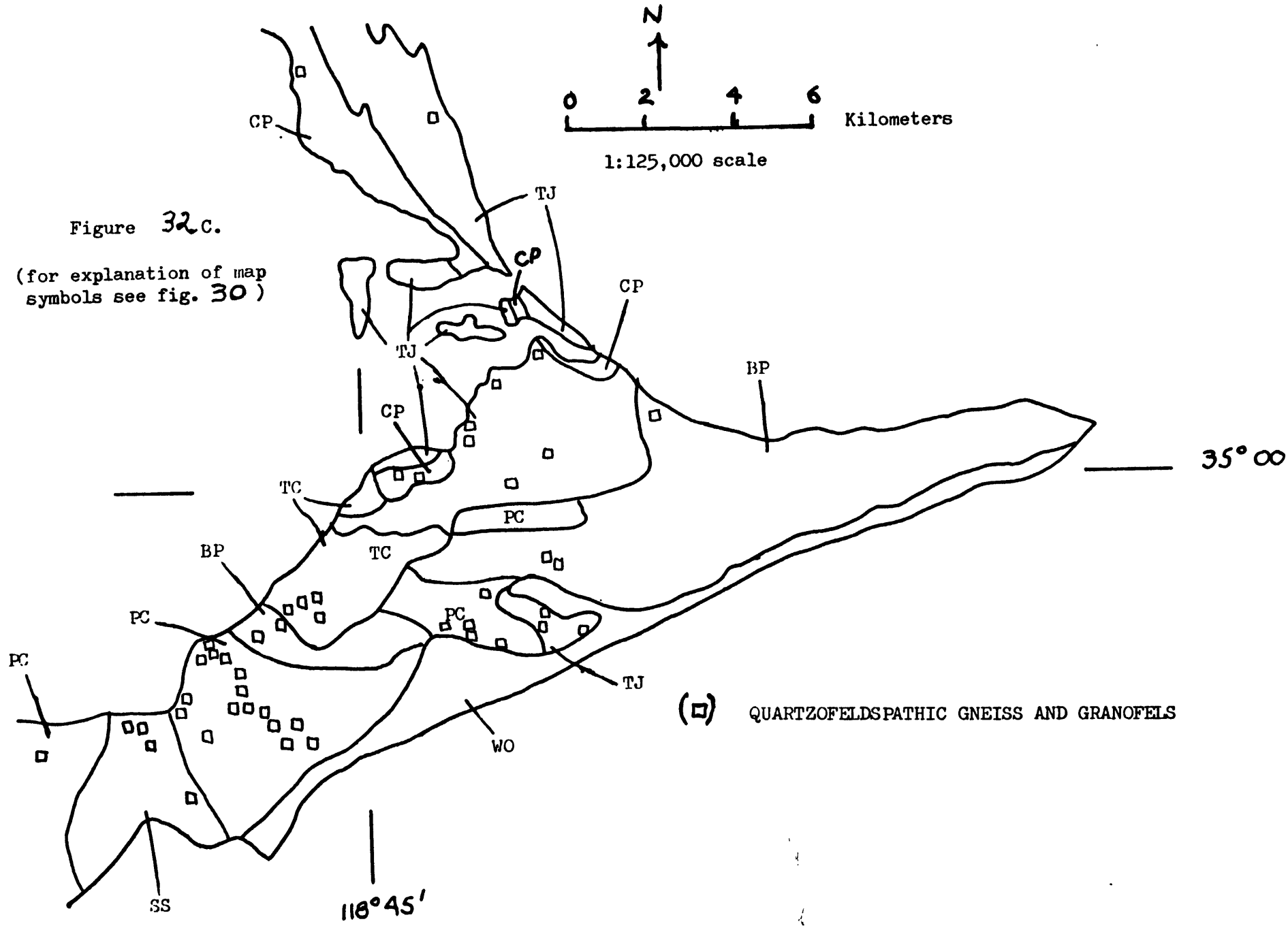

Figure 32c.

(for explanation of map symbols see fig. 30)

Table 1. Modes of granitic samples from Reservation Road

Sample Number	Plagioclase	K-feldspar	Quartz	Biotite	Hornblende		Other	S.I. $\times 10^{-5}$	
				Granodiorite of Hatchet Peak					
6709	47	16	30	7	–			600	
6710A	44	16	30	10	–			25	
6710B	34	7	25	14	(?)			400	
				Tonalite of Zumwalt Ranch					
6719	63	0.5	17	11	8		Opaque 0.5	2000	
6721	56	3	19	8	14			600	
6722	57	0.5	20	13.5	8.5		Opaque 0.5	4500	
6723	58	2	15	12.5	12.5		Opaque <1	2000	
				Mafic granitic body					
6715	51	3	17	14	15			100	
6716	57	0.5	9	18	15.5			1200	
6717	50	4	16	18	12			60	
				Felsic granitic body					
6712	32	32	30	6	–			5	
6713*	50	9	26	x (15) x				1200	

*[6713 more representative – 6712 may be a dike]

Table 3. Oxide ranges and averages by rock type and grand averages for all chemically analyzed rocks, southern Sierra Nevada, California

Oxide	Granite			Granodiorite			Tonalite			Quartz diorite			Granitic rocks	
	Range	Average	Weighted Average	Range	Average	Weighted Average	Range	Average	Weighted Average	Range	Average	Weighted Average	Average	Weighted Average
SiO_2	67-76.6	73.4	72.9	57.8-70.6	66.3	66.1	57.4-69.7	63.4	63.4	55.2-69.5	61.0	61.4	66.0	65.8
Al_2O_3	12.5-16.3	13.8	14.0	14.2-17.9	16.0	16.1	15-20.8	16.7	16.5	15.5-18	17.1	17.4	16.0	16.0
Fe_2O_3	0.2-1.7	0.9	0.9	0.3-3.5	1.4	1.5	0.7-2.6	1.5	1.5	0.9-3.5	2.3	2.7	1.4	1.5
FeO	0.2-2.5	1.0	1.2	0.5-4.7	2.5	2.4	1.8-5.8	3.4	3.6	1.9-7.1	3.7	2.9	2.7	2.7
MgO	0.1-1.3	0.4	0.5	0.4-3.2	1.5	1.5	1.1-4.5	2.4	2.4	1.4-4.4	2.7	2.2	1.7	1.7
CaO	0.4-3.5	1.5	1.6	1.9-6.4	4.0	4.0	3.8-6.9	5.6	5.4	5.2-8.2	6.4	6.3	4.3	4.3
Na_2O	2.3-4.2	3.5	3.5	2.6-4.3	3.6	3.7	2.3-4.6	3.3	3.5	2.8-4.3	3.5	3.9	3.5	3.6
K_2O	3.0-4.9	4.3	4.4	1.4-4.3	2.8	2.8	0.6-3.4	1.7	1.7	0.3-1.9	1.3	1.7	2.6	2.6
TiO_2	0.05-0.6	0.21	0.23	0.2-0.9	0.59	0.6	0.3-0.9	0.61	0.64	0.4-1.1	0.64	0.57	0.6	0.58
Total		99.01	99.23		98.69	98.7		98.61	98.64		98.64	99.17	98.8	98.8 *

*/ H_2O^+ and H_2O^- or LOI, and some minor oxides are not included. Many analyses total less than 100 percent.

□/ Weighted average based on areal extent of plutons

Table 4. Average and range of rubidium and strontium and initial strontium ratio (Sri) by unit for granitic rocks of the southern Sierra Nevada. (Data abstracted from Kistler and Ross, in press)

Unit	No. of samples	Rb (ppm)		Sr (ppm)		Sri
		Average	Range	Average	Range	
GRANITE						
Arrastre Creek	1	74	-	140	-	0.7040
Bodfish Canyon	1	194	-	41	-	0.7090
Brush Mountain	2	204	170-237	46	14-78	0.7085
Cannell Creek	6	134	58-171	275	29-517	0.7083
Five Fingers	3	88	77-93	717	544-809	0.7068
Kern River	4	136	105-155	175	147-203	0.7081
Noname Canyon	4	242	119-366	239	6-478	0.7088
Ony X	1	170	-	343	-	0.7080
Portuguese Pass	3	127	77-189	135	95-168	0.7063
Sherman Pass	1	182	-	76	-	0.7076
Tehachapi Airport	1	165	-	79	-	0.7096
Tejon Lookout	3	179	172-191	159	79-307	0.7073
GRANODIORITE						
Alder Creek	6	127	108-154	262	220-328	0.7064
Alta Sierra	4	57	43-64	578	527-676	0.7063
Brush Creek	1	133	-	408	-	0.7063
Castle Rock	12	109	82-195	557	349-695	0.7074
Deer Creek	1	74	-	195	-	0.7041
Gato-Montes	12	103	80-137	568	358-744	0.7079
Goat Canyon Ranch	1	71	-	530	-	0.7059
Hatchet Peak	1	121	-	174	-	0.7068
Hershey Ranch	1	78	-	230	-	0.7041
Keene	1	54	-	341	-	0.7054
Lebec	3	103	90-121	508	376-659	0.7074
Peppermint Mdw	3	78	77-79	604	577-621	0.7062

Table 4. (cont.)

Unit	No of Samples	Rb (ppm) Average	Rb (ppm) Range	Sr (ppm) Average	Sr (ppm) Range	Sri
Pine Flat	3	93	71-113	365	300-451	0.7062
Poso Flat	7	56	45-81	312	277-370	0.7047
Rabbit Island	8	96	57-124	646	378-956	0.7068
Sacatar	7	132	89-188	447	132-659	0.7105
Wagy Flat	2	67	60-74	603	583-623	0.7066
Whiterock	5	81	48-103	618	504-893	0.7074
TONALITE						
Antimony Peak	1	<5	-	603	-	0.7033
Bear Valley Spr.	16	62	19-104	333	250-399	0.7056
Carver-Bowen	3	53	44-71	359	282-514	0.7037
Dunlap Mdw	7	62	46-84	355	296-461	0.7062
Fountain Spr.	2	35	35-35	311	284-341	0.7039
Hoffman Canyon	1	90	-	634	-	0.7071
Mount Adelaide	3	38	20-58	504	418-640	0.7044
Walt Klein	8	54	33-79	340	288-399	0.7041
Zumwalt	1	41	-	320	-	0.7041
QUARTZ DIORITE						
Caliente	1	36	-	417	-	0.7044
Cyrus Flat	19	117	47-218	408	248-579	0.7080
Freeman Junction	2	43	36-50	493	456-531	0.7051 1/
Long Valley	1	43	-	925	-	"0.7056"
Walker Pass	11	44	27-77	625	396-762	0.7046

1/ $^{87}Sr/^{86}Sr$

Table 5 . Comparison of the chemical analysis of the Little Lake sample (Kistler and Peterman, 1978) with an average of two Paiute Monument samples from the Inyo Mountains (Ross, 1969).

	Little Lake	Paiute Monument
SiO_2	70.3	70.8
Al_2O_3	15.2	14.6
Fe_2O_3	1.5	1.6
FeO	1.3	1.1
MgO	0.68	0.55
CaO	1.9	2.2
Na_2O	3.4	3.4
K_2O	4.8	4.6
TiO_2	0.36	0.30
Other	1.11	1.04
Total	100.55	100.19

123

APPENDIX

Mode tables, modal triangular plots, and index maps* to supplement modal data of USGS Open-File Report 87-373 (Ross, 1987) for samples collected in 1987 and 1988.

Granite

Old Hot Springs Road

Granodiorite

Alder Creek

Basket Peak and Poso Creek

Deer Creek

Hatchet Peak

Hershey Ranch

Poso Flat

Tonalite

Carver-Bowen Ranch

Fountain Springs

Mount Adelaide

Walt Klein Ranch

Dark granitic rocks of Eclipse Hill (contaminated Walt Klein ?)**

Zumwalt Ranch

Miscellaneous

Cedar Creek (dikes and small masses-range of compositions)

Gabbronorite of Quedow Mountain (no modal plot)

---

* Index maps are all at 1:125,000 scale and "North-up". Numbered samples (with exceptions as noted) were collected in 1987 and 1988 after most modal data were published (Ross, 1987). Samples from Ross (1987) are located by black dots (•).

** Index map (sample location) with Walt Klein

Modes of the granite of Old Hot Spring Road (1988)

Sample	Plagioclase	K-feldspar	Quartz	Biotite	Hornblende	10^{-5} siu
6871A*	26	40	32	2	-	0
6874[a]	27	45	26	2	-	300

*contains minor pink garnet

[a]fine-grained, may be a dike

Table . Modes of the granodiorite of Alder Creek (1988)

6863	46	11	21	17	5	30
6864	43	13	25	14	5	20

Table . Modes of granodiorite of Basket Peak (1987)

Sample	Plagioclase	K-feldspar	Quartz	Biotite	Hornblende	10^{-5} siu	Spec. gr.
6600	51	18	21	8	2	25	2.65
6601	49	19	26	6	1	10	2.66

Modes of granodiorite of Poso Creek (1987)

6605	44	20	27	8	1	20	2.64
6609	46	17	28	8	1	20	2.64

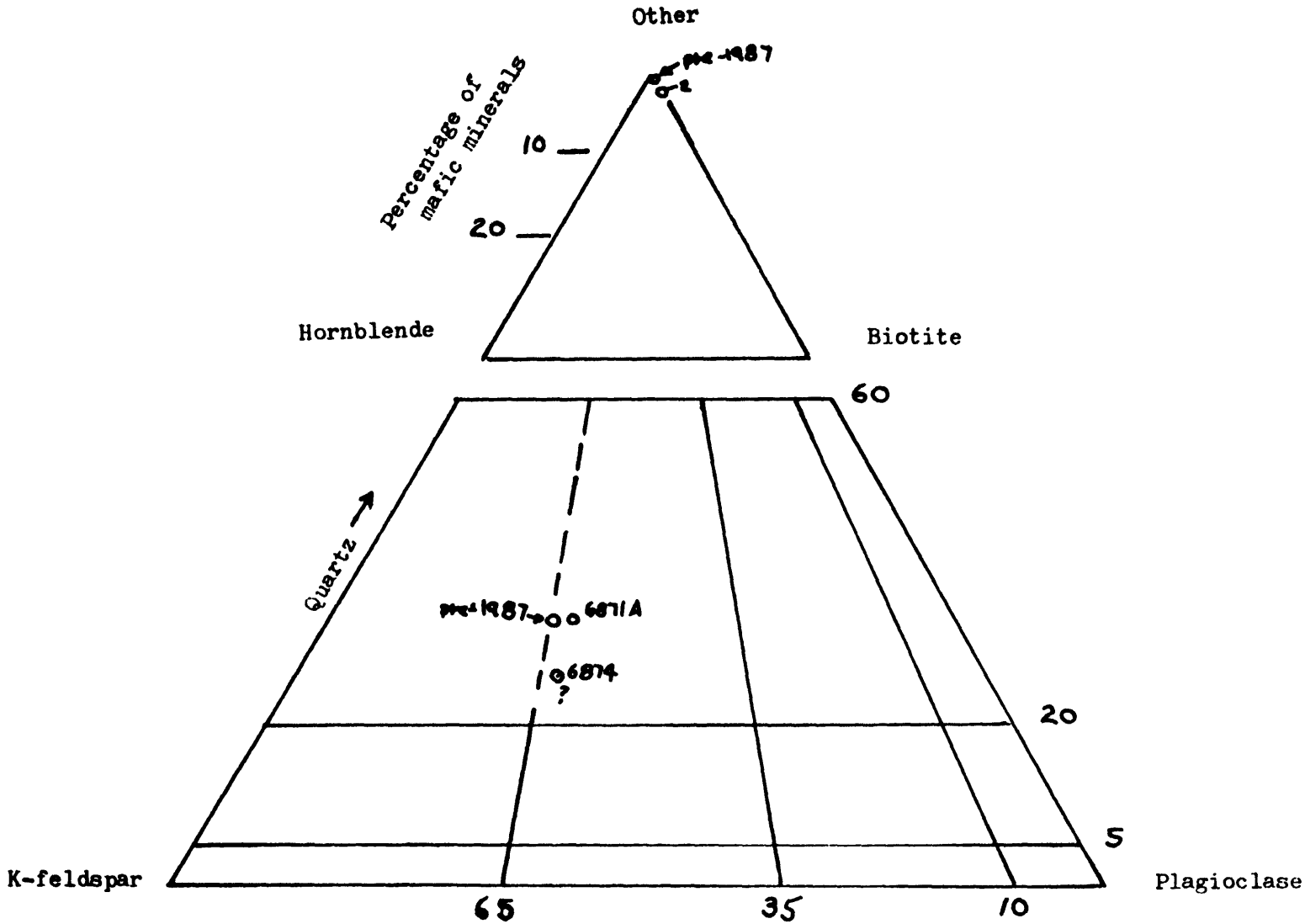

Modal plot of the granite of Old Hot Springs Road

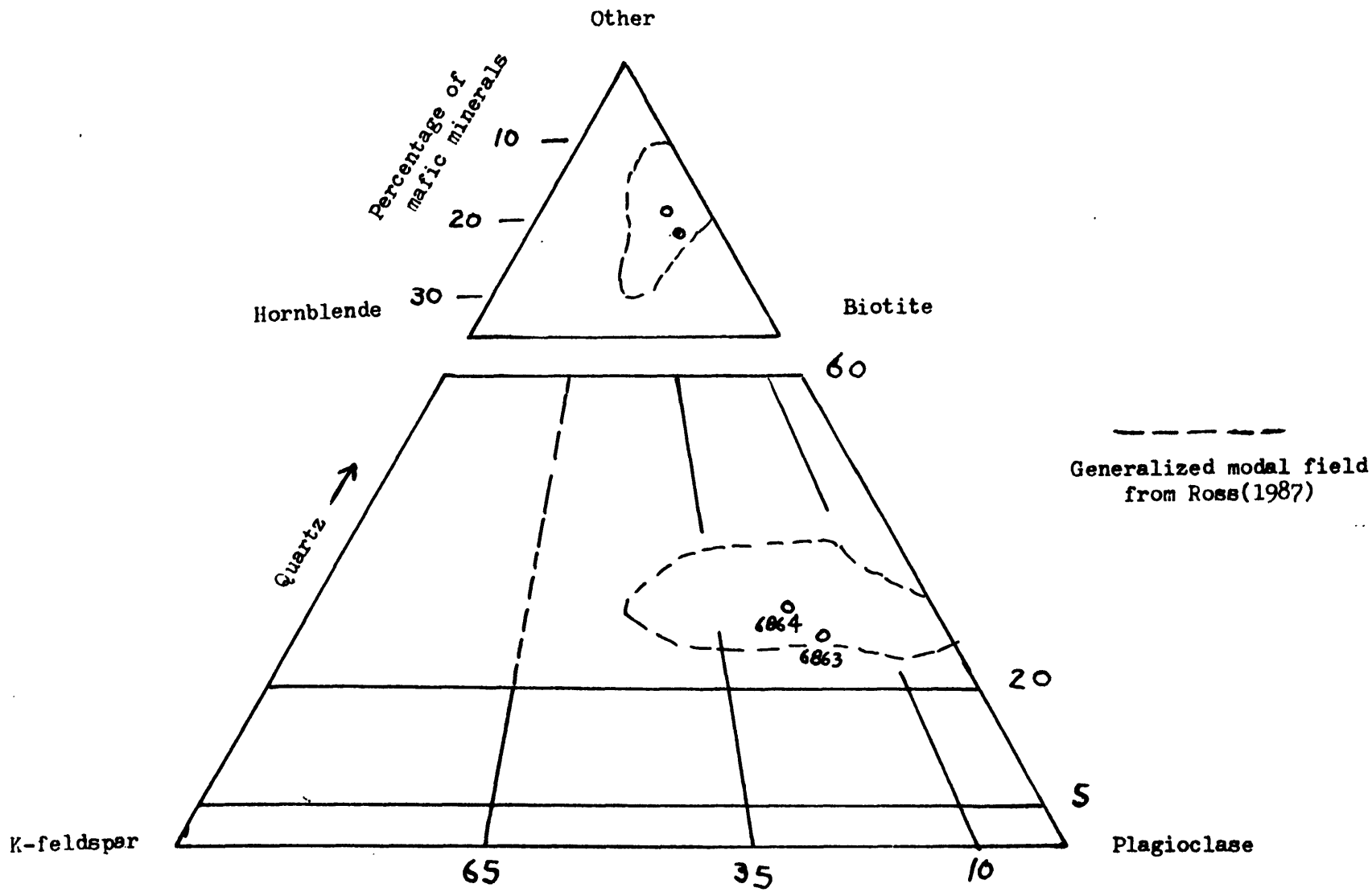

Modal plot of the granodiorite of Alder Creek

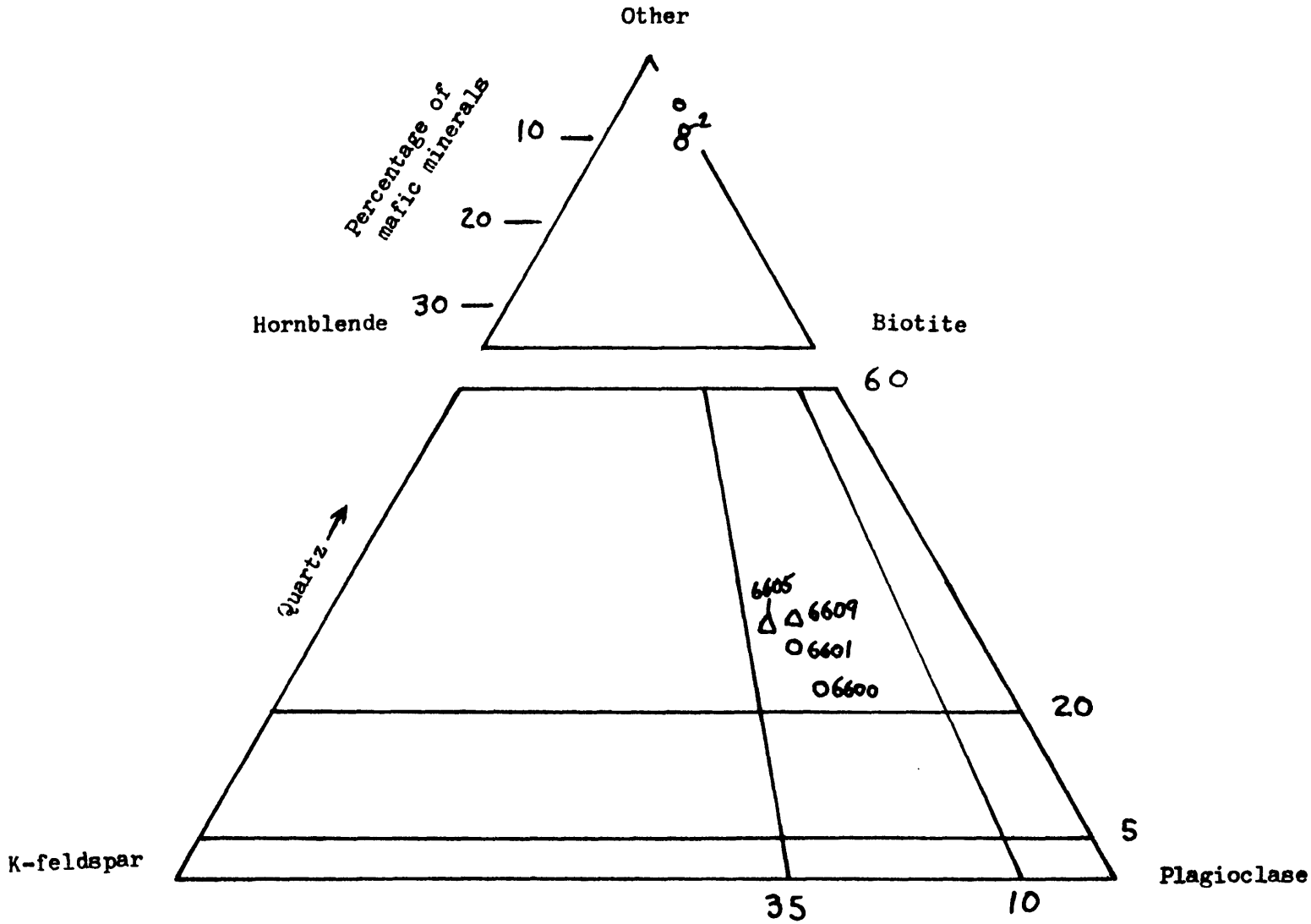

Modal plot of the granodiorites of Basket Peak (o) and Poso Creek (Δ).

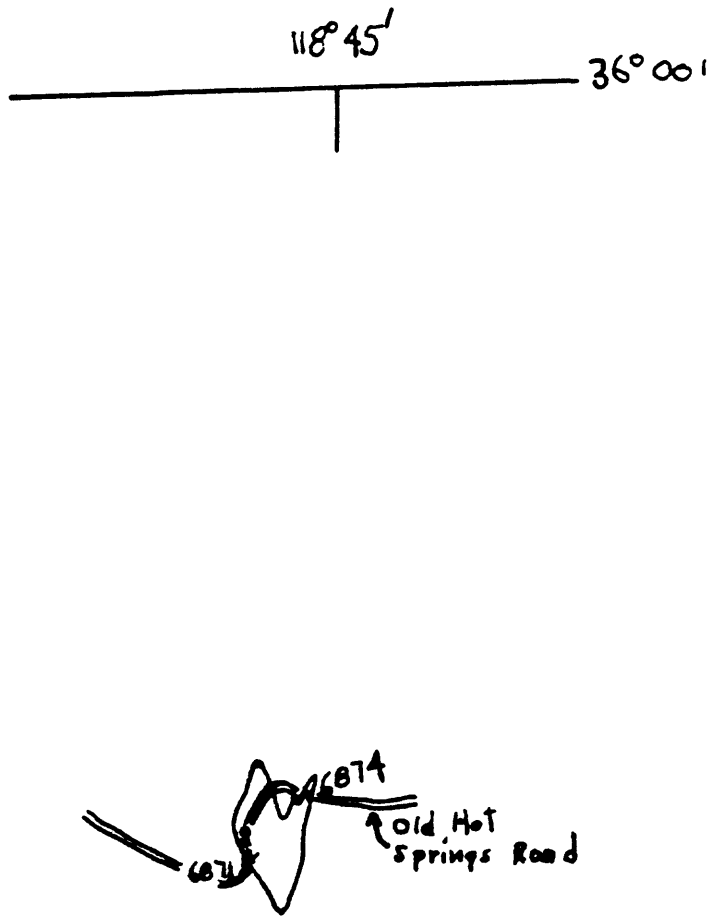

Location of modal samples of the granite of Old Hot Springs Road

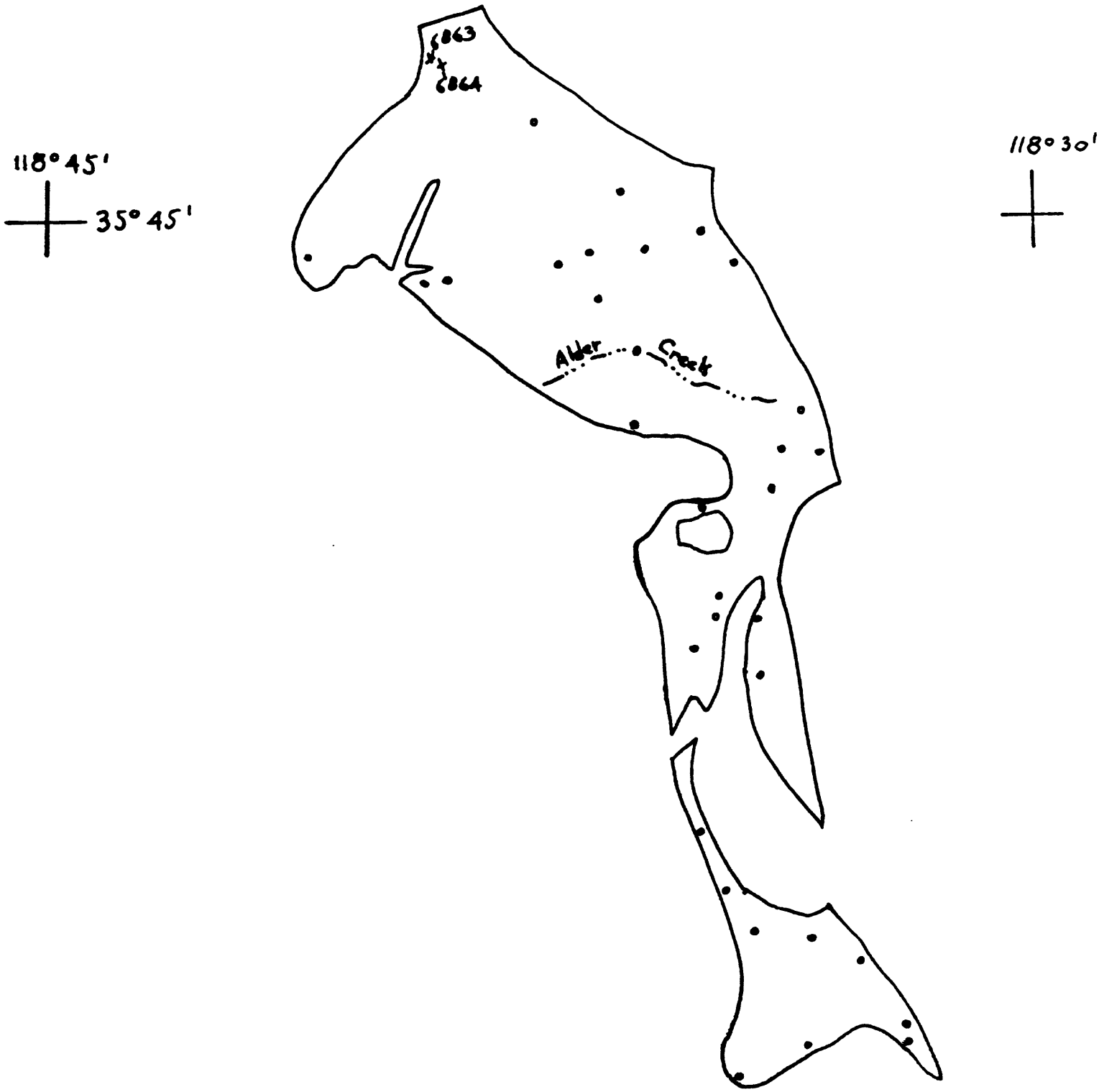

Location of modal samples of the granodiorite of Alder Creek

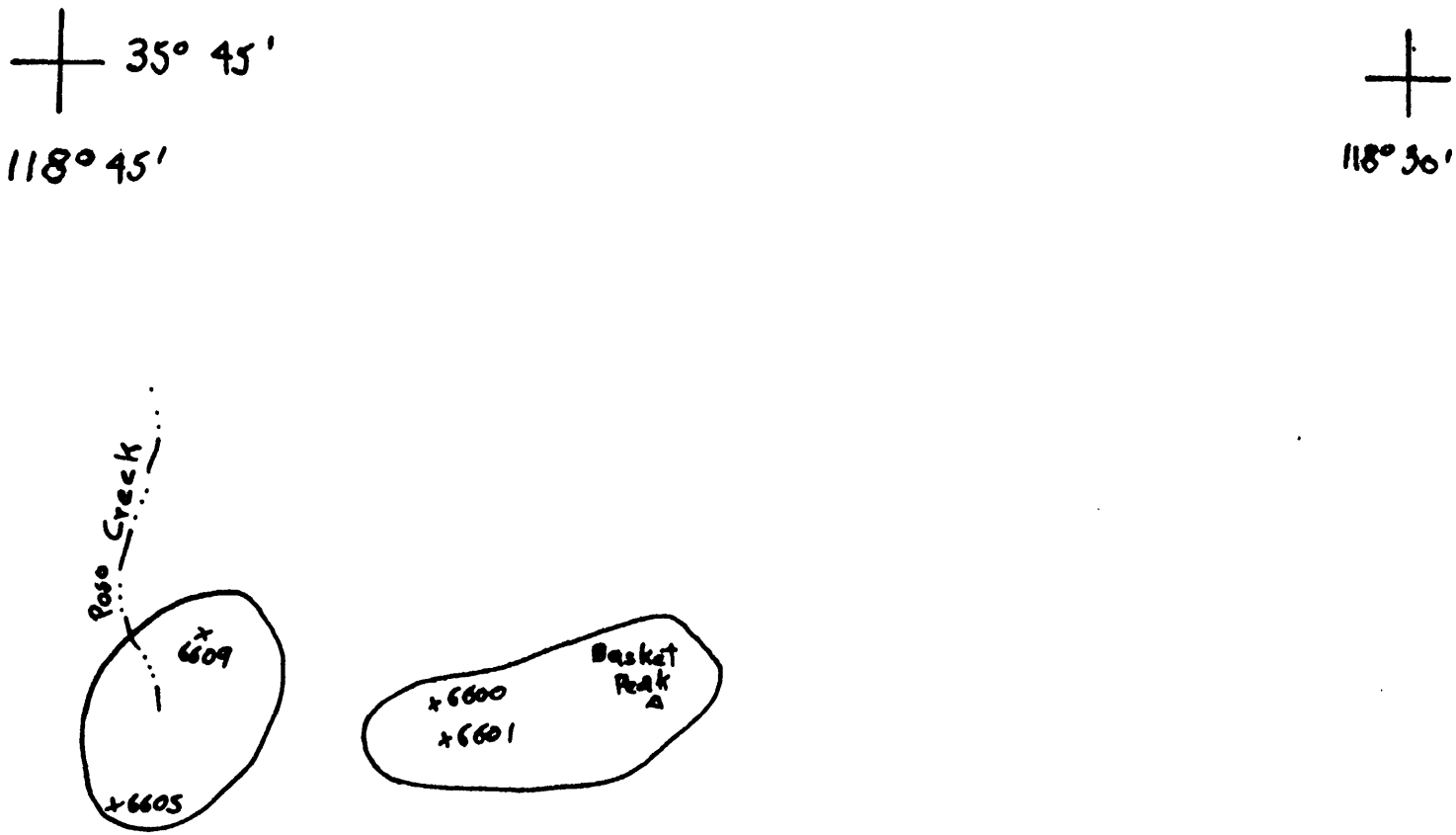

Location of modal samples of the granodiorites of Basket Peak and Poso Creek

Modes of the granodiorite of Deer Creek (1988)

Sample	Plagioclase	K-feldspar	Quartz	Biotite	Hornblende	Opaque	10^{-5} SIU
6113 □	54	3.5	29.5	13	< 1	-	2000
6115 □	53	6.5	25.5	12	3	-	1000
6116 □	55	5	33	7	< 1	-	1400
6117 □	47	16	28	8	1	-	1000
6118 □	46	19	27	7	0.5	0.5*	1000
6119 □	56	3	26	14	0.5	0.5*	-
6743	55	2	31	11	-	1	600
6746	56	1	31.5	11	-	0.5	1400
6747	48	22	23	7	< 1	<1	1000
6749	50	22	22	6	-	-	700
6751	64	1.5	23	11.5	-	<1	800
6753	54.5	21.5	13	11	-	<1	900
6762	67	-	17	15	1	<1	3000
6763	60	5	23	12	-	<1	2000
6765A	60	1.5	20.5	13	4.5	<1	1600
6766	56	4	32	7	-	1	2500
Average	55	8.5	25.5	10	1	<1	1393

* some sphene

□samples collected before 1988 when body called "Deer Creek-west body"

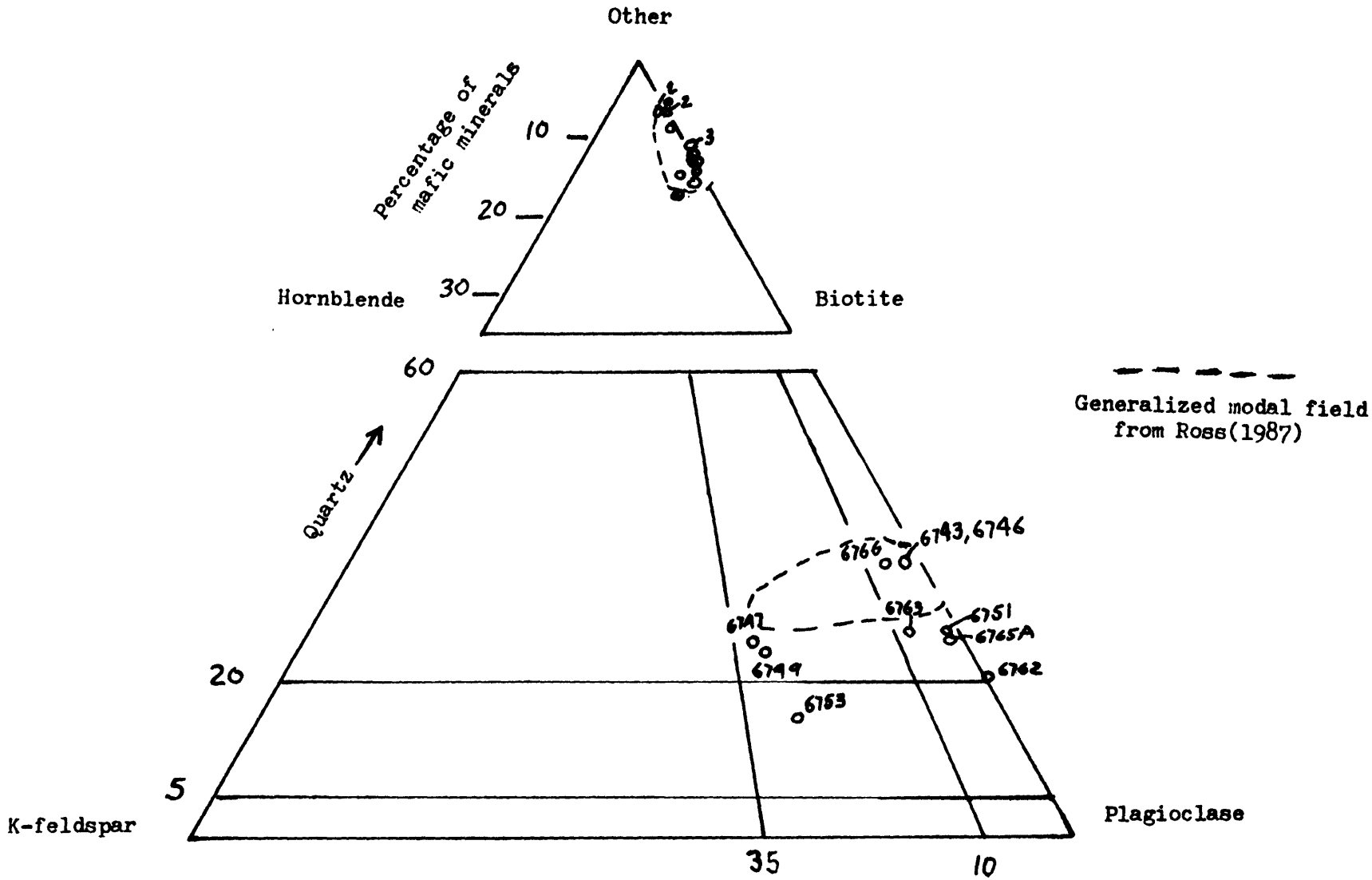

Modal plot of the granodiorite of Deer Creek

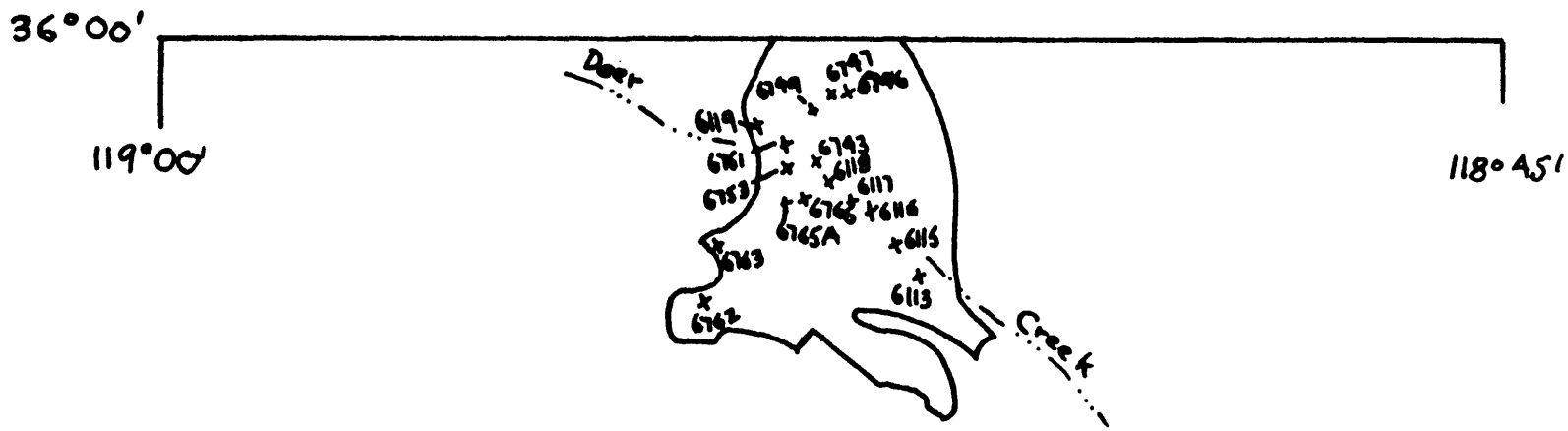

Location of modal samples of the granodiorite of Deer Creek

Modes of the granodiorite of Hatchet Peak (1988)*

Sample	Plagioclase	K-feldspar	Quartz	Biotite	Hornblende	10^{-5} siu
6709	47	16	30	7	-	600
6710A	44	16	30	10	-	25
6710B	54	7	25	14	?	400

*collected on Reservation Road north of the map area (See figure 4).

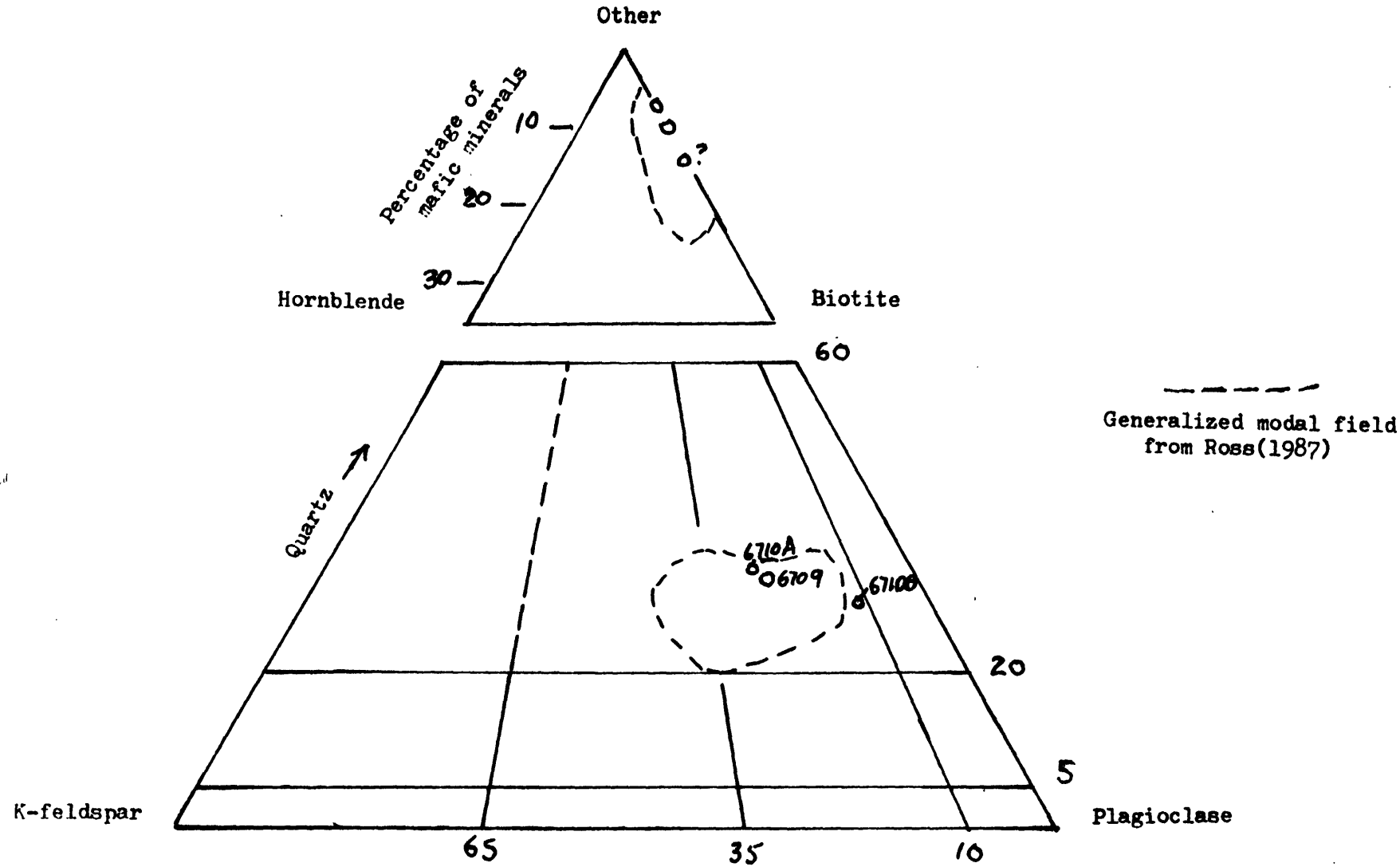

Modal plot of the granodiorite of Hatchet Peak

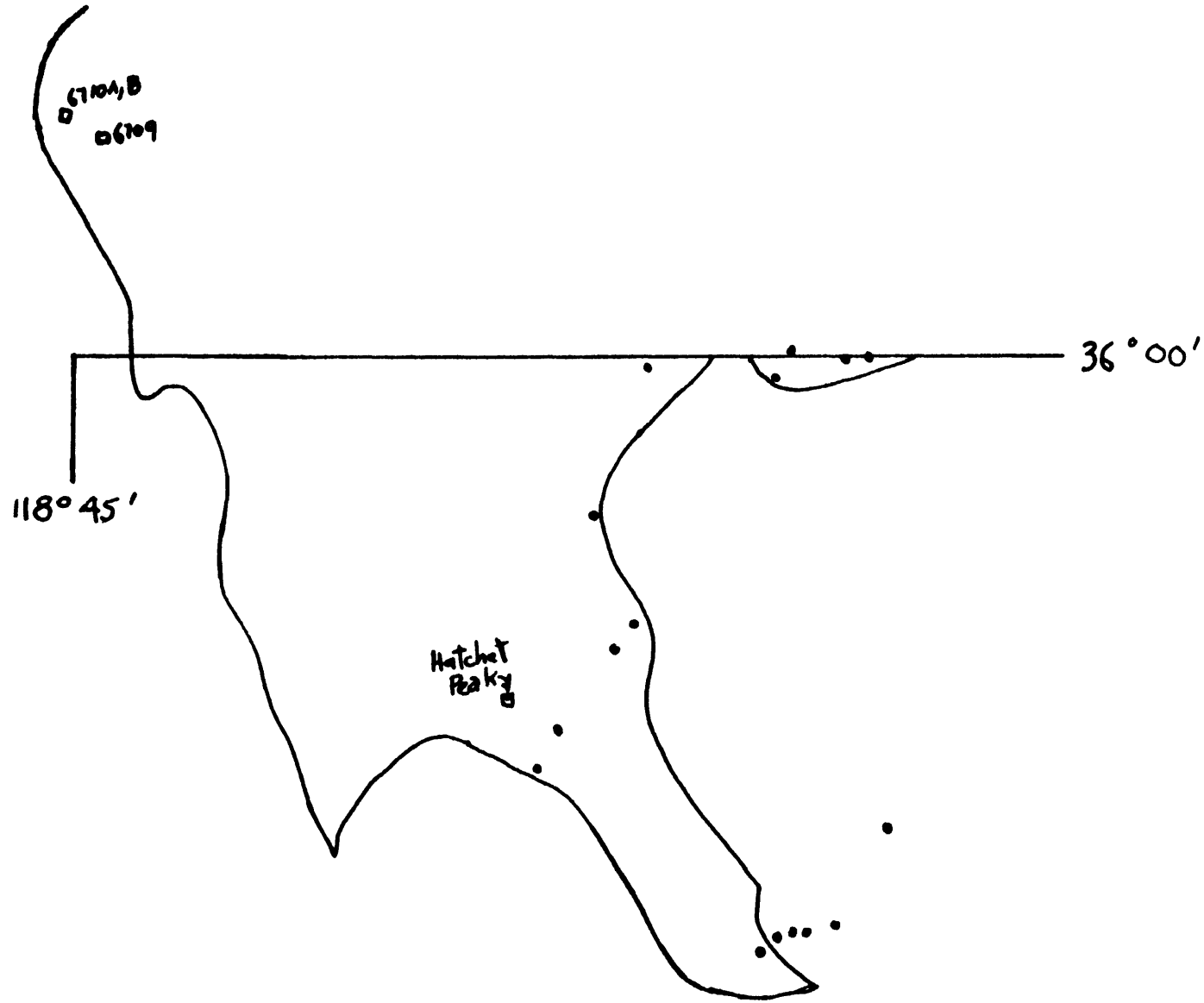

Location of modal samples of the granodiorite of Hatchet Peak

Modes of the granodiorite of Hershey Ranch (1988)*

Sample	Plagioclase	K-feldspar	Quartz	Biotite	Hornblende	Opaque	10^{-5} SIU
6008B	45	10	27	13	5	-	600
6009	50	10	25	12	3	-	1400
6010	41	12	32	11	4	-	500
6030	47	14	25	9	5	-	800
6031	46	9	34	9	2	-	400
6032A	46	10	28	11	5	-	400
6032B	41	13	28	13	5	-	300
6050	42	9	36	13	-	-	400
6051	39	23	34	4	-	-	200
6052	37	24	33	6	-	-	600
6053	42	11	29	13	4	-	500
6724	47	12	23	16	2	-	300
6726	58	3	19	18	2	-	400
6727	39	24	26.5	10	0.5	-	350
6728	47	10	23	12	8	< 1	800
6731	49	6	22	16	7	-	700
6732	51	7	22	13	7	-	700
6733	39	20	32	7	2	-	350
6870B	48	12	28	11	1	< 1	700
6872	43	17	30	9	1	-	400
6873	38	28	29	5	< 1	< 1	300
6876	46	10.5	28	12	3.5	-	700
Average	45	13	28	11	3	<1	536

*Formerly called "Deer Creek-east body" and includes some samples collected before 1988.

Early field mapping considered all the rocks now called the granodiorites of Deer Creek and Hershey Ranch as one unit called Deer Creek. Later magnetic susceptibility studies showed significant differences between the eastern and western samples, suggesting the possibility of two distinct plutons. Subsequent field work confirmed two separate granodiorites intrusive into the tonalite of Carver-Bowen Ranch.

In the field one might have difficulty separating these two granodiorites (as I had!) even with the intervening generally darker tonalite of Carver-Bowen, which is not everywhere all that distinct from the granodiorites. Commonly the Hershey Ranch body is coarser than the Deer Creek rocks, but there is considerable texture variation in both units. Probably the best distinction in the field is the presence of abundant inclusion swarms, schlieren, and almost gneissic zones in the Deer Creek unit compared to their scarcity in the Hershey Ranch unit. Field and petrographic differences between the two granodiorites are subtle and it would be difficult to separate the collected samples into two piles. The magnetic susceptibility difference between the two granodiorites is perhaps the most definitive way to separate them.

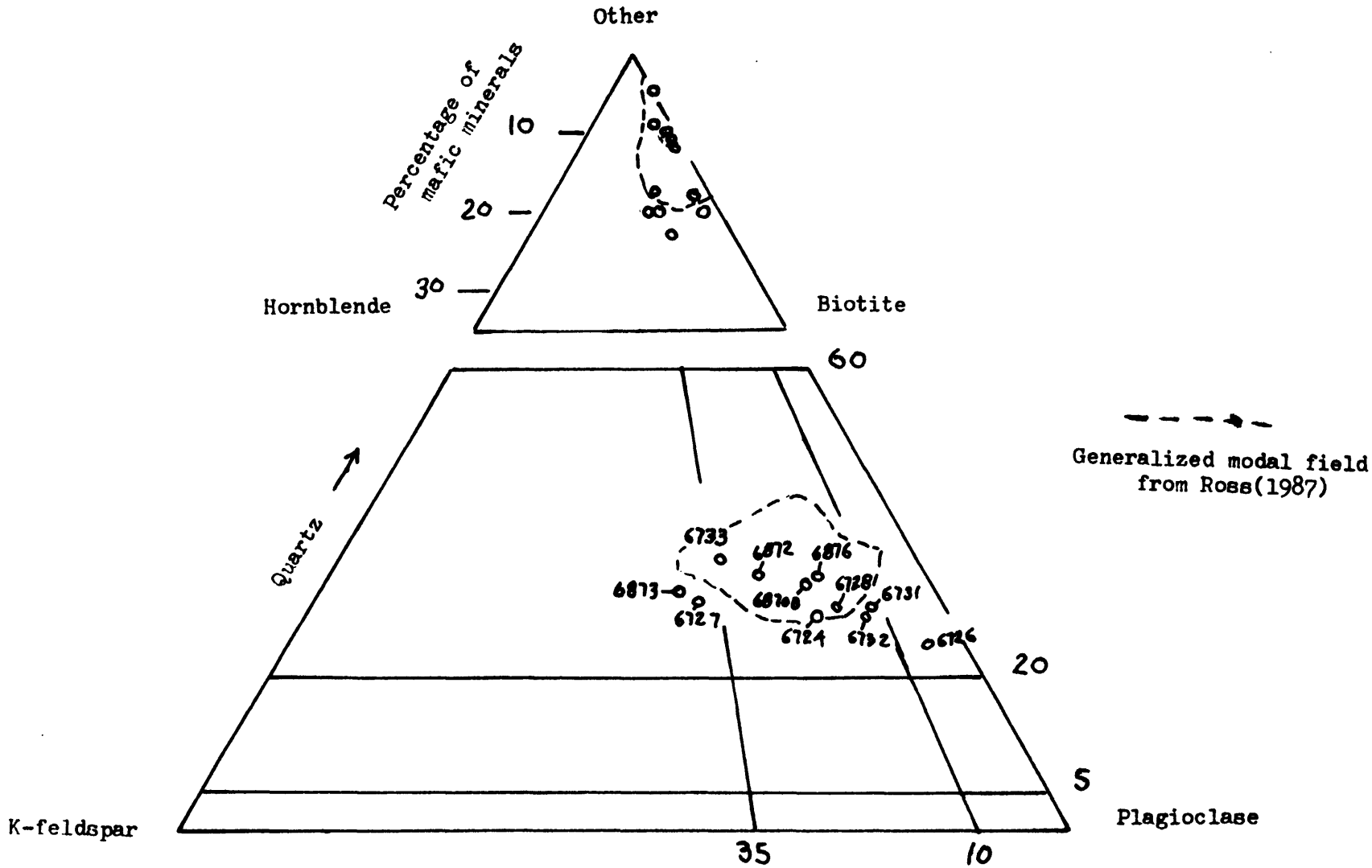

Modal plot of the granodiorite of Hershey Ranch

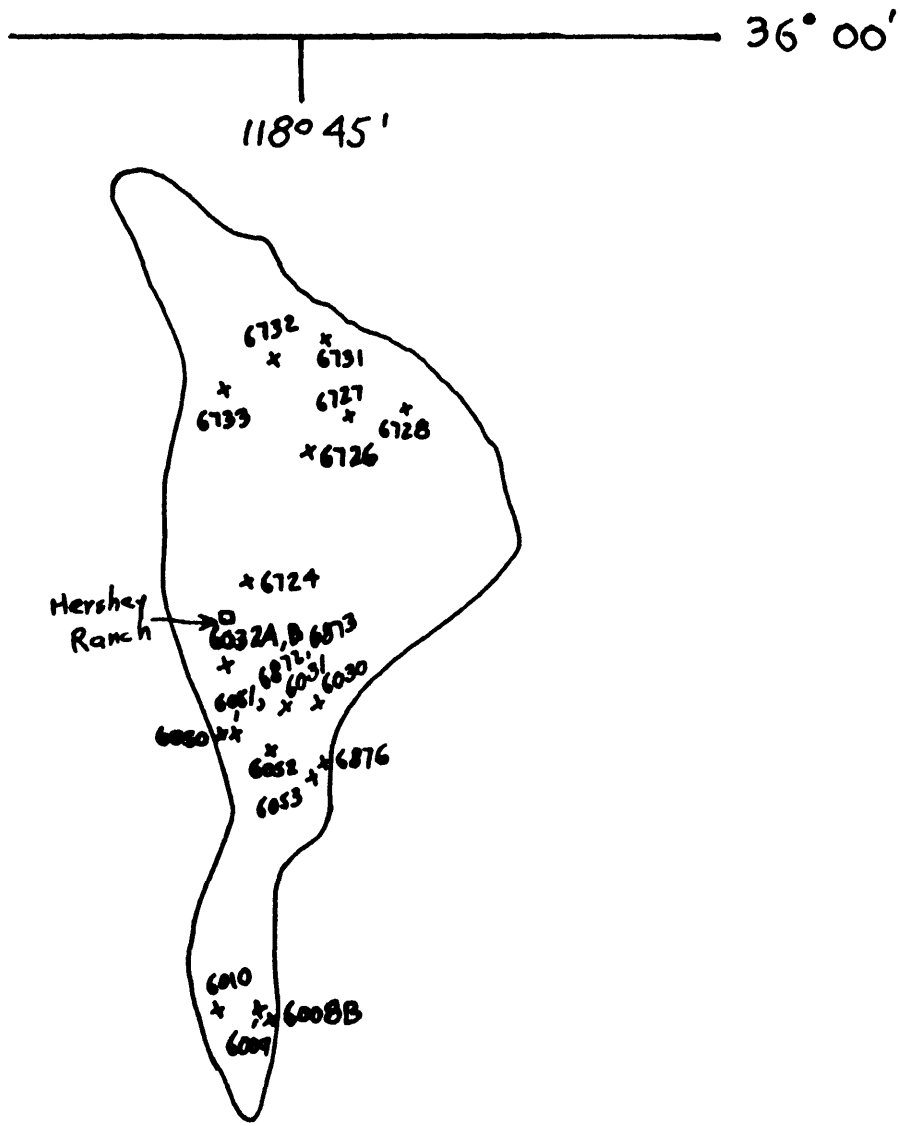

Location of modal samples of the granodiorite of Hershey Ranch

Modes of the granodiorite of Poso Flat (1987)

Sample	Plagioclase	K-feldspar	Quartz	Biotite	Hornblende	10^{-5} SIu	Spec. gr.
6278R-B	53	5	23.5	12.5	6	40	2.73
6342R	60	-	16	15	9	40	2.77
6356R	50	4	25	14	7	100	2.74
6554	57	<1	18	22	13	40	2.67
6557	51	10	29	8	2	15	2.67
6559	52	2	20	12	14	40	2.71
6560	53	4	26	13	4	20	2.67
6563A	52	5	27	13	3	20	2.69
6565	49	9	24	10	8	40	2.74
6570	55	5	21	13	6	25	2.67
6572	45	7	22	16	10	45	2.67
6573	49	10	17	14	10	50	2.72
6574	51	6	17	13	13	100	2.77
6576	48	5	25	10	12	20	2.71
6584	53	4	21	15	7	20	2.75
6585	45	10	25.5	10	9.5	20	2.71
6591	42	17	25	9	7	15	2.69
6593	42	13	23	10	12	30	2.72
6595	52	9	20	10	9	20	2.74
6603	60	<1	11	14	15	40	2.81
6612A	53	<1	27.5	10.5	9	30	2.69
6627	58	<1	22	19	1	700	2.71
6628	44	11	29	12	4	500	2.68
6629	57	<1	18	16	9	25	2.74
6630A	52	2.5	23.5	14	8	25	2.74
6630B	58	<1	23	12	7	25	2.75
6636B	53	11	20	9	7	25	2.66
6638	54	1	22	15	8	40	2.75
6644	50	12	25	10	3	800	2.70
6647	46	7	29	14	4	40	2.68
6648B	50	2	28	14	6	30	2.71
6704	45	9	26	11	9	20	2.66
6707A	50	5	22	12	11	40	2.76
6708	51	8	19	11	11	30	2.74
Average	51	5.5	23	12.5	8	90*	
Standard deviation	4.8	4.5	4.2	2.9	3.5		

*Average is 35 without the three high readings (800,700, and 500)

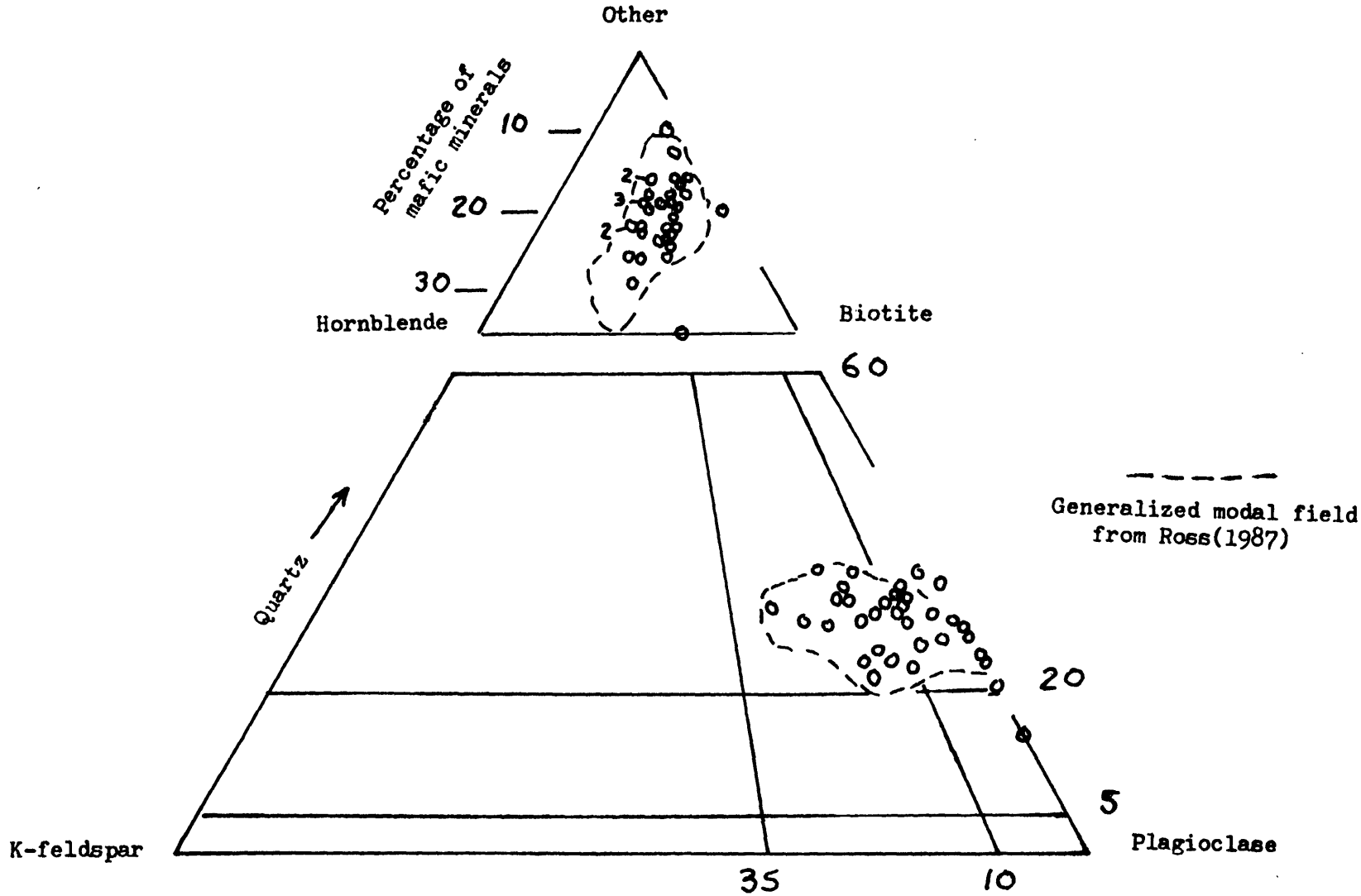

Modal plot of the granodiorite of Poso Flat

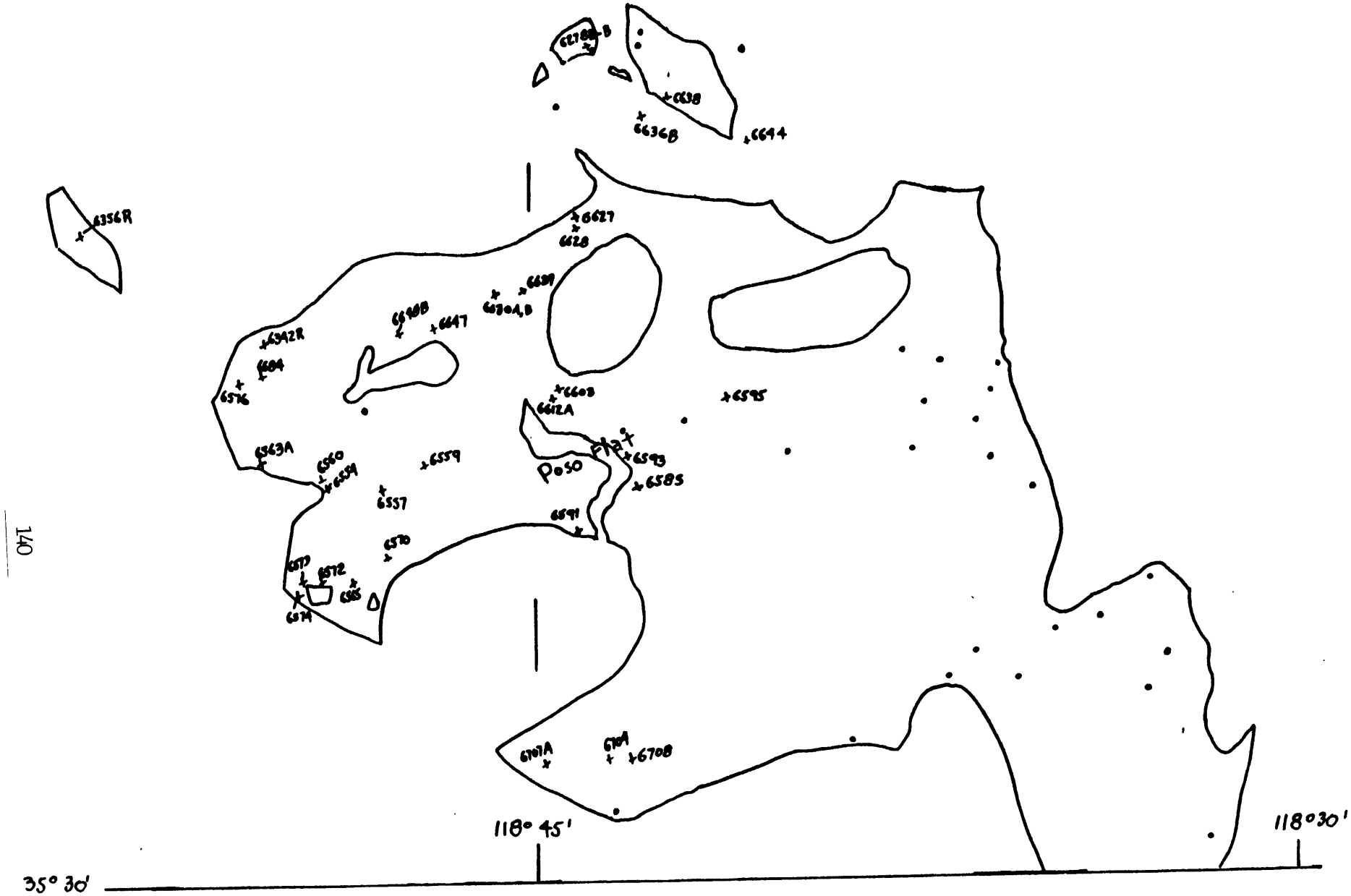

Location of modal samples of the granodiorite of Poso Flat

Modes of the tonalite of Carver-Bowen Ranch (1988)

Sample	Plagioclase	K-feldspar	Quartz	Biotite	Hornblende	Opaque	10^{-5} SIU
6735	47	7	18	15	13	-	500
6736	55	-	13.5	20	11	0.5	400
6738	57	1	16	13	12	1	1300
6767	53	8.5	19	12.5	7	< 1	1600
6768	53	5	17	14	11	< 1	1600
6771	(no mode)						1800
6772	55.5	4	21	11	8	0.5	1800
6773	57	2	17	10	14	-	1200
6843	61	-	11	14	14	< 1	1800
6851	67	< 1	11	21	1	-	40
6856-1	55	-	12	14	19	-	600
6859	59	-	10	12	18.5	0.5	
6865	61	-	10	18	11	-	50
6866	61	-	8	19	12	-	200
6867	65	-	4.5	19.5	11	< 1	120
6868	56	-	10	18	15	1	3000
6877	53	2	13	16	16	< 1	100
Average	57	2	13	16	12	< 1	

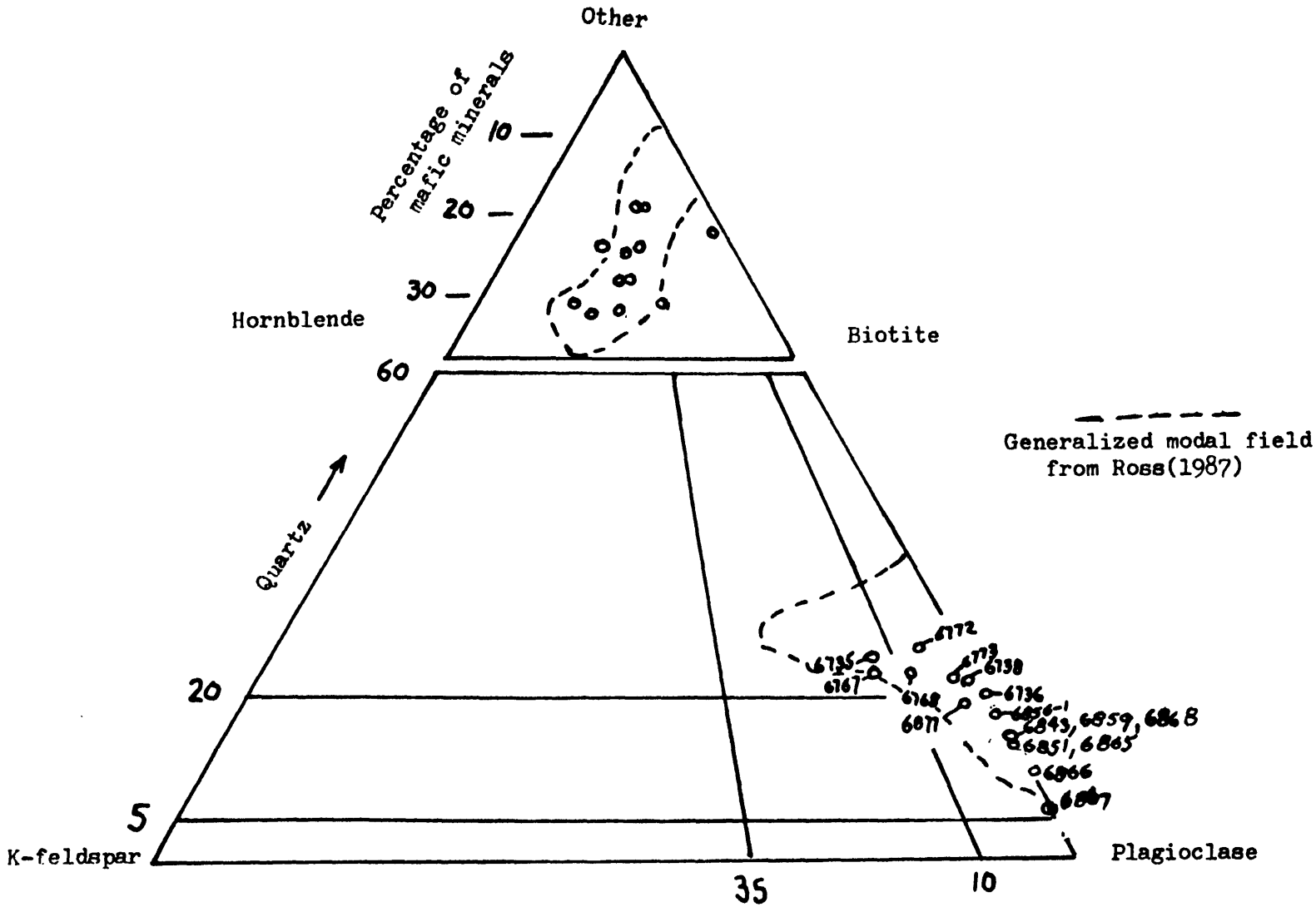

Modal plot of the tonalite of the Carver-Bowen Ranch

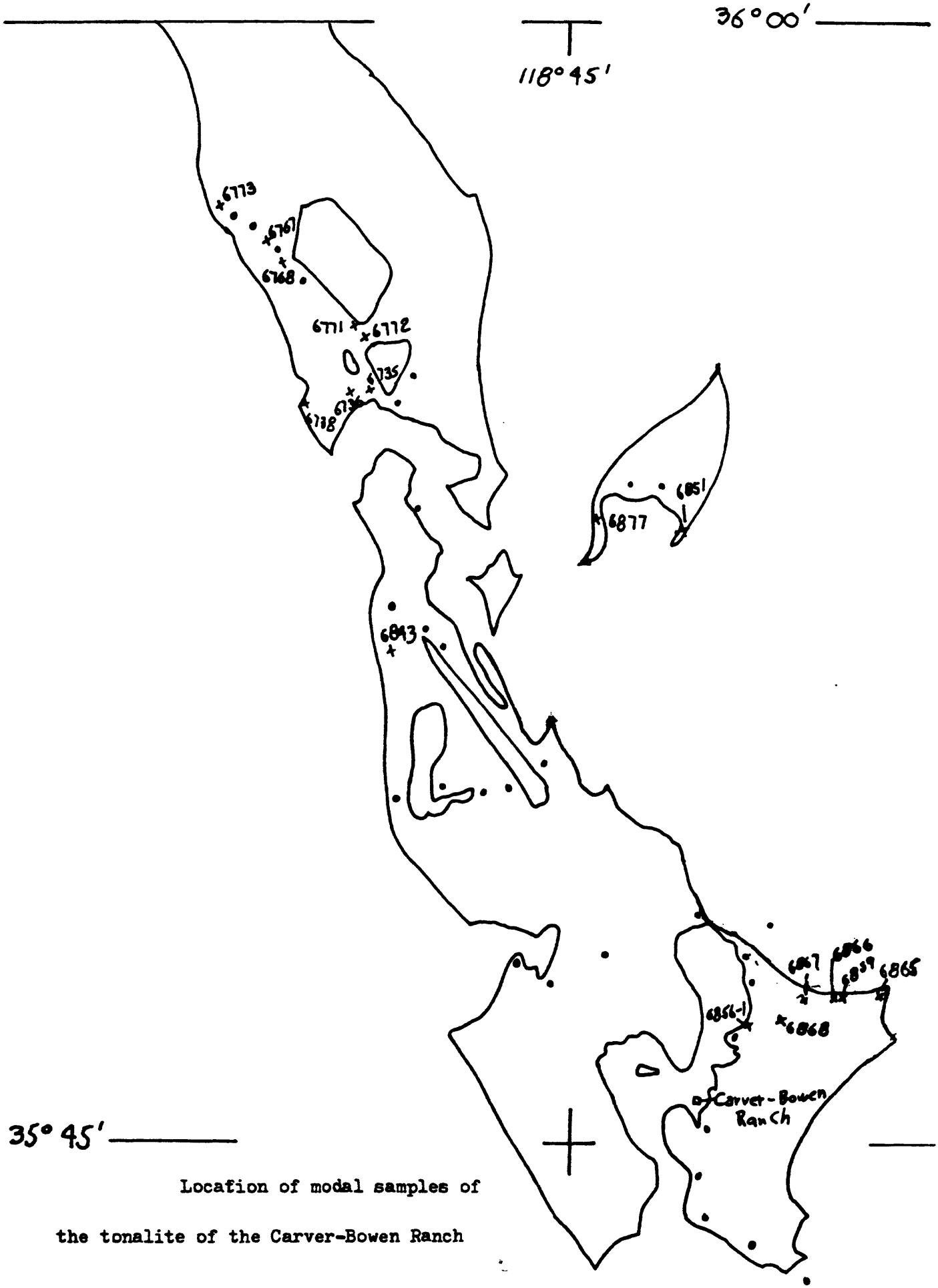

Locafion of modal samples of

the tonalite of the Carver-Bowen Ranch

Modes of the tonalite of Fountain Springs (1988)

Sample	Plagioclase	K-feldspar	Quartz	Biotite	Hornblende	10^{-5} siu	
6739	58	1	23	14	5	400	
6740	52.5	1	24	18.5	4	1200	(opaque 1)
6742	59	1	30	11	-	500	
6799	57	1	23	13	6	500	
6839	54	5	22	14	5	160	
6882	54	3	30	10	3	20	
6885A	50	4	22	13	11	40	
6888	54	2	23.5	12	8.5	30	
6890 1/	56	-	14	14	16	300	
6892	(no mode)					60	
6893	50	5	25	16	4	300	
Average	54	2	24	14	6	320	

1/ Darker than average Fountain Springs with relatively low quartz. May be contaminated or tonalite of Carver-Bowen (but magnetic susceptibility is much lower than average Carver-Bowen). Relation with "normal" Fountain Springs to the south is unknown.

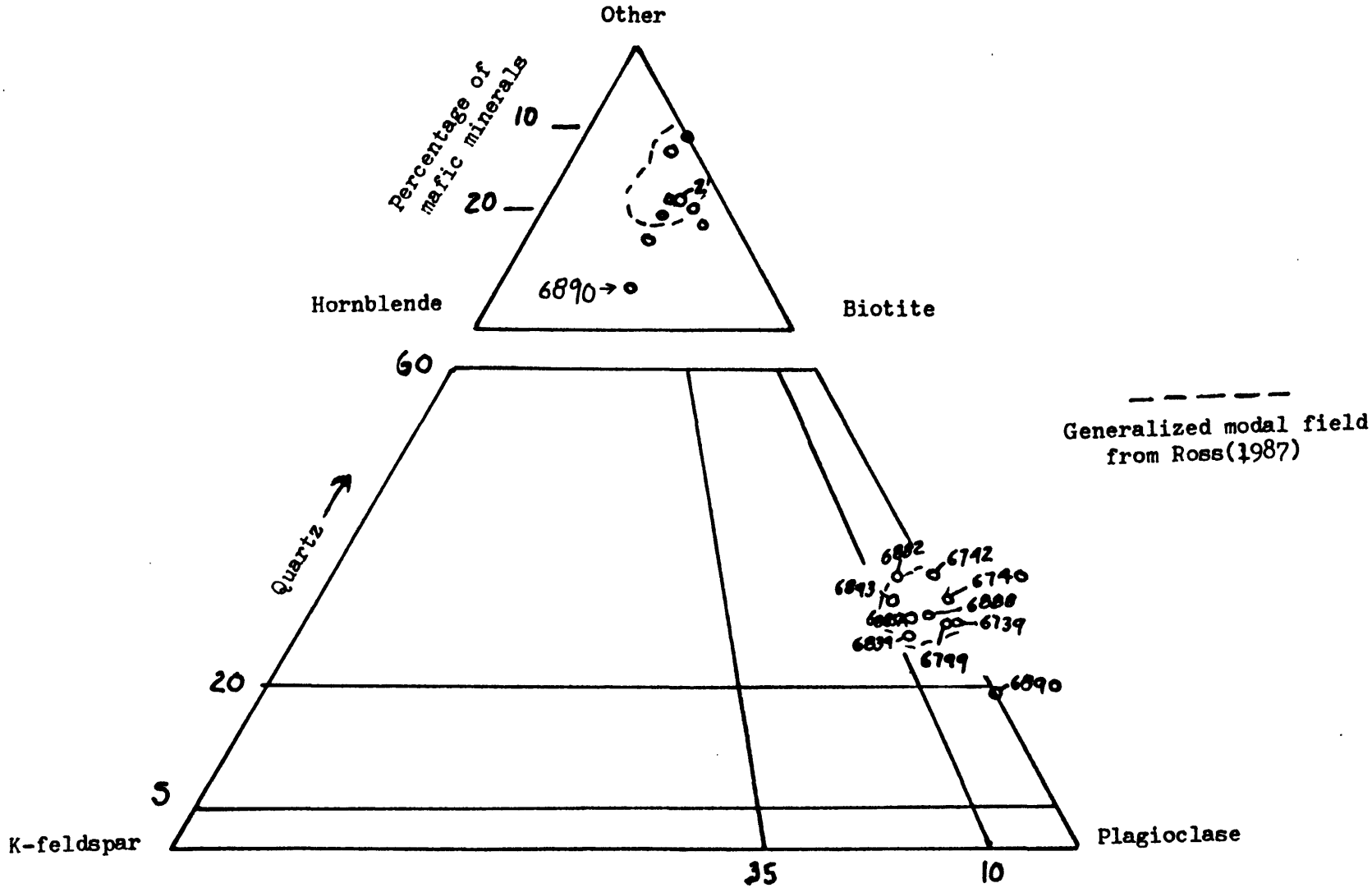

Modal plot of the tonalite of Fountain Springs

Location of modal samples of the tonalite of Fountain Springs

Modes of tonalite of Mount Adelaide (1987)

Sample	Plagioclase	K-feldspar	Quartz	Biotite	Hornblende	10^{-5} SIU	Spec. gr.
6544A	57	1	26	14	2	25	2.68
6545	63	1	21	13	2	25	2.71
6547	59	<1	25	15	1	20	2.69
6549B	56	2	30	12	-	10	2.66
6553	60	1	27	12	-	40	2.67
6567	60	<1	25	11	4	45	2.66
6568	67	<1	21	10	2	45	2.71
6569	57	-	23	15	5	70	2.71
6587	55	3	30	12	-	20	2.63
6588	51	7	35	7	-	15	2.64
Average	58.5	1.5	26	12	2	32	2.68
Standard deviation	4.4	2.2	4.4	2.4	1.8		
	Felsic phase						
6546	55	6.5	35.5	3	-	5	2.63

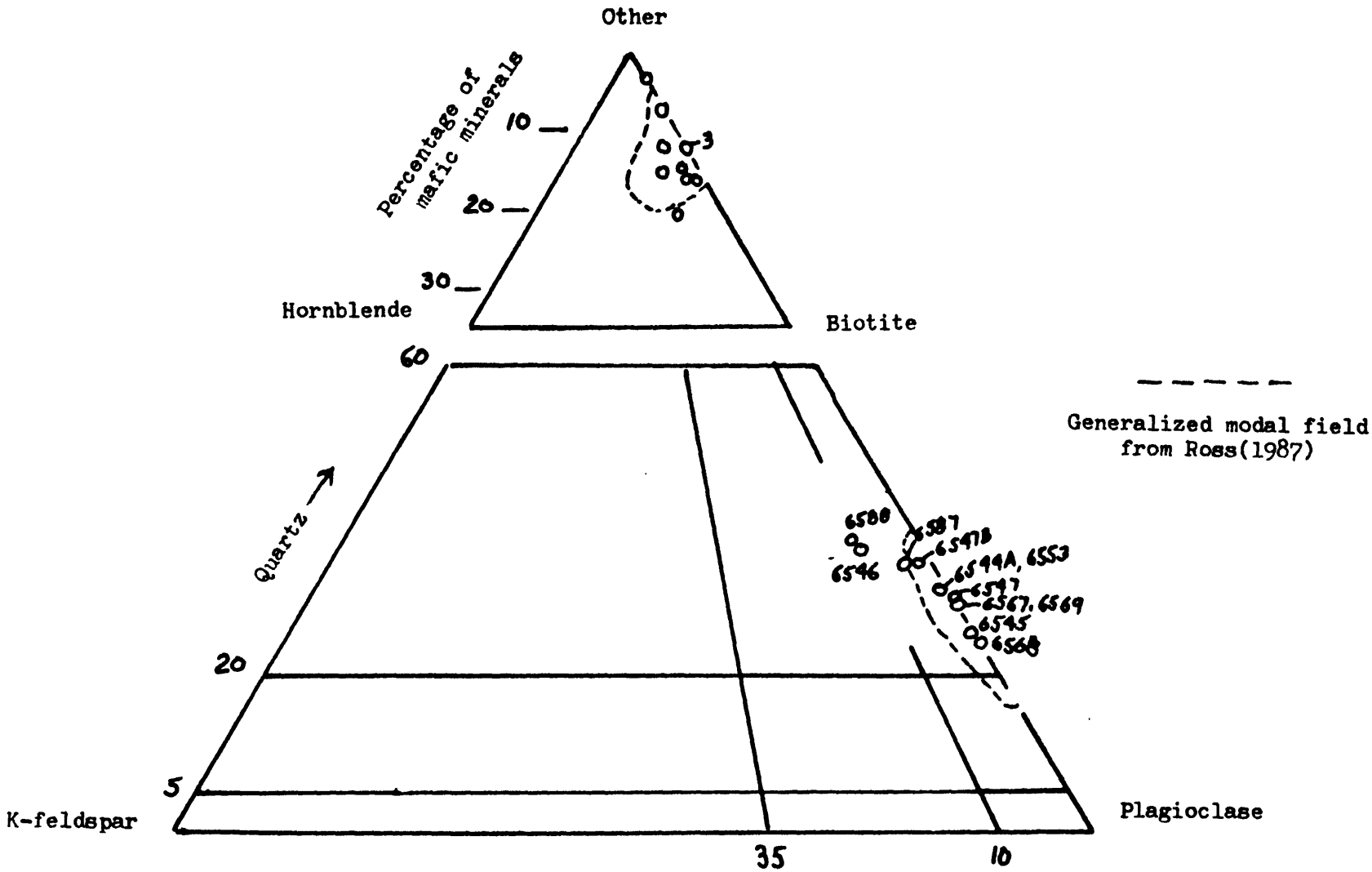

Modal plot of the tonalite of Mount Adelaide

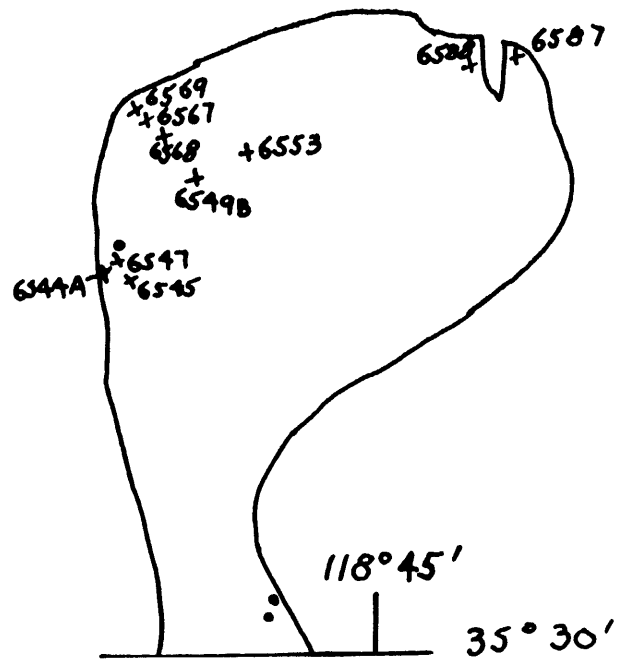

Location of modal samples of the tonalite of Mount Adelaide

Modes of the tonalite of Walt Klein Ranch (1987, 1988)

Sample	Plagioclase	K-feldspar	Quartz	Biotite	Hornblende	10^{-5} SIu	Spec. gr.
6281B	49	13	28	10	-	250	2.67
6305B	45	13	29	9	4	100	2.71
6317	54	1	26	14	5	20	2.69
6577	59	< 1	21.5	14.5	5	20	2.72
6579	61	2	24	12	1	20	2.65
6581	64	-	18	11.5	6.5	1600	2.77
6583	61	-	20	13	6	130	2.68
6626A	56	5	27	11	1	1000	2.65
6656	57	< 1	25	13	5	45	2.68
6657	52	8	27	13	-	600	2.65
6658	54	3	31	11	1	400	2.66
6663	58	3	24	13	2	500	2.71
6664	58	-	24	15	3	30	2.72
6665	54	< 1	28	11	7	20	2.74
6668	57	< 1	21	13	9	90	2.73
6669	51	-	28	14	7	20	2.66
6671	59	1	28	9	3	30	2.70
6679	51	3	27	11	8	30	2.72
6681	49	7	30	10	4	70	2.70
6682	48	5	26	16	5	40	2.73
6685	49	7.5	24	12.5	7	60	2.70
6697A	41	10	21	14	10	40	2.77
6777	52.5	2	23	13	9.5	600	
6780	50	2	30	16	2	60	
6781	59	2	21	14	4	80	
? 6783	61	3	8	9	19	50	
6785	59	-	29	12	-	15	
6787	56	-	29	14	1	30	
6797	52	7	25	13	3	60	
6800	49	3	29	12	7	180	
6802	56	2	26	14	2	160	
6803	51	2	34	9	4	60	
6804	48	6	33	12	1	80	
6812	(no mode)					40	
6813	56	-	19	16	9	50	
6818	56	-	18	15	11	30	
6826	57	4	21	11	7	10	
6831	51	6	24	14	5	70	
6832	53	3	23	13	8	30	
6834	50	7	22	16	7	40	
6835	54	3	24	13	6	70	
6837	58	-	22	11	9	40	
6774	(no mode)					10	
6778	"					600	
6827A	"					25	
6827B	"					15	
6817A	"					25	
Average	54	3	24.5	13	5.5	105 *	
Standard deviation	4.9	3.5	4.7	1.9	3.9		

* Average without samples 6581 and 6626A

Modes of dark granitic rock near Eclipse Hill (Walt Klein?) (1988)[1/]

Sample	Plagioclase	K-feldspar	Quartz	Biotite	Hornblende	10^{-5} siu
6096	53	5	19	14	9	25
6692	45	7	27	13	8	30
6693	51	6	19	14	10	30
6696	54	<1	20	13	13	30
6805	52	<1	23	15	10	30
6807	47	<1	21	15	17	40
6809B	54	-	11	19	16	60
6815	57	-	12	17	14	50
Average	52	2	19	15	12	37

1/ Outcrops of the undoubted texturally distinct tonalite of Walt Klein poke up through the argillaceous metasedimentary rocks of the White River pendant around the Father Garces historical monument in Grizzly Gulch (about 6 kilometers southwest of the small community of White River, White River 15' quadrangle). Associated outcrops, undoubtedly part of the same unit, are darker, somewhat gneissic, and lack the distinctive Walt Klein texture. The hererogeneity here in Grizzly Gulch gives more confidence to assignment of some other rocks, particularly those near Eclipse Hill, to the Walt Klein unit even though they lack the distinctive isolated and near-euhedral coarse crystals of hornblende and biotite considered "typical" Walt Klein texture.

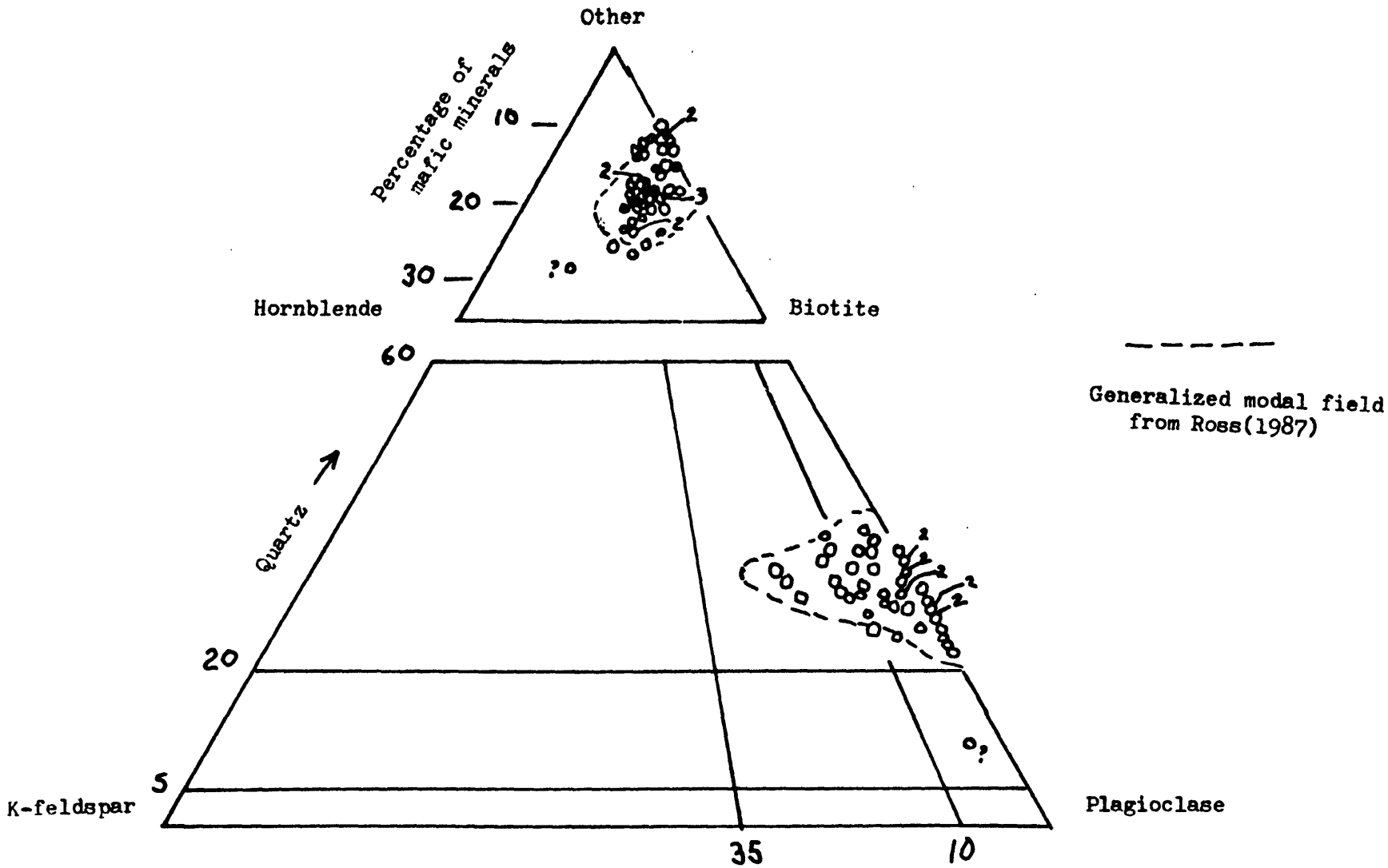

Modal plot of the tonalite of Walt Klein Ranch

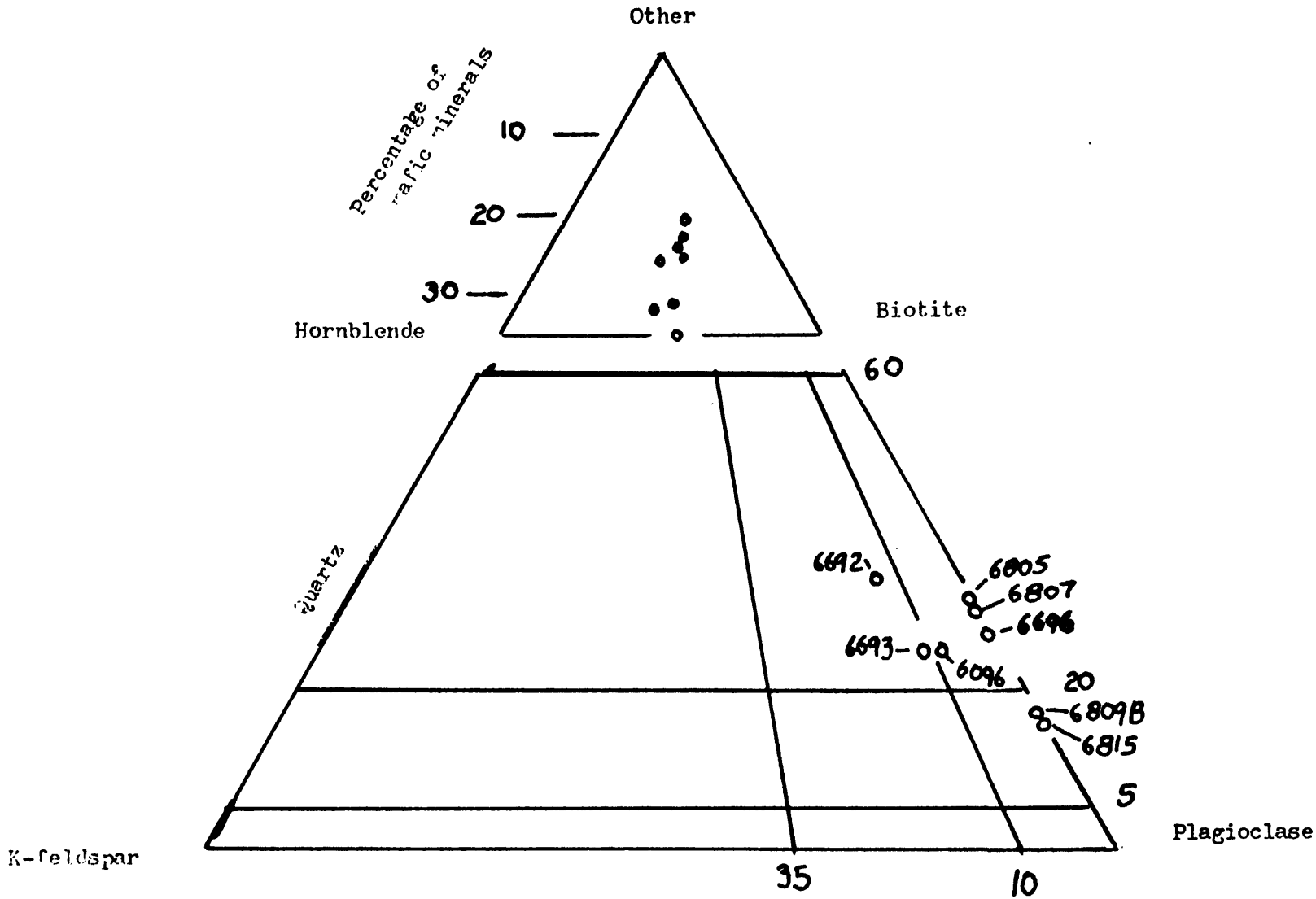

Modal plot of dark granitic rock near Eclipse Hill (Walt Klein?)

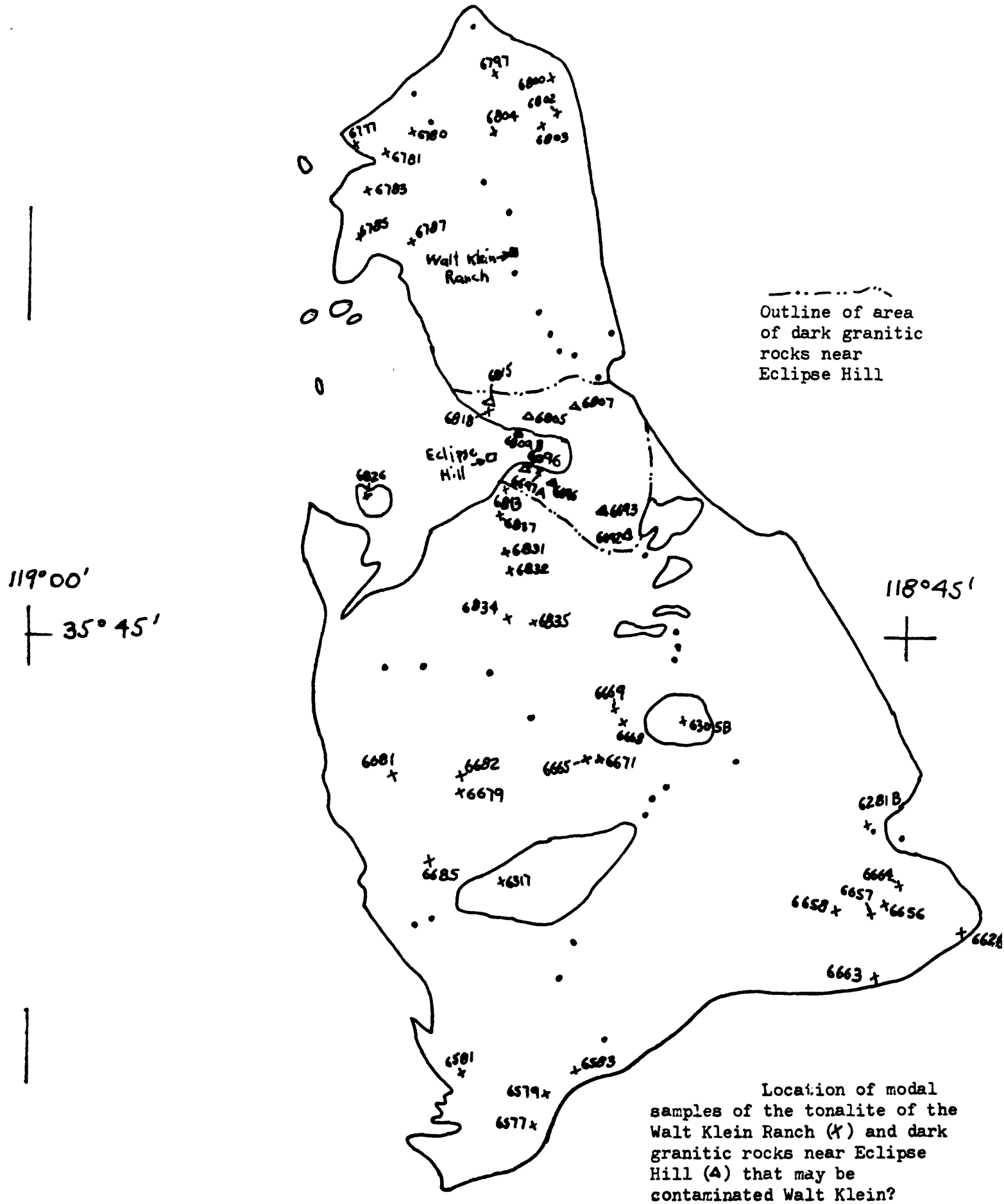
Walt Klein Ranch
Eclipse Hill
Outline of area of dark granitic rocks near Eclipse Hill
119°00'
35°45'
118°45'
Location of modal samples of the tonalite of the Walt Klein Ranch (✕) and dark granitic rocks near Eclipse Hill (▲) that may be contaminated Walt Klein?

Modes of the tonalite of the Zumwalt Ranch (1988)

Sample	Plagioclase	K-feldspar	Quartz	Biotite	Hornblende	Opaque	10^{-5} SIU
6719*	63	0.5	17	11	8	0.5	2000
6721*	56	3	19	8	14	-	600
6722*	57	0.5	20	13.5	8.5	0.5	4500
6723*	58	2	15	12.5	12.5	<1	2000
6652	53	7	20	13	7	<1	1200
6754	54.5	5	20	12	8.5	<1	900
6755	49	17	23	8	3	<1	1400
6756	53	6	20	13	8	-	600
6760	59	<1	9	16	16	-	1200
Average	56	5	18	12	9	<1	1600

*collected on Reservation Road north of the map area (see fig. 4).

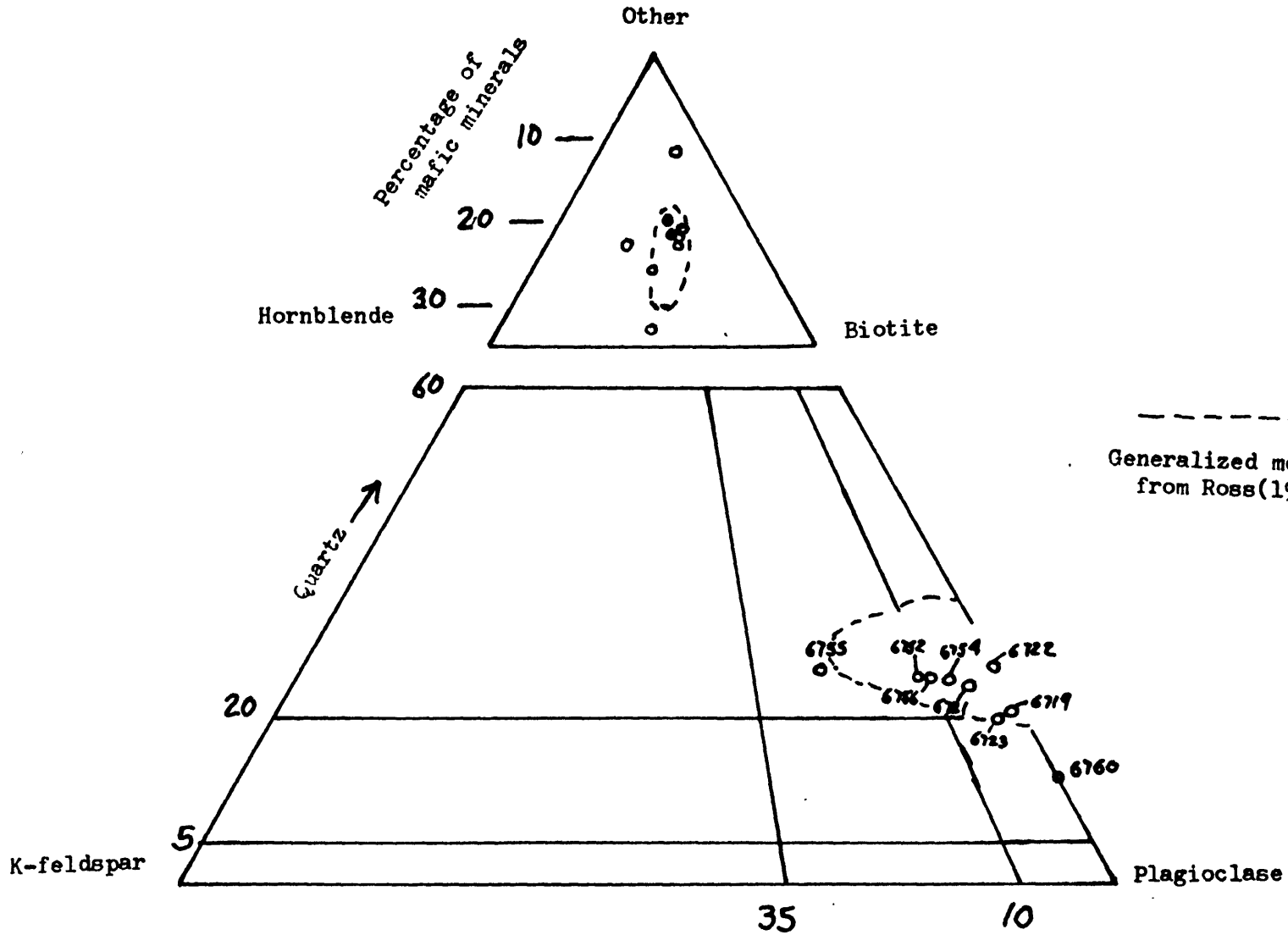

Modal plot of the tonalite of Zumwalt Ranch

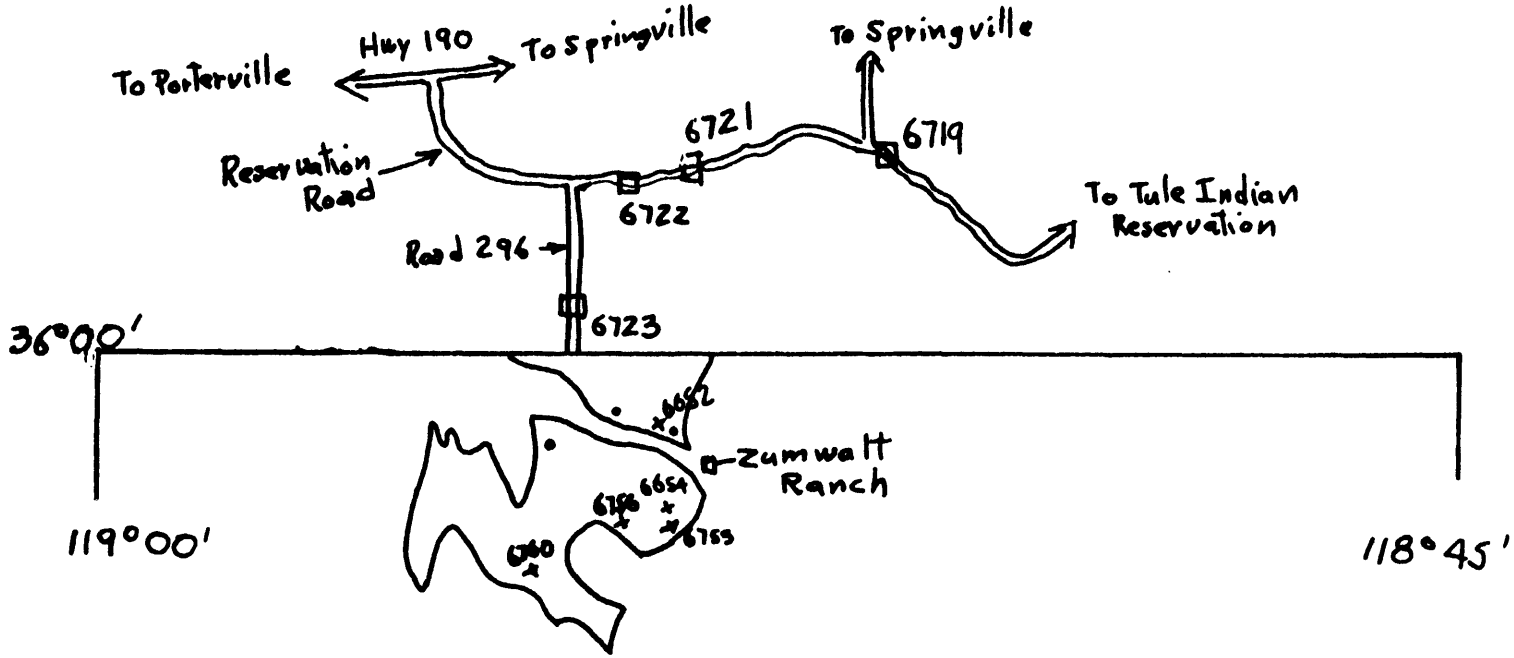

Location of modal samples of the tonalite of the Zumwalt Ranch

Modes of the Cedar Creek "type" (dikes and small masses) 1/

Sample	Plagioclase	K-feldspar	Quartz	Biotite	Hornblende	Other	10^{-5} siu	Specific Gravity
			Granite and granodiorite					
6287R-A	41	27	28	4	-	-	15	2.64
6286R	52	13	24	10	1	-	-	-
6350R	42	18	37	3	-	Opaque<1	-	-
6615	42	29	26	3	-	-	60	2.67
6623	43	25	29	3	-	-	0	2.67
6624B	59	12.5	16.5	12	<1	-	-	-
6635	48	19	23	10	-	-	400	2.64
6636A	32	37	29	2	-	-	400	2.61
6645	41	26	30	3	-	-	0	2.61
6650B	46	21	29	4	<1	-	-	-
6677	42	23	31	4	-	-	40	2.62
6698A	45	18	29	8	-	-	5	2.63
6698B	50	11	27	11	1	-	-	-
6829	46	33	15	6	-	-	5	-
			Tonalite					
6304R	51	6	33	10	-	-	70	2.65
6349R	63	2	20	15	1	Opaque<1	10	-
6613	56	3	28	8	5	-	1600	2.70
6622	54	3	25	10	8	-	1400	2.72
6624A	54	6	25	11	4	-	400	2.68
6625	58	4	26	12	?	-	4000	2.67
6659	54	3	34	9	1	-	900	2.66
6690	54	2	37	7	-	-	40	2.61
6687	50	-	38	10.5	1.5	-	-	-
6703	55	-	34	10	-	Opaque 1	-	2.73
RWK-3	59	4	22	12	2	Opaque 1 Tourm <1	3000	-
6806	63.5	-	24*	12.5	-	-	25	-
6808A	57	-	34*	9	-	-	10	-
6816	53	1	34*	12	-	-	20	-

* Small, rounded phenocrysts; textural resemblance to granodiorite of Evans Flat

Modes of the Cedar Creek "type" (cont.)

Sample	Plagioclase	K-feldspar	Quartz	Biotite	Hornblende	Other	10^{-5} siu	Specific Gravity
			Quartz diorite (and low quartz tonalite)					
6624C	64.5	-	11	18.5	6	Opaque<1	-	-
6631	63	-	8	9	18	Pyrox. 1 Opaque 1	-	-
6643	59	4	18	14	5	-	250	2.76
6648A	57	-	8	12	22	Opaque 1	-	-
6688A	56	-	17	12	15	-	35	2.79
6702	53.5	-	15.5	10	19.5	-	-	-

1/ Samples formerly assigned to tonalite of Woody (Ross, 1987) are now considered part of the Cedar Creek type.

Tonalite: 6304R, 6315, 6318, and 6349

Quartz diorite: 6313

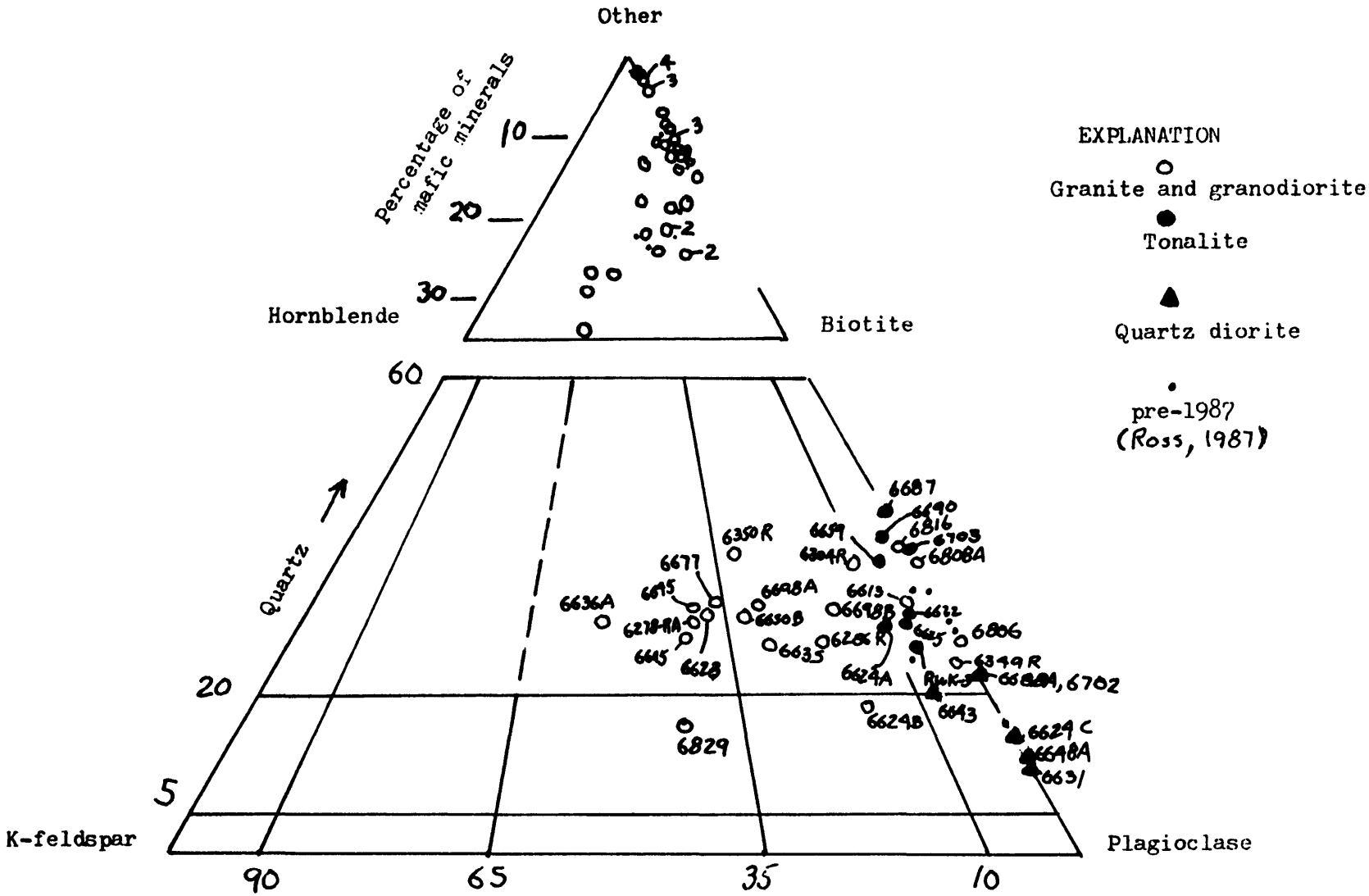

Modal plot of the Cedar Creek "type" (dikes and small masses of various compositions)

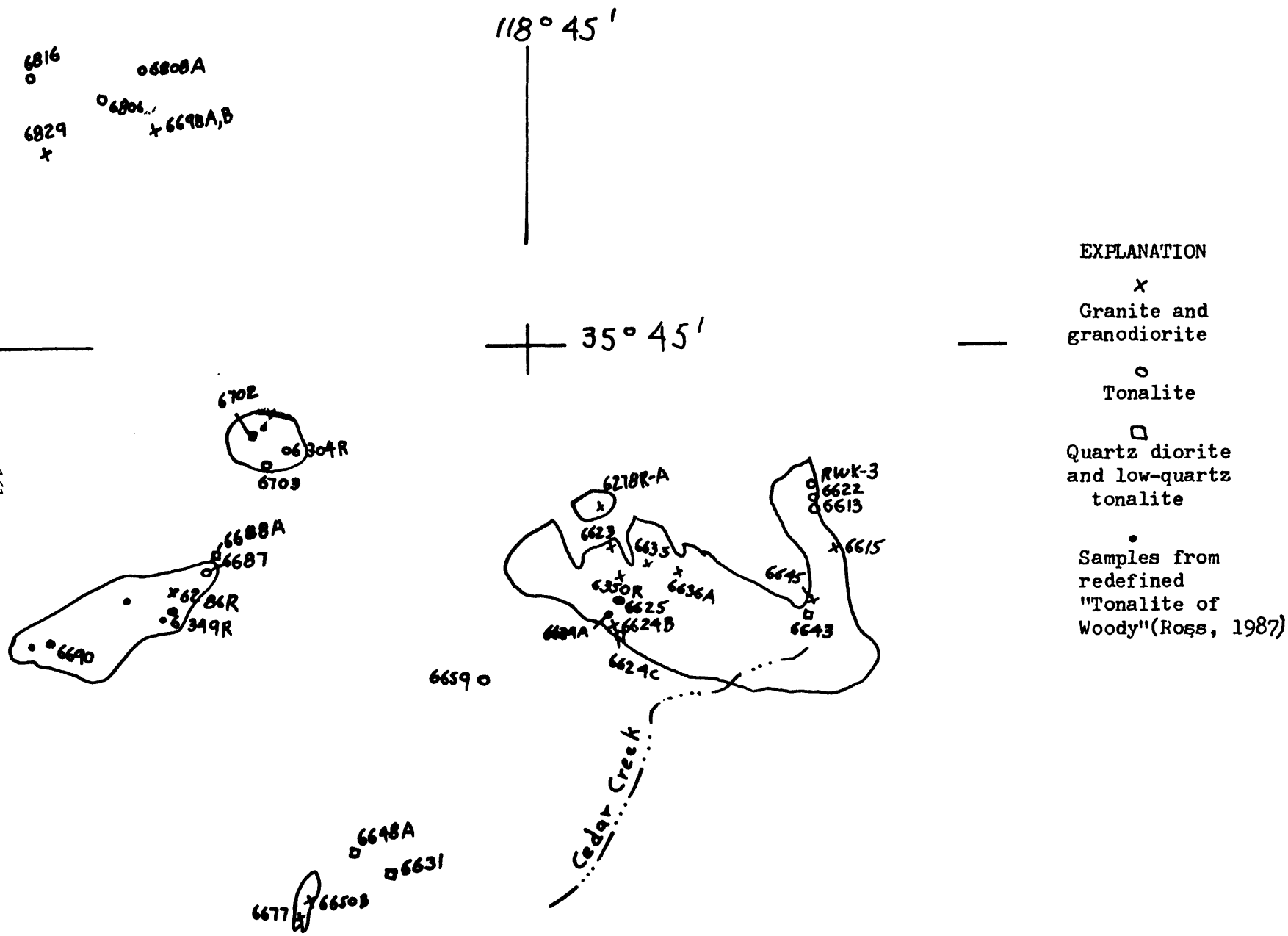

Location of modal samples of the Cedar Creek "type"(dikes and small masses with a wide range of compositions)

Modes of the gabbronorite of Quedow Mountain and related rocks (1987, 1988)

Sample	Plagioclase (An) [3]	Quartz	Biotite	Hornblende	Pyroxene opx	Pyroxene cpx	Opaque minerals	Total mafics [2]	10^{-5} siu
6045	67	6	9	9	8		1	-	-
6255 [5]	60	7	14.5	6	12.5 [1]		-	-	1000
6262 [5]	63	5	16	3	13 [1]		-	-	150
6563B	54	3	2	40	-	-	-	-	-
6575A	52	7	2	38	1	-	-	-	-
6632A	67.5	<1	1.5	21	8 [1]		2	-	-
6633A	66	1	3	28	-	2	<1	-	-
6634	60	-	-	1	37	-	2	-	-
6676A	60	4	3	33	-	-	-	-	-
6678	54.5	4	4	31.5	-	3	3	-	-
6734	65.5 (55)	1.5	1	<1	20	9	3	-	900
6775	86 (60)	-	<1	1	7	3	3	-	600
6860 [5]	64 (55)	6.5	11	10	5	3	0.5	-	50
6861 [5]	72 (62)	2	4	1	15	5	1	-	40
6862 [5]	54 (65)	0.5	0.5	18	12	12	3	-	60
6870A	69.5	1	3?	24? [4]	?		2.5	29.5	7000
6871B	72	2	4?	20.5? [4]	?		1.5	26	5000
6891A	74 (55)	<1	-	11	9	3	3	-	2500

1/ Mostly golden brown crystals of hypersthene, but at least some clinopyroxene

2/ On some gabbroic slabs the distinction between mafic minerals is difficult

3/ The most calcic estimate from extinctions of several grains

4/ May include some pyroxene

5/ Finer grained bodies (Rhymes Campground type) that have relatively low magnetic susceptibility and generally contain more quartz than typical samples of the gabbronorite of Quedow Mountain. These bodies are probably a finer grained, more quartz-rich, facies of the gabbronorite of Quedow Mountain